Proteolytic modification of elastase and chemokine activities by neutrophil elastase and proteinase 3

Dissertation zur Erlangung
des Doktorgrades der Naturwissenschaften
an der Fakultät für Biologie
der Ludwig-Maximilians-Universität München

angefertigt am
Max-Planck-Institut für Neurobiologie,
Abteilung Neuroimmunologie
und
Helmholtz Zentrum München,
Comprehensive Pneumology Center

vorgelegt von
Thérèse Thuy Dung Dau
aus Stuttgart

München

November 2013

Erstgutachterin:	Prof. Dr. Elisabeth Weiß
Zweitgutachterin:	PD Dr. Barbara Lösch
Mitgutachter:	Prof. Dr. Marc Bramkamp
	Prof. Dr. Kirsten Jung
Sondervotum:	PD Dr. Dieter Jenne
Einreichung der Dissertation:	05.12.2013
Datum der mündlichen Prüfung:	06.06.2014

Eidesstattliche Erklärung

Ich versichere hiermit an Eides statt, dass die vorgelegte Dissertation von mir selbständig und ohne unerlaubte Hilfe angefertigt ist.

München, den ....
(Unterschrift)

Erklärung

Hiermit erkläre ich, *

- dass die Dissertation nicht ganz oder in wesentlichen Teilen einer anderen Prüfungskommission vorgelegt worden ist.
- dass ich mich anderweitig einer Doktorprüfung ohne Erfolg **nicht** unterzogen habe.

München, den..... .....
(Unterschrift)

Für meine Eltern

Acknowledgments

I am very grateful and want to thank…

my supervisor **PD Dr. Dieter Jenne**, that he always had time to discuss scientific problems with me and encouraged me to develop new ideas. He taught me to be critical and to approach problems from several angles. I truly enjoyed and learned a lot through our scientific discussions and I sincerely respect his vast knowledge.

my doctoral thesis supervisor **Prof. Dr. Elisabeth Weiß** that she took the time to support and supervise me. I am also grateful for her interest and advice concerning my work. I am also very thankful to the members of my thesis examination committee, namely **PD Dr. Barbara Lösch**, **Prof. Dr. Marc Bramkamp** and **Prof. Dr. Kirsten Jung** for their time and contribution to this work.

Prof. Dr. Hartmut Wekerle for giving me the opportunity to do my PhD thesis at the Max-Planck-Institute of Neurobiology and for his continued interest and opinions at progress reports.

Prof. Dr. Oliver Eickelberg for housing our group in the Comprehensive Pneumology Center (CPC) of the Helmholtz-Zentrum München. I am grateful for the for the warm welcome we received.

the members of my thesis committee, **Prof. Dr. Michael** and **Prof. Dr. Peter Nelson** for their time and great input during our meetings. They truly helped me see things in a different light, when I got stuck somewhere.

all the members of the Jenne group, **Heike Kittel**, **Lisa Stegmann**, **Natascha Perera** and **Lisa Hinkofer** for creating a great work atmosphere. I truly had a lot of fun with them and could always count on them for scientific and moral support.

my fellow PhD students and colleagues, **Marsilius, Marija, Sarah, Cora, Latika, Johannes, Kerstin, Franziska H.** and **Franziska U.** for a great time during my PhD. Sharing all the lab events and going on fun holidays with them brightened my PhD up.

my best friends **Mark** and **Jasmina,** my sister **Cécile** and my brother **André** for their moral support.

and last, but not least my parents for supporting me all these years and encouraging me all the way through.

Table of content

1 Summary

Neutrophils are key players of the innate immune system and are the most important effector cells of antibacterial defense. They carry an abundant pool of highly active neutrophil serine poteases that are mostly known for their destructive role during inflammation. In the past, much focus has been placed on proteinase 3 (PR3) and especially neutrophil elastase (NE) with regard to their destructive role during chronic inflammation. In recent years it has been shown that PR3 and NE are also regulators of inflammation and can influence the course of the inflammation. To deepen our understanding of the pro-inflammatory function of PR3 and NE, I analyzed their effects on chemokines in the first part of my thesis. I focused my work on one class of chemokines, the so-called ERL^+ CXC chemokines, which attract neutrophils. Of particularl interest was MIP-2 as it is expressed in neutrophils. I was able to show that recombinant PR3 and NE can process the N-terminus of MIP-2. This trimming enhances the chemotactic activity of MIP-2. Extending the N-, but not the C-terminus abolished the chemotactic properties of MIP-2. As only active MIP-2 can trigger internalization of the corresponding receptor, CXCR2, I used FACS analysis to determine the CXCR2 binding properties of MIP-2. CXCR2 internalization was not observed on PR3/NE deficient PMNs when using N-terminally extended MIP-2. Only wild type PMNs were able to convert inactive MIP-2 into an active form and to trigger CXCR2 internalization. I concluded that MIP-2 is a substrate of PR3 and NE and processing of MIP-2 enhances recruitment of neutrophils.

In the second part of my thesis, I focused on an alternative regulation of NE activity. I discovered that NE cleaves itself near the active site between A^{188} and G^{189}, thereby changing its substrate specificity. To compare the two-chain form with intact NE, the exact active amount of each form was determined by titration. While the two-chain form of NE was much more slowly inhibited by α-1-protease inhibitor (α1PI), the most important inhibitor of elastase in the plasma, it retained its substrate specificity towards a certain subset of substrates. Deficiency of α1PI is associated with a higher risk of emphysema. In view of the pathogenicity of NE in several lung diseases, synthetic elastase inhibitors have been developed in pharmaceutical companies as potential therapeutic agents. I showed that one of the available small molecule inhibitors inhibited the two-chain form of NE only weakly. In conclusion, I detected a proteolytically modified form of NE that was able to escape inhibition by α1PI. This has been so far overlooked and was not considered during drug development. My studies provided strong evidence that the two-chain form of NE retains its pathogenicity.

Zusammenfassung

Neutrophile Granulozyten sind ein wesentlicher Bestandteil des angeborenen Immunsystems und sind die wichtigsten Effektorzellen für die bakterielle Abwehr. Sie führen große Mengen an hochaktiven Neutrophilen-Serinproteasen mit sich. Letztere sind besonders wegen ihrer destruktiven Rolle bei Entzündungsprozessen bekannt und bedeutsam geworden. Der Schwerpunkt in der Erforschung von Proteinase 3 (PR3) und Neutrophilen-Elastase (NE) war bisher auf ihre pathogene und destruktive Funktion bei chronischen Entzündungen gerichtet. Erst in den letzten Jahren wurde jedoch deutlich, dass PR3 und NE Entzündungsprozesse steuern und somit Entzündungsverläufe beeinflussen können. Um die entzündungsförderlichen Effekte von PR3 und NE zu charakterisieren, habe ich die Wirkung von PR3 und NE auf Chemokine untersucht. In meiner Arbeit habe ich mich vor allem auf die sogenannten ELR^+ CXC-Chemokine konzentriert, welche hauptsächlich Neutrophile anlocken. Mein Interesse galt vor allem MIP-2, da dieses auch von Neutrophilen produziert wird. Ich wies nach, dass PR3 und NE gezielt das N-terminale Ende von MIP-2 prozessieren. Die Verkürzung des N-Terminus von MIP-2 erhöht die chemotaktische Aktivität von MIP-2. Die Verlängerung des N-, nicht aber die des C-Terminus, hebt die chemotaktischen Eigenschaften von MIP-2 auf. Da der entsprechende Rezeptor, CXCR2 genannt, nur nach Stimulierung mit aktivem MIP-2 internalisiert wird, habe ich die Bindung von MIP-2 an CXCR2 mittels Durchflusszytometrie bestimmt. Eine CXCR2-Internalisierung fand in Granulozyten mit PR3/NE-Defizienz nicht statt, wenn N-terminal verlängertes MIP-2 verwendet wurde. Nur Wildtypzellen konnten inaktives MIP-2 in aktives MIP-2 umwandeln und damit die CXCR2-Internalisierung auslösen. Ich schlussfolgerte daraus, dass MIP-2 von PR3 und NE prozessiert wird und dies die Rekrutierung der Neutrophilen beschleunigt.

Im zweiten Teil meiner Arbeit, untersuchte ich eine alternative Regulierung der NE-Aktivität. Ich entdeckte, dass NE sich in der Nähe des aktiven Zentrums zwischen A^{188} und G^{189} selbst schneidet und dadurch seine Substratspezifität verändert. Um die intakte und die zweikettige NE-Form zu vergleichen, wurde die exakte Menge an aktiver NE für beiden Formen mittels Titration ermittelt. Obwohl zweikettige NE viel langsamer von α-1-Protease Inhibitor (α1PI), dem wichtigsten Elastaseinhibitor im Plasma, inhibiert wird, behält die zweikettige NE ihre Substratspezifität für eine Subgruppe von Substraten bei. Eingeschränkte Inhibition durch α1PI erhöht bekanntermaßen das Risiko für

Emphysem. Aufgrund der pathogenen Rolle von NE bei Lungenkrankheiten und anderen chronisch-entzündlichen Erkrankungen wurden synthetische Elastaseinhibitoren von vielen pharmazeutischen Firmen entwickelt. Ich konnte zeigen, dass ein niedermolekularer Elastase-Inhibitor, ein bereits in klinischen Studien verwendeter Wirkstoffkandidat, den uns AstraZeneca zur Verfügung stellte, die zweikettige NE-Form nur sehr schlecht inhibiert. Ich konnte schließlich eine proteolytisch modifizierte Form der NE nachweisen, die sich der Inhibierung durch α1PI partiell entzieht. Diese Form wurde bisher übersehen und daher nicht bei der Medikamenten-Entwicklung berücksichtigt. Viele Hinweise in meinen Studien weisen darauf hin, dass NE nach autoproteolytischer Modifikation ihre Pathogenität beibehält.

2 Introduction

2.1 Neutrophil granulocytes

Our body has developed a fine tuned immune system to fight microorganisms that are able to cross the physical barriers of our body such as the skin. The first line of defense is formed by leukocytes of the innate immune defense system with neutrophils as the key players. A distinctive feature of granulocytes is the lobulated nucleus, which earned them the name polymorphonuclear cells (PMNs). Neutrophils are the most dominant subclass of PMNs. They make up 40-70% of all peripheral blood leukocytes, while eosinophil and basophil granulocytes only constitute less than 5% of leukocytes. The importance of PMNs can be seen in patients with neutropenia, who show an increased risk of infections with PMN counts considerably reduced and below 1500 per µl. Patients with neutrophils below 500 per µl have a severe risk of serious infections (Janeway et al., 2005; Metcalf, 1991).

Neutrophils are the first cells to arrive at an inflammatory site after residential macrophages are alerted to local danger signals. They form the majority of leukocytes within the first hours of inflammation before they are followed by blood derived macrophages (Janeway et al., 2005; Lawrence et al., 2002). Once arrived at the inflammatory site, they release the contents of their granules and start with the destruction of invading microorganisms. These granules are densely packed stores filled with proteins like myeloperoxidase, defensins, antibacterial peptides and proteases that enable the PMNs to react fast to immediate dangers (Borregaard et al., 2007). There are three different kinds of granules, primary (azurophilic), secondary (specific) and tertiary (gelatinase) granules. They are formed during different stages of granulocyte development and thus differ in their contents (Borregaard, 2010). PMNs internalize pathogens via phagocytosis, where phagosomes fuse with lysosomes to so called phagolysosomes (Janeway et al., 2005). The neutral pH of phagolysosomes activates neutral proteases like the neutrophil serine proteases (NSPs), which are kept inactive by the low pH and binding to proteoglycans in the primary granules. During the so called respiratory burst PMNs produce reactive oxygen species (ROS) which together with other antimicrobial proteins from the lysosomes, kill the engulfed bacteria (Dale et al., 2008; Janeway et al., 2005). Although killing microorganisms is an important function, it is not

the only function of PMNs. PMNs are also involved in wound healing and regulation of the immune response during inflammation (Appelberg, 2007; Nathan, 2006).

2.2 Neutrophil serine proteases

Neutrophil serine proteases (NSPs) are a family of structurally related proteases that consists of four active members: neutrophil elastase (NE), cathepsin G (CG), proteinase 3

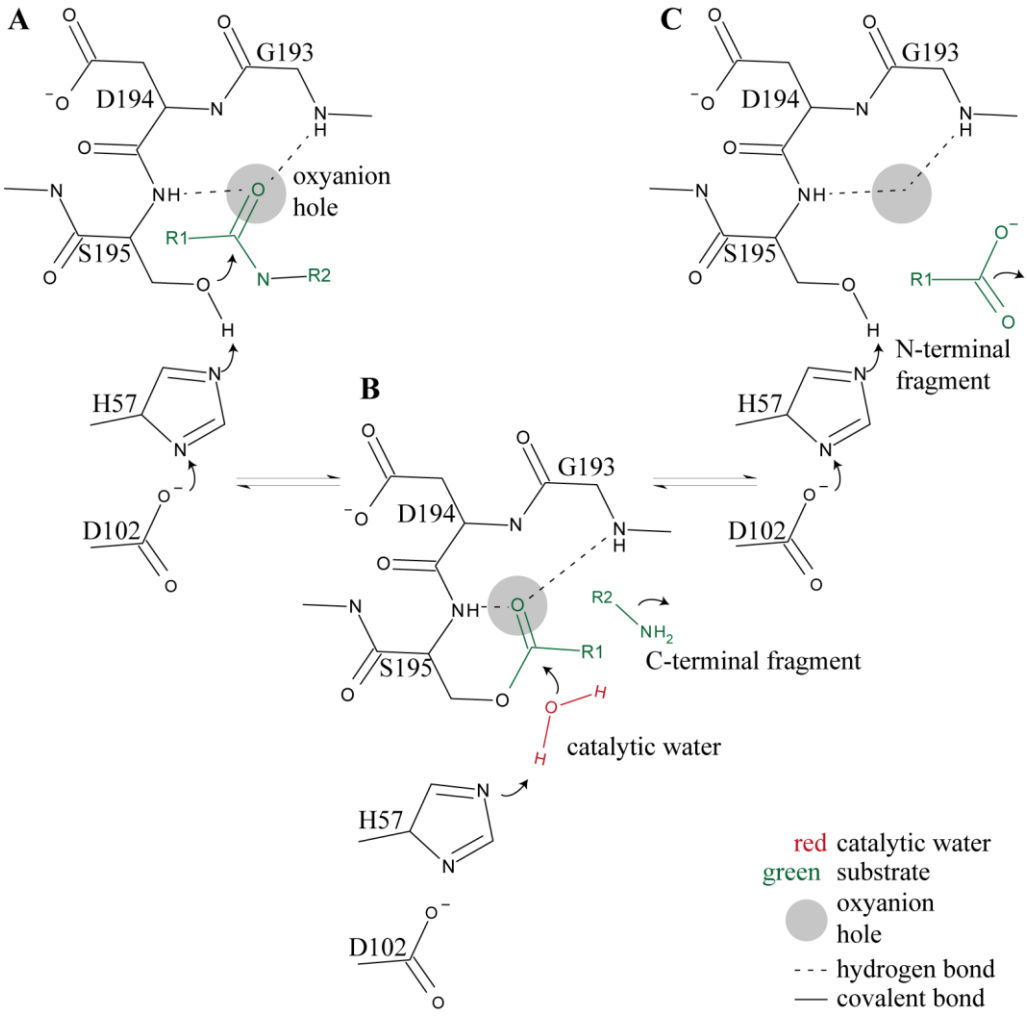

Fig 2.1: Mechanism of serine protease catalysis. (**A)** features the initial state of active center. The hydroxyl group of Ser^{195} is polarized to a highly nucleophilic state with the help of Asp^{102} and His^{57} and attacks the main chain of the substrate. The resulting tetrahedal intermediate is kept stable by the oxyanion hole (grey circle) and His^{57}. The tetrahedal intermediate is split into the acyl-enzyme complex (**B**) and the amino group of the C-terminal fragment after receiving a proton from His^{57}. The acyl-enzyme complex is attacked by the catalytic water resulting in a different tetrahedal intermediate that is again stabilized by the oxyanion hole and a protonated H^{57}. In (**C**) the carboxylic acid product is released and the original state of the active center is restored.

(PR3), and neutrophil serine protease 4 (NSP4) (Perera et al., 2012; Pham, 2006). They are chymotrypsin-like serine proteases, whose active center features the catalytic triad His^{57}, Asp^{102} and Ser^{195}.

The reaction can be divided into two steps, the acylation and deacylation step (**Fig 2.1**) (Berg et al., 2003; Hedstrom, 2002). The carboxylate group of Asp^{102} forms a hydrogen bond with the imidazole ring from His^{57}, which in turn forms a hydrogen bond with Ser^{195}. Because of these interactions the oxygen of Ser^{195} becomes strongly nucleophilic. During the acylation reaction the hydroxyl group of Ser^{195} attacks the main chain of the substrate and forms a tetrahedal intermediate (not shown), which is stabilized by the oxyanion hole. Once the amine group receives a proton from the His^{57} the tetrahedal intermediate collapses into the acyl-enzyme complex and the C-terminal part of the substrate and (Berg et al., 2003; Hedstrom, 2002). During the deacylation step a water molecule attacks the acyl-enzyme complex and protonates His^{57}. The resulting tetrahedal complex (not shown) is kept stable by the oxyanion hole before it splits into a carboxylic acid product and the restored catalytic triad (Berg et al., 2003; Hedstrom, 2002).

A large proportion of the NSPs are active in the phagolysosome, where they degrade ingested microorganisms. Their microbicidal ability is crucial for the defense against bacteria and fungi (Belaaouaj et al., 2000; de Haar et al., 2006) (Reeves et al., 2002). NSPs are also known to degrade the extracellular matrix (ECM) which is useful for extravasation, but uncontrolled excessive activity can also lead to serious tissue damage (Chua and Laurent, 2006; Pham, 2006). Besides their destructive role, emerging evidence indicates that NSPs can also regulate the inflammatory process (Kessenbrock et al., 2011; Pham, 2006).

2.2.1 Regulatory functions of NSPs

The small fraction of NSPs that is released into the extracellular space upon activation is thought to have a regulatory function. Externalized NSPs are bound to the membrane and to neutrophil extracellular traps (NETs) (Brinkmann et al., 2004; Campbell et al., 2000; Kessenbrock et al., 2009; Owen et al., 1995) Another factor contributing to a prolonged activity, is the local level of active inhibitors. These can be inactivated through oxidation or proteolysis (Liu et al., 2000; Owen and Campbell, 1999). NSPs are probably involved in immune complex (IC)-mediated inflammation, since IC-mediated inflammation is impaired in NSP-deficient mice (Kessenbrock et al., 2008; Raptis et al., 2005).

Recently, it was shown that the anti-inflammatory protein progranulin is degraded by NE and PR3 (Kessenbrock et al., 2008). Progranulin inhibits tumor necrosis factor α (TNF-α)-induced immune responses, thereby reducing the respiratory burst and degranulation (Zhu et al., 2002). Lack of PR3 and NE leads to an accumulation of progranulin resulting in decreased inflammation (Kessenbrock et al., 2008).

Pham *et al.* showed that CG indirectly enhanced integrin clustering by an as yet unknown mechanism. Consequence of this effect is the reduced secretion of macrophage inflammatory protein 2 (MIP-2) from neutrophils. MIP-2 belongs to the family of chemokines and is crucial for recruiting PMNs. Indirect regulation of chemokine levels are probably not the only way NSPs can modify chemokine activity.

2.2.2 Pathophysiological functions of NSPs

Despite the important role of NSPs in immune defense, a tight regulation of their activity is necessary, as an imbalance between proteases and inhibitors often leads to disease. NSPs are especially involved in chronic inflammatory diseases like emphysema and chronic inflammatory lung diseases, which will be discussed in detail later (Roghanian and Sallenave, 2008b). The following diseases are examples that emphasize the need to control the timing, localization and intensity of NSP activity. In addition, NSPs also play an important role in granulomatosis with polyangiitis, an autoimmune disease, independent of their activity (Korkmaz et al., 2010).

2.2.2.1 Hereditary neutropenias

One example that demonstrates the importance of timing and sorting of NSPs can be seen in cyclic and severe congenital neutropenia. This disease is often associated with mutations of ELANE, the gene encoding NE, resulting in a misplacement of NE (Dale et al., 2002; Klein, 2009). The function of NE in pathogenesis is not known yet. However, several observations indicate that mislocalization and/or misfolding of NE is one important factor that either induces apoptosis or inhibits differentiation of myeloblasts into neutrophils (Horwitz et al., 2007).

2.2.2.2 Papillon-Lefevre-syndrome

The activity of NSPs needs to be tightly controlled. Too high or too little activity can result in disease, as can be seen in patients suffering from Papillon-Lefèvre syndrome (PLS). In these patients the dipeptidyl peptidase I (DPPI) is missing (Dalgıc et al., 2011),

which is essential for the activation of NSPs. Because DPPI is missing, NSPs stay in their pro-protease or zymogen form, thus PLS patients have no active NSPs. In fact, even the protein level of zymogen NSPs is reduced (de Haar et al., 2004, 2006). These patients often have severe periodontal disease (periodontitis) as well as palmoplanter hyperkeratosis, thickened skin on palms and soles (Dalgıc et al., 2011).

2.2.2.3 Granulomatosis with polyangiitis

Granulomatosis with polyangiitis (GPA) is an autoimmune disease defined by the presence of antineutrophil cytoplasmic autoantibodies (ANCA) and necrotizing vasculitis (Korkmaz et al., 2010). These antibody recognize mainly PR3 (Kallenberg et al., 2006). Although inflammation can take place in every organ, the upper and lower respiratory tract as well as the kidneys are the most affected (Korkmaz et al., 2010).

2.2.3 Chemokines as substrates of NSPs

Chemokines are a family of chemoattractant cytokines that bind to G protein-coupled receptors expressed on leukocytes (Janeway et al., 2005). The conserved N-terminal cysteines of chemokines are used to divide the chemokines into four classes: CXC, CC, XC and CX3C (Baggiolini, 2001). The C stands for cysteine and the X for any amino acid residue. The receptors were named according to which chemokine class they bind. The CXC class is further subdivided into chemokines that feature an ELR motif before the CXC motif or not (Baggiolini, 2001). In this study we focus on CXC chemokines containing the ELR motif (ELR^+-CXC chemokines), because they bind to the CXCR2 receptor, which is expressed on neutrophils (Baggiolini, 2001; Janeway et al., 2005).

2.2.3.1 Interleukin-8

The most important and best studied ELR^+CXC chemokine in humans is CXCL8, also known as interleukin-8 (IL-8). Interestingly IL-8 is also expressed by neutrophils at relatively high levels (Scapini et al., 2000). Various naturally occurring IL-8 isoforms have been identified with different posttranslational modifications (Mortier et al., 2008; Proost et al., 2008). One example is the citrullination of Arg5. It does not change the chemotactic and angiogenic properties of IL-8 *in vitro*, but improves the stability of IL-8 *in vivo* (Proost et al., 2008). The most common modification of IL-8 is the trimming of the N-terminus (Mortier et al., 2008; Wolf et al., 2008). The amino-terminal domain with its ELR motif is essential for receptor activation (Clark-Lewis et al., 1991), thus changing

its length influences the chemotactic activity of IL-8. Several proteases *in vitro* are able to process IL-8 that can either enhance or inactivate IL-8 activity (**Fig 2.2**) (Mortier et al., 2008; Wolf et al., 2008). For example matrix metalloproteinase 12 (MMP-12) inactivates IL-8 by destroying the ELR motif (Dean et al., 2008). In contrast, cleavage of IL-8 after Ala^{7} by PR3 converts IL-8 to a more chemotactic form (Nourshargh et al., 1992; Padrines et al., 1994).

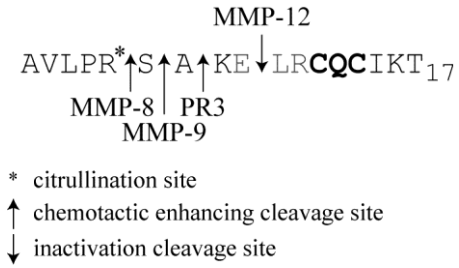

Fig 2.2: Naturally occurring modifications of IL-8 at the N-terminus. This figure shows the N-terminal sequence of IL-8 from Ala^{1} to Thr^{17}. MMP-12 cleaves within the ELR motif of IL-8, thereby inactivating it. Trimming of the N-terminus by MMP-8, MMP-9 and PR3 enhances chemotactic activity of IL-8. Citrullination of IL-8 has no influence on chemotactic activity, but enhances stability of IL-8 *in vivo*.

2.2.3.2 Murine CXC ELR^{+}

While there are seven human ELR+-CXC chemokines, only four were found in mice: MIP-2, LIX, KC, DCIP-1. None of these are true homologues of IL-8, but like IL-8 macrophage inflammatory protein (MIP-2 or CXCL2) is very abundantly expressed in neutrophils and can therefore be regarded as the appropriate murine equivalent of IL-8 (Pham, 2006). Very little is known how chemokine processing occurs *in vivo*.

2.3 Neutrophil Elastase

Neutrophil elastase, named for its ability to degrade elastin, is abundantly expressed in neutrophils. The high NE concentration of over 5 mM in azurophilic granules suggests an important role for elastase (Liou and Campbell, 1995). As already mentioned NE influences inflammation by processing and degrading inflammatory regulators (Kessenbrock et al., 2008; Pham, 2006). It has also been reported that the clearance of gram-negative bacteria is impaired in NE knockout mice (Belaaouaj et al., 1998). Internalized bacteria were not killed and could escape from the phagolysosome (Belaaouaj et al., 1998). Despite its importance in antimicrobial defense, NE has been

studied much more, because of its pathogenic role in inflammation. Due to its ability to degrade elastin and other components of the ECM, NE is often closely connected to tissue destruction in chronic inflammatory diseases (Barroso et al., 2006; Chua and Laurent, 2006; Heinz et al., 2012; Henriksen and Sallenave, 2008; Roghanian and Sallenave, 2008a).

2.3.1 NE in lung diseases

Unopposed NE activity is highly destructive and can lead to disease. Especially in chronic inflammatory lung diseases, where high NE activity between 0.5 to 5 µM in the airways can be detected, NE aggrevates the disease (Döring et al., 1995). In the following the two most relevant lung diseases concerning NE will be introduced.

2.3.1.1 Chronic obstructive pulmonary disease

Chronic obstructive pulmonary disease is a compendium of lung diseases that all show an irreversible airflow reduction, with chronic bronchitis and emphysema as the most prominent symptoms (Barnes et al., 2003). Since injection of human NE (hNE) into the lung results in emphysema, excess NE activity is regarded as one major risk factor for emphysema development (Barnes et al., 2003; Fujita et al., 1990; Senior et al., 1977). Adding to this line of reasoning, patients lacking the most important NE inhibitor alpha-1-protease inhibitor (α1PI) often develop emphysema (Fujita et al., 1990; Roghanian and Sallenave, 2008b). Degradation of ECM, promotion of proinflammatory proteins and stimulation of mucin production are the most important pathogenic features of NE during COPD (Roghanian and Sallenave, 2008b).

2.3.1.2 Cystic fibrosis

Cystic fibrosis is a hereditary recessive disease. Mutation of the gene encoding the cystic fibrosis transmembrane conductance regulator results in thickening of the mucus as well as severe and chronic inflammation of the lung with massive neutrophil infiltration (Kelly et al., 2008; Voynow et al., 2008). High levels of NSPs are reported to increase mucus secretion (Voynow et al., 2008). Additionally, high NE activity leads to epithelial disruption and prolongs inflammation (Kelly et al., 2008; Roghanian and Sallenave, 2008b; Voynow et al., 2008). Similar to COPD, disruption of the protease-antiprotease balance in favor for the protease gives rise to disease (Kelly et al., 2008; Voynow et al., 2008).

2.3.2 Regulation of NE activity

The previous chapters showed how important it is to keep a tight grip on the activity of NSPs. While the activity of other proteins can be controlled by up- or down-regulation of the expression of those protein, NSPs are only expressed during neutrophil development in the bone marrow and stored in azurophilic granules (Pham, 2006). Therefore other mechanisms e.g. the lowering of the pH, biosynthesis of zymogen precursors and inhibitors are used to maintain control over NSP activities.

2.3.2.1 pH

As NSPs are toxic to the neutrophil, they are kept inactive in the azurophilic granules through a low pH. During the catalysis His^{57} acts as a base and accepts the proton of Ser^{195} (**Fig2.1**) (Hedstrom, 2002). At a low pH His^{57} (pKa = 6.08) is protonated and thus is unable to act as a base any longer. Furthermore, NSPs are bound to proteoglycans (Pham, 2008). The presence of superoxide anion triggers the K^+-flux into the phagolysosome (Reeves et al., 2002). The K^+-influx increases the osmolarity and solubilizes the NSPs in the phagolysosome. The oxygen radicals neutralize the pH, thereby activating the NSPs (Reeves et al., 2002).

2.3.2.2 Proteolysis

It is a common principle of nature to regulate protease activity by other proteases. The most prominent examples are the clotting cascade and the complement system, where the components of these cascades are available in their zymogen form (Janeway et al., 2005). Each protease activates a zymogen, which in turn activates another zymogen (Janeway et al., 2005). Some proteases can even activate themselves by autoprocessing as can be seen with MMP-9 and trypsin (Brodrick et al., 1978; Kay and Kassell, 1971; Makowski and Ramsby, 2005).

2.3.2.2.1 Processing by other proteases

In general, proteases are expressed as zymogens and are activated by the removal of the propeptide with the help of another protease. As already mentioned, the protease responsible for converting Pro-NSPs into mature NSPs is DPPI (Pham, 2008). DPPI removes a two amino acid long peptide, thereby freeing the N-terminus Ile^{16}-Val^{17} (Hedstrom, 2002; Pham, 2006). The liberated Ile^{16} builds a salt bridge with the Asp^{194},

inducing a conformational change in the protease, which results in the formation of the oxyanion hole as well as the S1 site pocket (Hedstrom, 2002).

2.3.2.2.2 Self-cleavage

There are actually several examples for self-activating proteases. Self-activation is probably an enhancing mechanism to accelerate conversion of the zymogen. Besides self-activation, self-cleavage also can lead to inactivation or change of specificity. Trypsin is a very good example for different modalities of influencing the activity of a protease by self-cleavage.

Trypsin belongs to the family of serine proteases and is active as a digestive enzyme at neutral pH in the duodenum (Chen et al., 2001; Hedstrom, 2002). Trypsinogen, the zymogen of trypsin, is expressed in the pancreas and then secreted to the duodenum, where enterokinase starts its conversion to trypsin (Chen et al., 2001; Rinderknecht, 1986). Active trypsin then in turn activates other digestive proteases (Rinderknecht, 1986).

Interestingly, enterokinase only initiates trypsin activation. The newly formed, active trypsin actually converts trypsinogen to trypsin (Brodrick et al., 1978; Chen et al., 2001; Kay and Kassell, 1971). This reaction is largely dependent on pH and Ca^{2+}-concentration (Brodrick et al., 1978; Kay and Kassell, 1971; McDonald and Kunitz, 1941). As previously described for NSPs, cleavage of the Lys^{15}/Ile^{16} bond enables Ile^{16} to interact with Asp^{194} (Bode, 1979; Bode et al., 1978).

Although trypsin is active in the duodenum, deregulated trypsin activity actually leads to pancreatitis (Chen et al., 2001; Whitcomb et al., 1996). Premature activation of trypsin in the pancreas instead of the duodenum triggers the disease (Chen et al., 2001). Whitcomb et al. were the first to report that mutation of the Arg^{122} in the cationic trypsinogen causes pancreatitis. The mutation eliminates an internal autolysis site, through which trypsin can inactivate itself. Since then, many other mutations have been reported that all have the same effect of eliminating the autolysis site (Chen et al., 2001). Removal of this self-regulating mechanism of trypsin can lead to pancreatitis. This finding once again underlines the importance of self-cleavage as a regulatory mechanism.

It has been reported that trypsin features an additional self-cleavage site between Lys^{188}/Asp^{189} (Smith and Shaw, 1969). Cleavage of this bond changes the specificity of trypsin to a chymotrypsin-like specificity (Keil-Dlouhá et al., 1971). The S1 pocket is

formed by the residues 189—192, 214-216 and 224-228 (Hedstrom, 2002). The residue Asp^{189} is very important for the Arg and Lys specificity of trypsin and lies at the bottom of the S1 pocket (Hedstrom, 2002). Cleavage between Lys^{188} and Asp^{189} changes the conformation of the S1 pocket which leads to the chymotrypsin-like specificity. Although the biological function of this cleavage has not been elucidated yet, its existence is important for trypsin production. Commercially available trypsin is methylated to avoid this particular self-cleavage and treated with tosyl phenylalanyl chloromethyl ketone (TPCK) to suppress chymotrypsin-like activity from already nicked trypsin.

2.3.2.3 Inhibition with serpins

Normally, large amounts of inhibitors are expressed to keep protease activity under control. For serine proteases the most important inhibitors are the serpins. As the name indicates most members of the serpin superfamily are **ser**ine **pr**otease **in**hibitors, although this family also includes non-inhibitory members like ovalbumin. There are 36 members known in humans that are involved in inflammation, coagulation and fibrinolysis (Huntington, 2011).

Serpins have three β–sheets, 8-9 α-helixes and a reactive center loop (RCL) (Gettins, 2002). In its native conformation the 20-24 residue long RCL is a flexible loop that lies outside of the main structure and therefore is freely accessible by the protease (Huntington, 2011). Curiously, the native conformation of the serpins is not the most stable conformation. In its active state, the β–sheet A consists of five strands (Gettins, 2002; Gooptu and Lomas, 2009). The serpins switch to a hyperstable conformation by inserting the RCL into the β–sheet A, which turns the β–sheet A into a complete antiparallel β–sheet (Gettins, 2002; Gooptu and Lomas, 2009).

Covalent inhibition of proteases by serpins occurs in two consecutive steps. First, the protease is reversibly inhibited by the formation of a Michaelis complex (Gettins, 2002; Gooptu and Lomas, 2009). In the second step an ester bond is formed between the protease and serpin, resulting in an irreversible inhibition (Gettins, 2002; Gooptu and Lomas, 2009). Incorporation of the RCL into the β–sheet A is favored upon cleavage of the RCL by the protease (Gettins, 2002; Gooptu and Lomas, 2009). The classical orientation of serpins features the RCL on top of the serpin, so in a canonical complex the protease sits above the serpin (Huntington, 2011). After the acyl-enzyme complex is formed, the RCL inserts into the β–sheet A and the protease is relocated to the bottom of

the serpin (Gettins, 2002; Huntington, 2011). The structural change distorts the active center of the protease and destroys the oxyanion hole (Gettins, 2002; Huntington, 2011). That is why the deacylation cannot occur and the protease is trapped with a covalent bond to serpin. If the deacylation is faster than the rearrangement of the serpin, the serpin will merely serve as a substrate and the protease will not be inhibited (Gettins, 2002).

2.3.2.3.1 α-1 protease inhibitor (α1PI)

A very important member of serpins is the plasma protein α-1 protease inhibitor (α1PI). Plasma protease inhibitors make up 10 % of all plasma proteins (Travis et al., 1988). Out of these inhibitors, α-1-protease inhibitor (α1PI) with a concentration of 20 -53 µM is the most abundant one in plasma (Hortin et al., 2008; Stoller and Aboussouan, 2012; Travis et al., 1988). While it has been first recognized for its ability to inhibit pancreatic trypsin and has thus been called α-1-anitrypsin formerly, α1PI is the best and most efficient inhibitor for NE (Travis and Salvesen, 1983). As an acute phase protein α1PI levels are increased during inflammation (Travis et al., 1988).

Lack of α1PI is associated with emphysema and patients suffering from α1PI deficiency are currently treated with intravenous application of α1PI (Gooptu et al., 2009). Several mutations have been found to cause α1PI deficiency. In Europe the most common mutation is the so called Z variant of α1PI (Z α1PI), where Glu^{342} is changed to Lys (Carrell et al., 1994; Gooptu et al., 2009). Glu^{342} is located at the hinge region between the β-sheet and the RCL and promotes α1PI polymerization (Carrell et al., 1994; Gooptu et al., 2009; Hopkins et al., 1993). α1PI plasma levels of individuals that are homozygous for Z α1PI have only 10 -15 % of a normal level (Carrell et al., 1994; Gooptu et al., 2009). Additionally, patients carrying the Z α1PI also often have liver diseases, because hepatocytes are the main producers of α1PI. Due to its tendency to polymerize, Z α1PI is retained in inclusion bodies and damages the hepatocytes by accumulation (Gooptu et al., 2009).

2.3.2.3.2 MNEI

Monocyte neutrophil elastase inhibitor (MNEI), also known as SERPINB1, belongs to the clade of OV-serpins (Benarafa et al., 2002). OV-serpins lack a secretory signalpeptide and are primarily active in the cytoplasm (Benarafa et al., 2002). MNEI is very efficient against all three NSPs, but its activity against CG seems especially essential for neutrophil survival (Cooley et al., 2001; Zhou et al., 2001).

3 Material and methods

3.1 Nucleic acid methods

3.1.1 Polymerase-chain reaction (PCR)

Using a heat resistant DNA polymerase, a defined DNA fragment can be easily multiplied. The PCR was used to obtain sufficient amount of DNA necessary for further cloning steps. A typical PCR cycle consists of a denaturation, annealing and elongation step. The conditions used are described in the tables below. The Phusion High-Fidelity DNA polymerase from Finnzymes (New England Biolabs) was used for the PCR.

PCR-mix

400 nM	primer 1
400 nM	primer 2
5-10 ng	template: plasmid
200 µM	dNTPs
1 x	HF-buffer (Finnzymes)
1.25 U	DNA polymerase

PCR program

	temperature	***time***	
initial denaturation	94°C	30 sec	
denaturation	94°C	15 sec	25 cycles
annealing	dependent on primers	1 min	
elongation	72°C	1 min/kb of product	
final elongation	72°C	10 min	

3.1.2 Restriction digest

For each digest we used a 3-5 times excess of enzyme (3-5 units/ µg DNA) with the recommended buffer and temperature. In general 1-5 µg DNA was digested. All enzymes besides AbsI (Novosibirsk, Russia), were pursued from New England Biolabs. To remove the enzymes and undigested vector, the cleaved products were run on a 1% agarose gel (see below) and QIAquick gel extraction kit (QIAGEN) was used to purify the DNA from the gel.

3.1.3 DNA gel electrophoresis

Running DNA fragments on agarose gels in an electrical field separates the DNA fragments by size. To the 1% agarose gels (w/v) 1 µg/ml ethidium bromide was added to visualize the DNA. The agarose gels were prepared with TAE buffer, which was also used as a running buffer for the gels. To identify the size of the fragments the Gene Ruler 1 kb marker (Ferments, Thermo Fisher Scientific) was used.

50 x TAE

242 g	Tris
57.1 ml	acetic acid
100 ml	0.5M EDTA, pH 8.8
	Fill up to 1 L with H_20

10 x sample buffer

0.25%	bromphenol blue
0.25%	xylene cyanol
50%	glycerol

3.1.4 Dephosphorylation

The digested vector is dephosphorylated to prevent the religation of the vector. Only the phosphorylated fragment can then close the plasmid again. For the dephosphorylation alkaline phosphatase (New England Biolabs) was used according to the manufacturer's instruction.

3.1.5 Ligation

Ligase joins together the 3'hydroxyl and 5'phosphate end of DNA fragments, resulting in a covalent diphosphoester bond. A phosphorylated 5'end and adenosine triphosphate (ATP) are necessary for this reaction.

During a common reaction 50 ng vector, 5 times molar excess of fragment and 1 µl T4 DNA ligase are incubated in 50 mM Tris-HCl, 10 mM $MgCl_2$, 1 mM ATP, 10 mM dithiothreitol, pH 7.5 for two hours at room temperature.

3.1.6 Transformation

For each ligation reaction 100 µl competent bacteria were thawn on ice. After adding the DNA (5 µl ligation preparation or 10 ng plasmid DNA) the bacteria were incubated on ice

for 20 min, followed by a heat shock at 42°C for 1 min. The sample was shortly cooled on ice again before 1 ml of Luria-Bertani (LB) medium was added. The bacteria were incubated to recover at 37°C for one hour. For the selection 100 µl of the suspension were plated on agar plates with antibiotics (ampicillin 100 µg/ml) and incubated at 37°C overnight.

LB-medium

1%	tryptone
0.5%	yeast extract
1%	NaCl
1.5%	agar (only for plates)

3.1.7 Competent cells

A single colony of the *E. coli* strain DH5α is grown in 50 ml LB medium at 37°C over night. With 4 ml of this culture a new 200 ml culture is set up. Upon reaching an OD_{590} of 0,375-0.6 the bacteria are cooled on ice for ten minutes in precooled 15 ml falcons. After centrifuging the cells at 4°C and 3000 rpm for 7 min, the pellet is resuspended in 10 ml ice cold $CaCl_2$ solution. This step is repeated to ensure the complete removal of media. After 30 min of incubation on ice, the bacteria are centrifugated and are resuspended in 2 ml ice cold $CaCl_2$ solution. Aliquots (100 µl) of the cells are shock frozen using a mix of dry ice and isopropanol. The competent cells are stored at -80°C. It is crucial to precool all buffers and centrifuges for the whole procedure.

$CaCl_2$-Lösung

60 mM	$CaCl_2$
15%	glycerol
10 mM	PIPES, pH 7

3.1.8 DNA purification

Transformed bacteria are stored as glycerol stocks (17.5% glycerol) at -80°C after verification. For DNA isolation an overnight culture (minipreps: 2-5 ml, maxipreps: 200 ml) is needed. The DNA is then isolated using the QIAprep Spin Miniprep Kit (QIAGEN) or Plasmid Maxi Prep (QIAGEN) or PureYield™ Plasmid Maxiprep System (Promega) respectively according to the manufacturer's instruction.

3.2 Protein methods

3.2.1 Antibody list

antigen	species	dilution	manufacturer	Cat. No.
murine MIP-2	rabbit	1:5000	Preprotech	500-P130
Human NE	rabbit	1:1000	Abcam	ab68672
Human NE	mouse	For IP	QED	13203
His-tag, 3D5	mouse	1:2500	E. Kremmer	-
human haptoglobin	rabbit	1:1000	Dako	A0030
Gr-1/ Ly-6G (mouse)	rat	1:200	BD Pharmingen	553126
CXCR2, 242216	rat	1:200	R&D Systems	MAB2164
IgG, FITC†	rat	1:200	BD Pharmingen	553988
murine IgG+IgM, HRP*	goat	1:2500	Pierce	31444
rabbit IgG, HRP*	goat	1:5000	Jackson ImmunoResearch	111-035-006

†Fluorescein isothiocyanate (FITC), * horseradish peroxidase (HRP)

3.2.2 Affinity chromatography

All recombinant proteins were expressed with a C-terminal his-tag, which binds to Ni^{2+} ions. The proteins were purified using nickel columns that mainly differ in their matrix material and have varying binding capacities. The protein is eluted with imidazole, which competes with the protein for the nickel binding sites.

3.2.2.1 HisTrap™ HP Columns (GE Healthcare)

The matrix of these columns is sepharose and these columns are compatible with ÄktaPrime Plus (GE Healthcare) that was used for the purification. Before loading, the supernatant was dialyzed against the washing buffer (20 mM Tris-HCl pH7.4, 300 mM NaCl). A continuous imidazole gradient was applied to elute bound proteins. For this washing buffer and elution buffer (20 mM Tris-HCl pH7.4, 300 mM NaCl, 1M imidazole) were mixed continuously. The maximum capacity of a column is 40 mg, of His-tagged proteins. These columns were to purify 250-600 ml supernatant of mNE and MIP-2. Z-α1PI was always purified with these columns as this protein did not bind to the PrepEase Histidine-tagged Protein Purification columns (Affymetrix).

3.2.2.2 PrepEase Histidine-tagged Protein Purification - High Specificity (Affymetrix)

The Ni^{2+} ions are bound to the dry silica-based resin via the chelating group tris-carboxymethyl ethylene diamine. Purification was performed according to the manufacturer's instruction. If a Tris-based buffer was needed in subsequent steps, then all buffers after the first wash were replaced by Tris-based buffers. These columns are good for fast purifications. The Histidine-tagged PrepEase Protein Purification columns MIDI (Affymetrix) were used to purify 50-250 ml supernatant as the maximum binding capacity of His-tagged proteins is 2.5 mg.

3.2.2.3 Ni-NTA Spin Kit (QIAGEN)

Ni-NTA spin columns are especially good for small sample volumes. The PrepEase Ni-NTA uses a silica-based resin, but has a different chelator, nitrilotriacetic acid (NTA). Compared to the PrepEase Ni-NTA binds the proteins stronger and higher concentrations of imidazole are required to elute the proteins. The 300 µg binding capacity however, is the lowest of all three columns. The columns were used for supernatants below 50 ml according to the manufacturer's instruction.

3.2.3 Activation of NSPs by enterokinase cleavage

Active NSPs may exert a toxic effect to the host cells and are therefore expressed in an inactive zymogen form. To keep them inactive, an N-terminal artificial propeptide is fused to the mature protein via an enterokinase cleavage site (D_4K). The salt bridge between the N-terminus Ile^{26} and Asp^{194} is necessary for an active NSP and can only form upon removal by propeptide with the enterokinase. For optimal enterokinase activity the reaction was always performed in 20 mM Tris and 300 mM NaCl at neutral pH (pH 7.4). Two different enterokinases were used. When the enterokinase from New England Biolabs was used 2 mM $CaCl_2$ is added to the normal enterokinase buffer to gain the full activity. The target protein should have a concentration of 0.3 -1.0 mg/ml. The ratio target protein to enterokinase (2 µg/ml) was always 1:14000. After the addition of the enterokinase (NEB) the digest was incubated at 37°C for two hours. The enterokinase from Roche did not need the addition of $CaCl_2$. The target protein should have a concentration between 0.3 -1.0 mg/ml. The enterokinase is than added at a ratio of 1:40 and incubated for two hours at 37°C.

3.2.4 Spectrophotometric quantification of proteins

The amino acid tryptophan, and to some extent tyrosine and cystine bonds absorb UV-light at a wavelength λ= 280 nm. The number and extinction coefficient of these amino acid residues in each protein is therefore very important for protein quantification and expressed by the molar extinction coefficient (ε) [$M^{-1}cm^{-1}$]. After measuring the absorbance (A) the concentration (c) can be calculated using the Lambert-Beer law (**Eq. 1)**. The path length (l) is normally 1 cm when using standard cuvettes. The free program ProtParam Expasy (SIB Swiss Institute of Bioinformatics) was used to determine ε from the amino acid sequence.

Eq. 1

$$c=\frac{A}{\varepsilon * l}$$

c	concentration
A	absorbance
ε	molar extinction coefficient
l	pathway length

3.2.5 Quantification of proteins with bicinchoninic acid (BCA) assay

Peptide bonds in proteins reduce Cu^{2+}-ions to Cu^{+}-ions. Cu^{+} in turn forms a chelate complex with two BCA-molecules which absorbs at λ= 562 nm. BCA assay of Uptima was used according to the manufacturer's instructions.

3.2.6 Enzyme-linked immunosorbent assay (ELISA)

ELISAs are used to detect and quantify specific target proteins in complex solutions with the help of specific antibodies. There are direct and indirect "sandwich" ELISAs. In a sandwich ELISA a target specific antibody is coated on the plate to capture the desired protein from the sample. A second horseradish peroxidase (HRP) coupled antibody which is also directed against the specific protein is used for detection. The HRP oxidizes the substrate 2,2'-azino-bis(3-ethylbenzothiazoline-6-sulphonic acid) (ABTS) The product of this reaction absorbs at λ= 405 nm.

MIP-2 Standard ELISA Development Kit (Preprotech) was used according to the manufacturer's instruction, because MIP-2 does not have any tryptophanes, which are necessary for reliable quantification through absorbance.

3.2.7 Discontinuous gel electrophoresis

Similar to agarose gels, polyacrylamid gels are used to separate proteins by size and charge. Because proteins, unlike DNA, do not have a common charge, sodium dodecyl sulfate (SDS) is used to charge all proteins negatively. To avoid an influence of the protein structure on the separation, the proteins are denatured and disulfide bonds are reduced with β-mercaptoethanol. This method is called SDS polyacrylamide gel electrophoresis (SDS-PAGE) under reducing conditions.

Most of the time 15% Tris-glycine gels were employed, but for the separation of small fragments (5-10 kDa) 18% Tris-tricine SDS-polyacrylamide gels with 5% crosslinker were used. Gels were always poured between two glass plates with 1 mm spacer (Biorad). The resolving gel is always poured first and then overlayed with water to get an even edge. After the gel has completed the polymerization reaction, the stacking gel is poured and the combs for pockets are inserted. Tris-tricine gels were always run with different cathode and anode buffer (200 mM Tris-HCl, pH 8.8). The 10 x cathode buffer was purchased from Sigma-Aldrich (T1165).

15% Tris-tricine SDS gel

	stacking gel	**resolving gel**
H_2O	2.5 ml	-
40% acrylamide/bisacrylamide (29:1)	0.5 ml	-
40% acrylamide/bisacrylamide (19:1)	-	3.6 ml
3 M Tris-HCl, pH 8,45; 0,4% SDS	1 ml	2 ml
10% APS	16 µl	32 µl
TEMED	16 µl	12 µl
bromophenol blue	-	0,2% (w/v)

Tris-glycine running buffer

50 mM	Tris,
384 mM	glycine
0,2%	SDS
	pH 8.6

Tris-glycine SDS gel

	stacking gel	**resolving gel**
H_2O	9.4 ml	13.6 ml
40% acrylamide/bisacrylamide (37,5:1)	20 ml	3.32 ml
1 M Tris-HCl, pH 6,8	10 ml	-
1,5 M Tris-HCl, pH 8,8	-	2.56 ml
20% SDS	200 µl	100 µl
10% APS	400 µl	200 µl
TEMED	18 µl	16 µl
bromophenol blue	-	0,2% (w/v)

4x loading dye

200 mM	Tris-HCl, pH 6,8
10%	SDS
40%	glycerol
30%	β–mercaptoethanol
0,2%	bromophenol blue

3.2.8 Staining of protein gels

To stop diffusion of proteins from the gels after electrophoresis, a fixation buffer with high organic solvent content is used at low pH. These conditions cause the proteins to unfold and their exposed hydrophobic parts interact and mediate the formation of forming insoluble complexes.

3.2.9 Coomassie blue staining

Directly after the discontinous gel electrophoresis the gel was incubated in the staining solution at room temperature for 1 hour. Afterwards the gel was incubated in the destaining solution at room temperature until the gel was destained to satisfaction and the bands clearly visible.

Staining solution

0.25%	Coomassie Brilliant Blue R-250
45%	methanol
10%	acetic acid

Destaining solution:

45%	methanol
10%	acetic acid

3.2.10 Silver staining

The gel is first fixated at room temperature for an hour. After three washes of 20-min duration in 50% ethanol, the gel is incubated in a thiosulfate solution (0.2 g/l $Na_2S_2O_3x5H_2O$) for one minute. The gels are washed three times before and after putting the gel in the silver solution. A stop solution is added when the staining is satisfying. For long term storage keep the gel in 50% methanol.

Fixation solution

500 ml	methanol
120 ml	acetic acid
0, 5 ml	37% formaldehyde
	Fill up to 1 L with H_20

Silver staining solution

0,2 g	silver nitrate
75 µl	37% formaldehyde
	Fill up to 100 ml with H_20

Developing solution

60 g	sodium carbonate
4 mg	sodium sulfate
0.05 ml	37% formaldehyde
	Fill up to 1 L with H_20

Stop solution

500 ml	methanol
120 ml	acetic acid
	Fill up to 1 L with H_20

3.2.11 Western blot

After SDS-PAGE protein bands are blotted on a membrane. A vertical electrical field causes the proteins to migrate out of the gel onto the membrane. The membrane is made

out of polyvinylidene fluoride (PVDF), which binds protein via hydrophobic interactions. Before use the membrane has to be activated with 100% methanol. There are two different types of blotting: semi-dry and tank-blot.

While the gel and the membrane is totally immersed in buffer during tank blotting, the membrane and gel are only wetted with buffer and fixed between two graphit plates during semi dry blotting. It is very important to remove air bubbles between the membrane and gel, because proteins can't be transferred across air. The membrane was blocked with 5% (w/v) Non-Fat Dry Milk Blocker (Bio-Rad) in PBS-T at room temperature for one hour. The first antibody was incubated overnight at 4°C. Before and after incubation with the second antibody (room temperature, 1 hour) the membrane was washed three times with PBS-T for ten minutes. For the development WestPico (pierce) was used according to the manufacturer's instruction.

When more than one antibody was used for one membrane, the membrane is shortly washed with PBS-T after developing. Then the membrane is incubated in stripping buffer at room temperature for 30 minutes. Afterwards the membrane is washed thrice with PBS-T for 5 minutes to remove the stripping buffer. The membrane was then blocked with 5% (w/v) Non-Fat Dry Milk Blocker (Bio-Rad) at room temperature for 1 hour, before the new antibody was added.

Western transfer buffer

150 mM	glycine
35 mM	Tris
	pH 8.3

PBS-T

140 mM	NaCl
2.7 mM	KCl
3.2 mM	Na_2HPO_4 x 12 H_2O
1.5 mM	KH_2PO_4
0.05% (v/v)	Tween 20
	pH 7.4

Stripping buffer

200 mM	glycine
0.1% (w/v)	SDS
	pH 2.2

3.2.12 Activity assay

A typical substrate for activity measurements always features a short peptide sequence linked to a chromophor or fluorophor, which can be only detected after its release by proteolytic cleavage via absorbance or fluorescence measurement. All quantifications were performed in activity buffer at room temperature.

Activity buffer

50 mM	Tris-HCl, pH 7,4
150 mM	NaCl
0.01%	Tween 20

3.2.12.1 Absorbance

In this work p-nitroanilide (pNA) and thiobenzyl ester (SBzl) were the only chromophors used. Only when the amide bond between pNA and the C-teminus of the peptide is cleaved a change in the absorbance at 405 nm occurs. Therefore, there is only one possible cleavage site that results in a detectable signal. The cleavage of the thiobenzyl ester (1 mM) cannot be detected directly. To monitor the reaction at 405 nm, you add 5,5´-dithiobis-(2-nitrobenzoic acid) (DTNB; 0.5 mM), which is hydrolised to the 2-nitro-5-thiobenzoate anion in the presence of free thiols. The working concentration for pNA is 0.5 mM.

3.2.12.2 Fluorescence

Förster resonance energy transfer (FRET)-substrate consist always of a fluorescence and quencher group. The fluorochrome, 2-aminobenzoyl (Abz) or 4-methylcoumarinyl-7-amide (Mca) is linked to a quencher, 2,4-dinitrophenyl (Dnp) or N-(2,4-dinitrophenyl)ethylenediamine (EDDnp) via a short peptide. Once the peptide is cleaved internally in the fluorochrome and quencher groups are separated and the fluorescence can be measured (excitation: 320 nm, emission: 405 nm). In this case the cleavage is not clearly restricted to a single peptide bond within the given peptide sequence.

The fluorochrome 7-amido-4-methylcoumarin (AMC) is attached to the C-terminal site of a peptide. Only when this amide bond is cleaved, 7-amino-4 methylcoumarin is released, which can then be detected (excitation: 350 nm, emission: 450 nm). This means that only one possible cleavage site exists.

3.2.13 Immunoprecipitation of MIP-2

PMNs were stimulated with 10 ng/ml TNF-α (Biosource; PMC3016), 200 ng/ml phorbol myristate acetate (PMA) (Sigma; P1585) and 40 ng murine MIP-2 (Preprotech, 250-15) and incubated at 37°C for four hours. The suspension was centrifuged (600 g, 15 min) and the supernatant take for further analysis. After the addition of 10 µg anti-MIP-2 anitbody (Preprotech, 500-P130) to the supernatant, the reaction was incubated at 4°C over night. To purify the MIP-2-antibody complexes 30 µl of pre-washed dynabeads Protein G (life technologies, 10004D) were added and incubated at 4°C for four hours. The beads were washed twice with PBS-T and then boiled in reducing sample buffer for SDS-PAGE.

3.2.14 Preparation of PMNs lysate

The cells were resuspended in RIPA buffer ($3*10^4$ cells/µl) to lyse them. After incubation on ice for 15 min, the cells were put thrice into an ultrasonic bath for 5 min. In between the sonification, the cells are cooled on ice for 5 min. In the end the cells are centrifuged at 20000 g for 5 min to remove cell debris and DNA.

RIPA buffer

50 mM	Tris-HCl pH 8.0
150 mM	NaCl
0.5 M	EDTA
1 mM	PMSF
0.5% (w/v)	Deoxycholic acid
0.1% (w/v)	SDS
0.5% (v/v)	Nonodet P-40

3.3 Kinetic methods

3.3.1 Burst titration

During burst titration the substrate reacts in a suicide mechanism with the protease molecule, thereby inhibiting the protease in the process. Each substrate molecule reacts only with one protease molecule. Trypsin was titrated with p-nitrophenyl-p-guanidinobenzoate. The amount of p-nitrophenol (ε= 8800 $M^{-1}cm^{-1}$) released equals the amount of trypsin and can be calculated by measuring the absorbance at 410 nm.

3.3.2 Titration

Titrated trypsin was used to determine the amount of active α1PI, which in turn was taken to determine concentration of sc- and tc-mNE. To fulfill the requirements, the concentration of the protease had to be at least 100-times higher than the dissociation constant K_i of the protease and α1PI. Trypsin was always used at 200 nM (K_i = 0,63 nM, (Hopkins et al., 1993)). K_i from mNE is not yet known, but judging from the K_i of hNE and antitrypsin (K_i = 330 pM, (Beatty et al., 1984), I used a concentration of 5-10 µM for mNE. In all experiments, inhibitor concentration was varied, while the protease concentration was kept constant. Remaining protease concentration activity was measured after incubation for one hour at 37°C. Plotting the inhibitor concentration against the relative velocity renders a linear regression. The intersection with the x- axis can be obtained by extrapolation. The x-axis intercept indicates the concentration of the protease in the sample.

3.3.3 K_M and k_{cat}

The reaction of an enzyme E converting a substrate S to a product P can be described with equation 2 (Berg et al., 2003). The reaction is divided into two parts. First the substrate (S) and enzyme (E) form a reversible complex (ES), then the substrate is cleaved, which leads to the product (P).

Eq. 2

$$E + S \underset{k_{-1}}{\overset{k_1}{\rightleftharpoons}} ES \xrightarrow{k_2} E + P$$

E	enzyme
S	substrate
ES	enzyme-substrate complex
P	product

This reaction is described by the Michaelis-Menten equation (**Eq. 4**) (Berg et al., 2003). The Michaelis Menten (K_M) concentration is the concentration of the substrate at which the half-maximum velocity is reached. Together with the catalytic constant (k_{cat}) this is an important parameter to judge, how well a substrate fits the enzyme. When all enzymes are binding a substrate then k_{cat} can be calculated with **Eq. 3**: $k_{cat}=v_{max}/[E]$. [E] is the total enzyme concentration.

Eq. 4

$$v = \frac{v_{max}*[S]}{K_M+[S]}$$

v	velocity
v_{max}	maximum velocity
[S]	concentration of substrate at any time
K_M	Michaelis-Menten constant

In this study we always used 23 nM sc-mNE or 231 nM tc-mNE respectively for the determination of K_M. Substrate concentrations [S] were varied from 1-80 µM and plotted against the reaction rate (v) and fitted to the Michaelis-Menten equation using GraphPad Prism (GraphPad Software, Inc., La Jolla).

3.3.4 Competitive inhibition

In this kind of inhibition, the inhibitor competes with the substrate for the enzyme. So enhancing the substrate concentration influences the inhibition. The maximum velocity v_{max} can still be reached, given [S] is high enough, but K_M increases with higher inhibition concentration [I] (Berg et al., 2003). For competitive inhibitors the inhibitor constant K_i is the same as the dissociation constant K_D.

Eq. 5

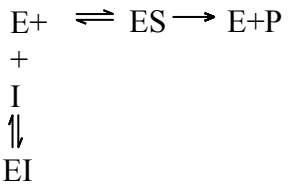

E	enzyme
S	substrate
ES	enzyme-substrate complex, reversible
P	product
I	inhibitor
EI	enzyme-inhibitor complex, reversible

The relation between [I] and K_M can be described as follows (Berg et al., 2003):

Eq. 6

$$\frac{1}{v_0} = \frac{1}{v_{max}} + \frac{K_M}{v_{max}}\left(1 + \frac{[I]}{K_i}\right)\left(\frac{1}{[S]}\right)$$

v	velocity
v_{max}	maximum velocity
[S]	concentration of substrate at any time
K_M	Michaelis-Menten constant

Through different Michaelis-Menten curves and by varying inhibitor concentrations, one can calculate the inhibitor constant K_i.

3.3.5 Irreversible inhibition

An irreversible inhibitor first forms a reversible complex with the enzyme. As soon as the protease has cleaved the inhibitor, an irreversible complex is formed. The substrate concentration only influences the first reaction, but not the second. So higher substrate concentrations can delay the inhibition but cannot completely abrogate it as seen in competitive inhibition. In an irreversible inhibition V_{max} is changed, while K_M remains the same.

Eq. 7

$$E + I \underset{k_{-1}}{\overset{k_1}{\rightleftharpoons}} EI \xrightarrow{k_2} EI^*$$

E	enzyme
I	inhibitor
EI	reversible enzyme-inhibitor complex
EI*	irreversible enzyme-inhibitor complex

The reaction of α1PI and NE is too fast for conventional K_i determination. Therefore different concentrations (50-300 nM) of inhibitor were mixed with 100 µM substrate before adding the protease. The resulting curve can be described with equation 7 (Duranton and Bieth, 2003).

Eq. 8

$$[P] = \left(\frac{v_0}{k_{obs}}\right)\left(1 - e^{-k_{obs}t}\right)$$

v_0	velocity at time point zero
k_{obs}	observed rate constant
[P]	concentration of product at any time
$K_{i(app)}$	apparent inhibitor constant
k_2	first-order rate constant
$[I]_o$	concentration of inhibitor at time point zero

The substrate concentration was five times higher than K_M, so no substrate depletion occurred. To ensure that inhibitor concentration was not significantly changed at least five times higher inhibitor than enzyme concentration was used. Fitting the curves in GraphPad Prism to equation 7 provided us with the observed rate constant (k_{obs}). Then k_{obs} values were plotted against inhibitor concentration and the resulting curve was fitted to following equation 8 and 9 (Duranton and Bieth, 2003).

Eq. 9

$$k_{obs} = \frac{k_2[I]_0}{[I]_0 + K_{i(app)}}$$

k_{obs}	observed rate constant
$K_{i(app)}$	apparent inhibitor constant
k_2	first-order rate constant
$[I]_o$	concentration of inhibitor at time point zero

Eq. 10

$$K_{i(app)} = K_i^*\left(1 + \frac{[S]_0}{K_M}\right)$$

$K_{i(app)}$	apparent inhibitor concentration
[S]	concentration of substrate at any time
K_i^*	equilibrium dissociation constant
K_M	Michaelis-Menten constant

EI* does not accumulate significantly at inhibitor concentration well below the equilibrium dissociation constant K_i*(K_i*= k_{-1}/k_1) . In this case the inhibition behaves like a simple bimolecular reaction (E + I → EI) (Duranton and Bieth, 2003) and equation 10 applies. This reaction is governed by a second-order association constant k_{ass}.

Eq. 10

$$k_{ass} = \frac{k_2}{K_i^*}$$

k_{ass}	second-order association constant
k_2	first-order rate constant
K_i^*	equilibrium dissociation constant

3.4 Cell biological methods

3.4.1 Cell culture

Expression was done in HEK-EBNA cell lines. This cell line is derived from primary human embryonic kidney cells that were transformed with adenovirus type 5. In addition, this cell lines has a codon optimized fusion protein EBNA1, which consists of a truncated nuclear protein of the Epstein-Barr virus EBNA1c and a protein from the Herpes Simplex virus VP16. EBNA1 enables the replication of plasmids that possess an oriP in mammalian cells. For expression the pTT5 expression system was used.
HEK 293 EBNA cells were cultured in serum free media (Gibco® FreeStyle™ 293 Expression Medium, (Life technologies) to reduce the amount of undesired proteins. Foam reducing agent Pluronic F-68 (0,1%) and geniticin selective antibiotic (G418 sulfate, 25 µg/ml) were also added to the medium.

3.4.2 Transfection

The proteins were expressed in the HEK 293 EBNA 1 cell line. The cells were cultured in FreestyleTM 293 Expression Medium (Invitrogen) with 0.1% (v/v) Pluronic® F-68 and 25 µg/ml Geneticin® G418. Cells are diluted to a concentration of $1*10^6$ cells per ml before transfection. The amount of DNA used for a transfection is proportional to the amount of transfected cells (for x ml cells, x µg DNA and 2 x µl polyethylenimine (PEI) is used). First DNA and PEI (1 mg/ml) are diluted separately in an equal volume of OptiPro (Life technologies) (70 µl OptiPro per one ml cell suspension). After mixing the OptiPro-PEI and OptiPro-DNA solutions together complexes are forming at room temperature within the next 20 min. The transfection solution is than added drop by drop to the cells. To stabilize the recombinant proteins in the supernatant 0.5% (v/v) Bacto TC Lactalbumin Hydrolysate (BD Biosciences) is added after 24 hours.

3.4.3 Isolation of granulocytes

3.4.3.1 Human granulocytes

Human granulocytes were isolated from whole blood on a discontinuous Ficoll gradient. To avoid coagulation of the blood, ethylenediaminetetraacetic acid (EDTA) covered syringes were used. EDTA-blood was diluted to a final volume of 40 ml with PBS and carefully underlayed with 10 ml Pancoll (δ=1,077 g/L). The high density of Pancoll ensures that only erythrocytes and granulocytes can cross through this layer during centrifugation (500 g, at RT, without brake for 30 min). After removing the supernatant containing PBMCs the erythrocytes are removed in two steps. First, we used dextran sedimentation for 30 minutes (1% dextran), to roughly separate the cells, as erythrocytes settle down faster. The supernatant is then centrifuged (1200 rpm, at RT for 15 min). To remove the remaining erythrocytes, the pellet is resuspended in 5 ml 0.2% NaCl solution for one minute, before 5 ml of 1.6% NaCl solution is added and everything is incubated again for a minute. The cell suspension is filled with PBS to 50ml and then centrifuged (1350 rpm, at RT for 5 min). A washing step with PBS follows (centrifuge 1350 rpm at 4°C, for 5 min). If necessary, the lysis can be repeated.

3.4.3.2 Murine granulocytes

The small size of a mouse and the corresponding small blood volume makes the isolation of murine PMNs (mPMNs) difficult. Better sources for mPMNs are bone marrow cells. Both femurs are flushed with PBS and the suspension centrifuged at 1200 rpm for 5 min. Cells were resuspended in 10 ml PBS and send through a cell strainer (BD biosciences). On the bottom of the discontinuous gradient is a 62% percoll solution (5.69 ml 10x HBSS + 9.32 ml percoll) and on top is the cell suspension. After centrifugation (30 min, 300 g, RT, without brake) the granulocytes and erythrocytes are in the cell pellet, while the PBMCs are left in the supernatant. The supernatant is carefully removed and a hypotonic lysis performed by resuspension of the cells in lysis buffer (9 ml 0.8%. NH_4Cl, 1 ml Tris-HCl pH 7,4). The cells are finally washed with PBS.

3.4.4 Identification of sc- and tc-NE in biological samples

Identification of human NE in human samples was done in two steps. The lysate of $3*10^6$ hPMNs (100 µl lysate), was inhibited with 20 nmol biotinylated NE-specific AAPV-chloromethyl ketone inhibitor (CMK) at 37°C for 30 min. The inhibitor reacts covalently

with NE. Then 4,4 µg anti-hNE antibody (QED, Cat.No.12303) was added and incubated overnight at 4°C. HNE-antibody complexes were captured with Protein G dynabeads (Life sciences). For analysis on a SDS-PAGE the beads were boiled at 95°C in reducing sample buffer for 5 min. Because of the biotin, the inhibited hNE could be detected with HRP-coupled streptavidin after SDS-PAGE. In murine samples mNE could be detected directly by western blot analysis, using an anti-hNE antibody (Abcam, Cat.No. ab68672) that cross reacts with mNE.

3.4.5 Chemotaxis assay

For a comparison of two chemokines the under-agarose-assay is the method of choice, because it allows a direct comparison of different chemokines in one experiment. An agarose layer is pured into a 35 mm dish. Holes with a distance between 2-4 mm are punched into the agarose layer for cells and chemokines. The dishes are incubated at 37°C and 5% CO_2 prior to the experiment. The cells are placed between the two chemokine reservoirs. In each experiment 7 µl of 0.1 mg/ml chemokine were put into a well and 7 µl of PMNs suspension (2.4 *10^7 cells/ml). The experiment has to be done at 37°C and in an atmosphere of 5% CO_2, because the agarose is buffered with bicarbonate. The cells can sense the chemokine gradient and start to wander under the agarose. This can be monitored with an optical microscope (20 x magnifications) and after 4-6 hours a picture is taken.

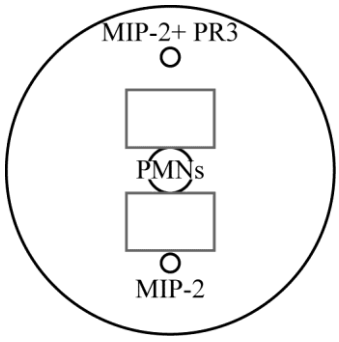

Fig 3.1: Under agarose assay In an agarose layer of a petri dish with 35 mm diameter holes for the PMNs and chemokines are punched. After the PMNs and the chemokines are filled in, the PMNs start crawling between the agarose layer and the bottom of the petri dish towards the chemokine. A picture with an optical microscope is taken and the cells are counted. The grey boxes mark the fields in which the cells are counted.

Agarose layer

5 ml	2 x HBSS (Gibco®, life sciences)
10 ml	RPMI + 20%FCS (Gibco®, life sciences)
0.2 g	Agarose LE (Biozym)
10 ml	H_2O

3.4.6 Flow cytometry

The cell suspension is focused in a liquid stream that only one cell at a time passes the laser beam. By means of light scatter, density and size of a cell can be determined. Expression of different markers can be identified by staining the cells with fluorescently labeled antibodies.

For each staining $1*10^5$ cells were used. The first antibody is diluted to a concentration of 2 µg/ml in PBS + 1% BSA and incubated at 4°C for 30 min. After three washes the cells with PBS the second antibody (2.5 µg/ml) was added to the cells and incubated at 4°C in the dark for 30 min. Cells were washed thrice again with PBS. Propidium iodide is added in the last washing step before analysis. At last cells were resuspended in 200 µl PBS.

Phosphate buffered saline (PBS)

136,89 mM	NaCl
2,68 mM	KCl
9,47 mM	Na_2HPO_4
1,76 mM	KH_2PO_4

4 Results

4.1 NSP regulate inflammation by processing of chemokines

4.1.1 N-terminal processing of MIP-2 by NE and PR3 in-vitro

4.1.1.1 Production of recombinant mPR3 and mNE

Murine PR3 and NE (mPR3 and mNE) were expressed in HEK293 EBNA cells using the pTT5 expression vector. As secretion of the proteases in the supernatant was desired, an N-terminal Igκ-signal peptide was added (**Fig 4.1 A**). Using a C-terminal His-tag, the

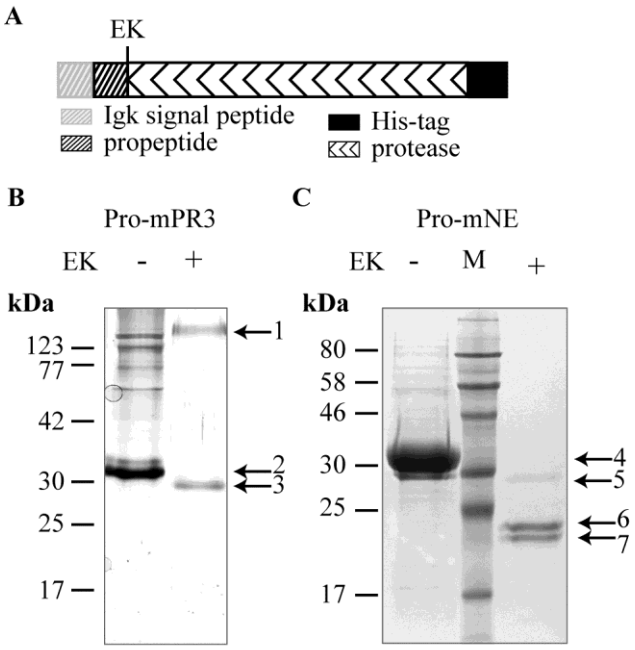

Fig 4.1: Production of recombinant mPR3 and mNE. (**A**) Both proteases (black, loosely hatched bar) were expressed in HEK293 cells with a C-terminal His-tag (black box) for purification. To prevent premature activation of these proteases, which would be toxic to the cells, an artificial propeptide (black, tightly hatched box) was added to the N-terminus. For removal of the propeptide an enterokinase (EK) cleavage site (vertical line, labeled EK) was inserted before the mature N-terminus of the NSPs. The exact sequence can be found in the appendix (**8.2.1** and **8.2.2**). (**B**) 600 ng pro-mPR3 before (left lane) and after (right lane) the addition of enterokinase, were compared on a silver stained gel. Although pro-mPR3 (band 2) was purified still some unknown proteins can be seen. Besides mature mPR3 (band 3) EK was detected (band 1) as EK has not been removed. (**C**) Five µg purified pro-mNE (band 4) before enterokinase was added were loaded on the left lane of the Coomassie stained gel. Three µg of mNE after EK digest and removal of EK were loaded on the right lane. The middle lane contains the prestained protein marker (NEB, P7708). In addition to the mature mNE (band 5) two smaller bands appeared (band 6,7). These bands are fragments of mNE and will be discussed later. Both gels were 15% SDS gels.

NSPs were purified with Ni-columns from the supernatant. Depending on the amount of supernatant different columns were used (see **chapter 3.2.2**). To protect the cells from the toxicity of the NSPs an artificial propeptide followed by an enterokinase cleavage site (DDDDK) keeps the protease inactive. Just like natural occurring zymogens, the artificial propeptide prevents the formation of the active conformation, the opening of the S1 pocket and generation of the oxyanion hole. Purification of NSPs from the supernatant yielded very clean fractions (**Fig 4.1 B, C**). The removal of the propeptide with enterokinase results in a size shift that is visible in a reducing 15% SDS-PAGE. The conversion of the zymogens was successful and complete, but for mNE I had three bands instead of one band were observed after the conversion. Band 1 is the mature intact form of mNE. The two lower bands 2, 3 are products of the self-cleavage of mNE as will be shown and discussed in detail later (4.2).

4.1.1.2 N-terminal processing of MIP-2 by neutrophil proteases

Murine MIP-2 with a concentration of 0.2 mg/ml (Preprotech) (mMIP-2) was incubated with either recombinant mPR3 or mNE (19 µg/ml) at 37°C for one hour in PBS. In the core facility of the MPI Biochemistry, Elisabeth Weyher examined the mixture using mass spectrometry analysis. Both mPR3 and mNE were able to cleave mMIP-2 after alanine at position four (**Fig 4.2 A**), which is similar to the cleavage site of hPR3 in human. As previously mentioned, processing of human IL-8 by hPR3 as well as by MMP-8 and MMP-9, enhances the chemotactic ability of IL-8 (Mortier et al., 2008; Padrines et al., 1994). MMP-12, which is found predominantly in macrophages, destroys the ELR-motif of hIL-8, which is essential for its CXCR2 binding capacity. This results in the inactivation of human IL-8. Given that hIL-8 can also be processed by MMPs, I used the fluorescence substrate Abz-GAVVASELR-Y(NO2)-D that features the N-terminal sequence of MIP-2 to test processing of mMIP-2 by other endoproteases of PMNs (**Fig 4.2 B**). Cleavage at any position of the peptide results in the generation of a fluorescence signal. The negative control consists only of substrate and buffer, while hNE was added as a positive control. As expected, PMN lysate from wt mice was able to cleave the substrate, because it contains mPR3 and mNE. PMN lysate from PR3/NE deficient mice was no longer able to generate a signal, thus the only endoproteases capable of processing mMIP-2 in neutrophils are mPR3 and mNE.

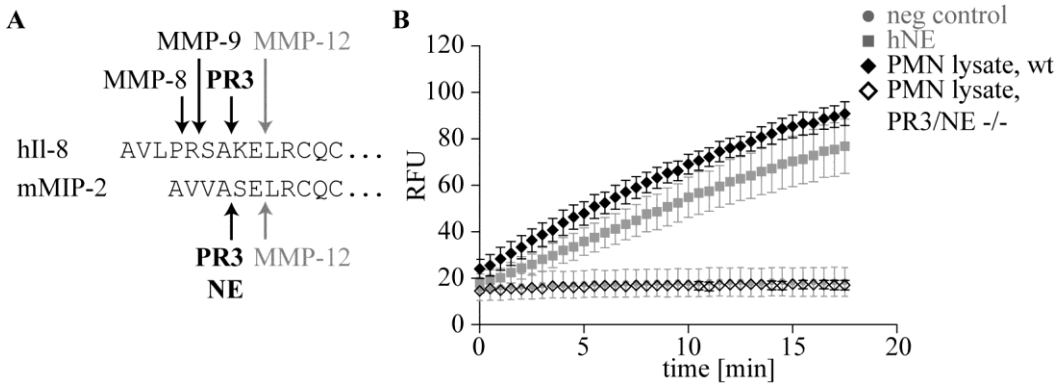

Fig 4.2: mNE and mPR3 are the only endoproteases processing MIP-2. (**A**) Chemotactic property of IL-8 is enhanced after the processing by MMP-8, MMP-9 and hPR3 *in-vitro*. By contrast, cleavage of MMP-12 inactivates hIL-8. I incubated mMIP-2 (0.2 mg/ml) with mPR3 or mNE (19 µg/ml) and gave the digest for mass spectrometry analysis to E. Wehyer (MPI Biochemistry). A cleavage site at Ala^4 was found, which is comparable to the cleavage site where hPR3 processes hIL-8. (**B**) A substrate covering the N-terminal sequence of mMIP-2 (Abz-GAVVASELR-Y(NO2)-D) was incubated with the lysate of from $1.5*10^6$ wt (filled, black squares) and PR3/NE deficient mPMNs (hollowed, black squares). Once the substrate is cleaved the quencher and fluorescent groups are separated, the fluorescence was measured (excitation: 320 nm, emission: 405 nm). Only wt (black squares) but not PR3/NE deficient (white squares) mPMNs were able to cleave the substrate, meaning other proteases of mPMNs were not able to cleave the N-terminal sequence of mMIP-2. The negative control (grey dots) consisted of substrate alone. For a positive control (grey squares) hNE was added to the substrate. Data (mean ± SD) are representative of 3 independent experiments each conducted in triplicate. The y-axis shows the fluorescence in relative fluorescence units (RFU).

To simulate a more in vivo-like situation, I isolated mPMNs from the bone marrow and stimulated them with TNF-α. Then I added MIP-2 and incubated this at 37°C for 4 hours. After an immunoprecipitation with anti-MIP-2 antibodies (Preprotech), I blotted the purified MIP-2 on a membrane for Edman sequencing. I was able to detect MIP-2(5-73) only with wt, but not with PR3/NE deficient mPMNs. The experiment was repeated thrice.

4.1.2 Chemotactic properties of MIP-2

4.1.2.1 Comparison of processed and intact mMIP-2

As already mentioned, PR3 processed hIL-8 is a more chemotactic form of hIL-8, so processed mMIP-2 might also change its chemotactic properties. The under-agarose-assay enabled me to compare unprocessed and processed mMIP-2 in one experiment. In a agarose layer holes were punched for the cells and chemokines. Between the chemokines

(7 µl with the concentration 0.2 mg/ml) 7 µl of 2.4*10^7 mPMNs were placed. After 4-6 hours a pictures were taken with an optical microscope (20 x magnifications) and the migrated cells were counted. The cell count was very heterogenous from experiment to experiment with 113-247 cells migrated mPMNs as the highest cell numbers. For better comparison cell count was normalized, with the highest cell count set to 100%. Unaltered mMIP-2 (MIP-2(1-73)), a mixture of mPR3 and mMIP-2 and PR3 alone were tested at the same time during one experiment (**Fig 4.3 A**). Almost none mPMNs migrated towards the negative control, mPR3, because mPR3 itself is not chemotactic (8%) (**Fig 4.3 B**). A moderate amount of cells (20%) crawled towards mMIP-2(1-73), while five times more PMNs responded to processed MIP-2 (MIP-2(5-73)). Murine MIP-2 that was processed by mPR3 is therefore clearly more chemotactic than intact MIP-2(1-73).

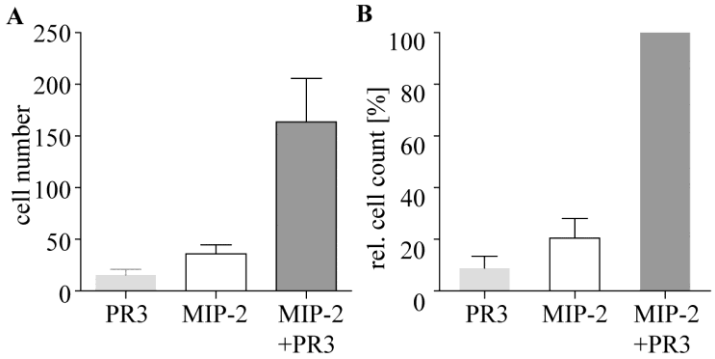

Fig 4.3: Processing of MIP-2 enhances its chemotactic activity. For the comparison of chemokines, 7 µl mPMNs (2.4*10^7 cells/ml) are placed between the chemokines (0.2 mg/ml) into holes in an agarose layer. The mPMNs can sense the chemokine gradient and start to crawl under the agarose towards the chemokine source. Using an optical microscope the migrated cells are counted. (**A**) The total cell count for mPR3 (light grey bar), intact MIP-2 (white bar) and processed MIP-2 (dark grey bar) were compared to each other. (**B**) As the cell number of migrated cells varied much between the experiments (113-247 PMNs for MIP-2+PR3), I normalized the cell count to the highest value, which was set to 100%. Processed MIP-2 attracted five times more mPMNs than intact MIP-2. Data (mean ± SD) are representative of 3 independent experiments.

4.1.2.2 Production of processed and intact MIP-2

Only MIP-2(1-73) is commercial available at present. Therefore it was necessary to express both forms of mMIP-2 in our lab for further experiments. As described for NSPs, both mMIP-2 forms were expressed in HEK293 EBNA cells. The constructs consisted of an Igκ-signal peptide and a C-terminal his-tag (**Fig 4.4 A**). I was able to express and purify clean MIP-2(5-73) with a correct N-terminus (**Fig 4.4 B**), verified by Reinhard

Mentele (Core facility of MPI of biochemistry) via Edman Sequencing. Expression of full length MIP-2(1-73) without a propeptide was unsuccessful, as 30% of MIP-2(1-73) was shortened by one amino acid residue at the N-terminus. To protect the N-terminus of the MIP-2(1-73) against exopeptidases, a small propeptide with cleavage site for removal by enterokinase was added N-terminally to MIP-2(1-73). In order to apply equal treatment to both forms, I also tried to use the same propeptide with MIP-2(5-73). Unfortunately, the propeptide of MIP-2(5-73) could not be removed by enterokinase. This is the reason why I expressed MIP-2(5-73) without propeptide, while MIP-2(1-73) was expressed with a propeptide. I purified both forms of MIP-2 using either PrepEase MIDI columns or HisTrap™ HP columns, depending on the amount of supernatant, and was able to get clean preparations of MIP-2 (**B, C**). Successful conversion of pro_MIP-2(1-73) with enterokinase was analyzed by SDS-PAGE and was demonstrated by Edman sequencing in the Core facility of the MPI Biochemistry (Reinhard Mentele).

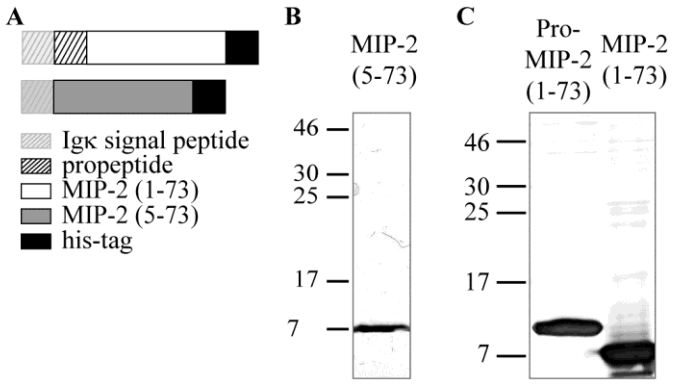

Fig 4.4: Production of processed and intact MIP-2. (**A**) The pTT5/HEK293 expression system was used to produce two MIP-2 variants. Both constructs have a C-terminal his-tag (black bar) for purification. MIP-2(1-73) (white bar) has an additional propeptide (black, hatched bar) to protect it against exopeptidases from HEK293 cells. The propeptide ended with an enterokinase cleavage site, so the propetide could be removed precisely after purification. The sequence is listed in the appendix (**8.2.3** and **8.2.4**) (**B**) Purified MIP-2(5-73) (400 ng) was separated on a 15% SDS gel and stained with silver. (**C**) The conversion of purified pro-MIP-2(1-73) by enterokinase was checked after SDS-PAGE and silver staining. 4.5 µg of pro-MIP-2(1-73) before and after the digest was loaded.

4.1.2.3 CXCR2 internalization after stimulation with MIP-2

It is still unclear why MIP-2(5-73) is more chemotactic than MIP-2(1-73). One reason is the different receptor binding capabilities of the two MIP-2 forms. I isolated mPMNs

from wt mice and incubated $1*10^5$ mPMNs with 200 ng MIP-2(1-73), 200 ng MIP-2(5-73) or PBS at 37°C for 5 min. After the mMIP-2 variants bound to CXCR2, the MIP-2-CXCR2 complex was internalized, thus the amount of receptors on the surface was reduced (**Fig 4.5 A**). Murine PMNs were then stained with anti-CXCR2 receptor antibody (2 µg/ml) to quantify the remaining CXCR2 on the surface. As this antibody is a rat antibody, a FITC-coupled anti-rat antibody (2.5 µg/ml) was used for visualization in FACS.

Before MIP-2 treatment, there were 38±1% CXCR2 positive PMNs (**Fig4.5B**). After incubation with MIP-2(1-73) and MIP-2(5-73), 9±4% and 10±3%, respectively, remained CXCR2 positive. In each experiment 10000 PMNs per population were counted. The data are mean ± SEM of three independent experiments.

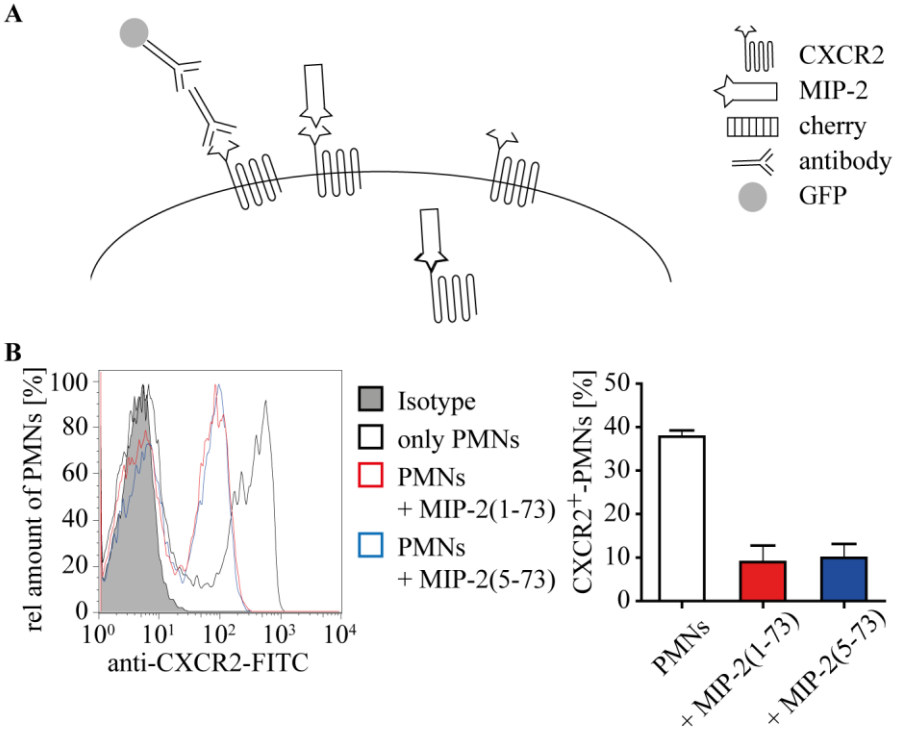

Fig 4.5: CXCR2 internalization after stimulation with MIP-2. (**A**) $1*10^5$ Murine PMNs, isolated from the bone marrow, were first incubated with 200 ng MIP-2 or PBS at 37°C for 5 min. After binding of MIP-2, receptors were internalized and therefore disappeared from the surface. Immediately after the incubation PMNs were stained with anti-CXCR2 (2 µg/ml) to detect the remaining CXCR2 (second antibody: FITC-coupled anti-rat; 2.5 µg/ml). (**B**) The $CXCR2^+$-PMNs were counted after exposure to MIP-2(1-73) (red) and MIP-2(5-73) (blue) and compared to unstimulated PMNs (black). The left panel shows an example of such an experiment. The right panel shows a summary of all experiments. Both MIP-2 variants were able to induce receptor internalization. No significant difference could be discerned. Data shown are mean ± SEM from all experiments with n=3 and always 10000 cells were counted for each staining.

4.1.3 Further MIP-2 variants

4.1.3.1 Production of further MIP-2 variants

I produced fusion proteins between MIP-2 and two different fluorescence proteins, cherry and ruby, to visualize mMIP-2 processing *in-vitro* and *in-vivo* (**Fig 4.6 A**). As described above, constructs before, I expressed both fusion proteins in HEK293 EBNA cells by using an Igκ-signal peptide for secretion and a C-terminal his-tag for purification. In the first construct the fluorescence protein cherry was N-terminally fused to MIP-2(1-73) (Ch_MIP-2). Since the N-terminus is very important for chemotactic activity, I also made a construct in which the fluorescence protein ruby was inserted between MIP-2(5-73) and its his-tag (MIP-2_Ru) at the C-terminus. Both proteins were well expressed in HEK293 EBNA cells and could be isolated from the supernatant in highly pure form using

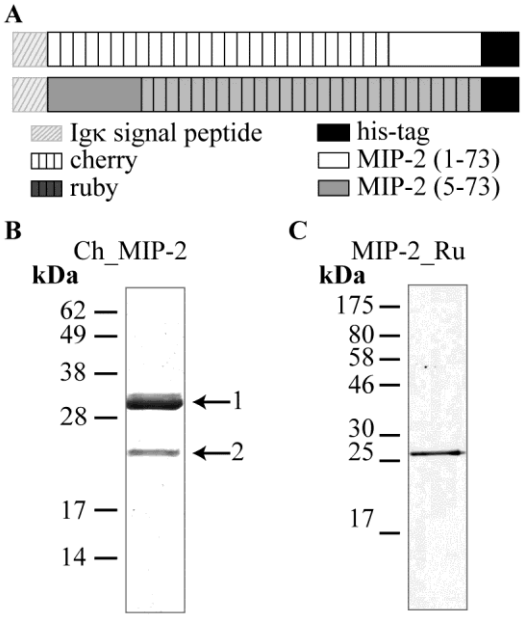

Fig 4.6: Production of further MIP-2 variants. (**A**) As with the proteins described above, the pTT5/HEK293 expression system was used for recombinant production. Both MIP-2 constructs have a C-terminal his-tag (black bar) for purification and an Igκ-signal peptide (grey, hatched bar) for secretion. In the Ch_MIP-2(1-73) construct, the fluorescence protein cherry (white, hatched bar) has been placed N-terminal to MIP-2(1-73) (white bar), while for the MIP-2_Ru construct the fluorescence protein ruby (dark grey, hatched bar) has been C-terminally positioned to MIP-2(5-73) (dark grey bar). The sequence is listed in the appendix (**8.2.5** and **8.2.6**) (**B**) 3.3 µg purified Ch_MIP-2 (band 1) was run on a 15% SDS polyacrylamide gel and stained with Coomassie. The additional lower band 2 is probably a degradation product resulting from an unwanted N-terminal cleavage in HEK-293. (**C**) MIP-2_Ru was purified and 560 ng was loaded on a 15% SDS gel that was stained with silver.

PrepEase MIDI columns or HisTrap™ HP columns (**B**). Purification of Ch_MIP-2 yielded a second band of approximately 26 kDa. Since this band still bound to the Ni-column and co-purified with Ch-MIP-2, I suggest, that Ch_MIP-2 was nicked and shortened within the N-terminal region by endoproteases from HEK293 cells.

4.1.3.2 Processing of Ch_MIP-2 with mNE or mPR3

Cherry was linked to MIP-2(1-73) and initial cleavage by mPR3 or mNE separated cherry (28 kDa) from MIP-2(5-73) (7 kDa) (**Fig 4.7** A, **B**). To see whether the cherry domain sterically blocks the cleavage site of mPR3 or mNE, I incubated 30 µg Ch_MIP-2 (**Fig 4.7**, band 1) with 1.67 µg active mPR3 or mNE and ran an SDS-PAGE to analyze the size shift. After 10,20,30,60 and 120 min aliquots containing 4 µg Ch_MIP-2 and 222 ng protease were taken and immediately boiled with reducing sample buffer at 95°C. A band with the size of cherry appeared (**Fig 4.7**, band 2) after 10 minutes of incubation of Ch_MIP-2 with mNE. After 2 hours Ch_MIP-2 was completely cleaved and only cherry remained. MIP-2(5-73) was too small and was therefore not retained on this gel. The reaction with mPR3 was considerably slower, but still mPR3 was able to digest Ch_MIP-2 almost completely after 120 min.

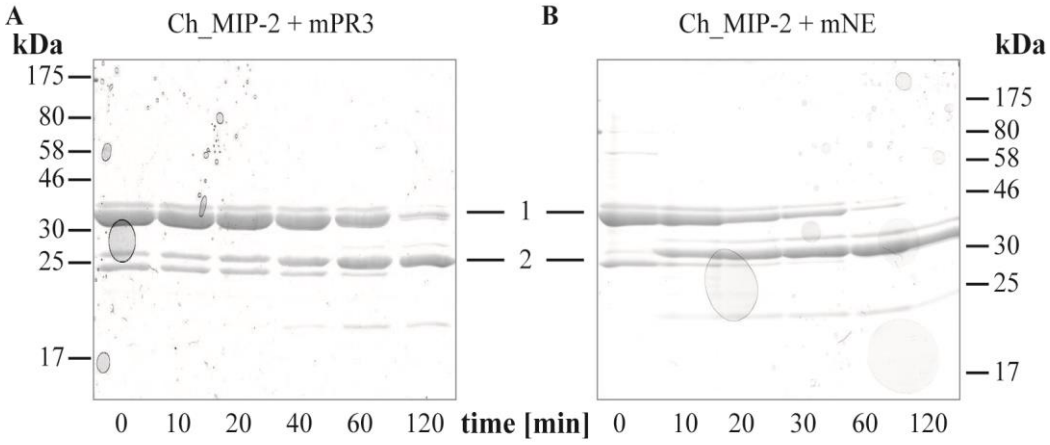

Fig 4.7: Processing of Ch_MIP-2 by mNE and mPR3. (**A**) For each experiment 1,67 µg mPR3 was incubated with 30 µg Ch_MIP-2 at 37° (ratio of 1:18). At every time point an aliquot was retrieved and immediately boiled at 95°C with sample buffer. Each lane contains 4 µg Ch_MIP-2 and 222 ng mPR3. Ch_MIP-2 has a size of 35 kDa big (band 1) and is split into cherry (28 kDa) and MIP-2(5-73) (7 kDa) after cleavage. Only the bigger band of cherry (band 2) can be seen in this Coomassie-stained 15% SDS polyacrylamide gel. (**B**) The experiment from **A** was repeated with mNE instead of mPR3. 30 µg Ch_MIP-2 was incubated with 1.67 µg mNE and aliquots containing 4 µg Ch_MIP-2 and 222 ng mNE were retrieved at different time points. The aliquots were loaded on a Coomassie-stained 15% SDS gel. Both mPR3 and mNE were able to cleave Ch_MIP-2 into cherry and MIP-2(5-73).

4.1.3.3 CXCR2 internalization after stimulation with MIP-2 variants

As already mentioned the N-terminal extension of MIP-2 by cherry may influence its chemotactic ability. To investigate this, Ch_MIP-2 and MIP-2_Ru, which have about the same size, were compared to each other with regard to CXCR2 internalization (**Fig 4.8**). I incubated and stained wt mPMNs as described in chapter **4.1.2.3**. Murine PMNs ($1*10^5$) were incubated with equal amounts of Ch_MIP-2 or MIP-2_Ru (860 ng) at 37°C for 5 minutes. Immediately afterwards the cells were cooled on ice and stained with anti-CXCR2 antibody (2 µg/ml). The second antibody, FITC-coupled anti-rat antibody was used at a concentration of 2.5 µg/ml. While 32±9% of wt mPMNs had a high CXCR2 expression, only 5±4% and 6±5% respectively, remained CXCR2 positive after incubation with either Ch_MIP-2 or MIP-2_Ru.

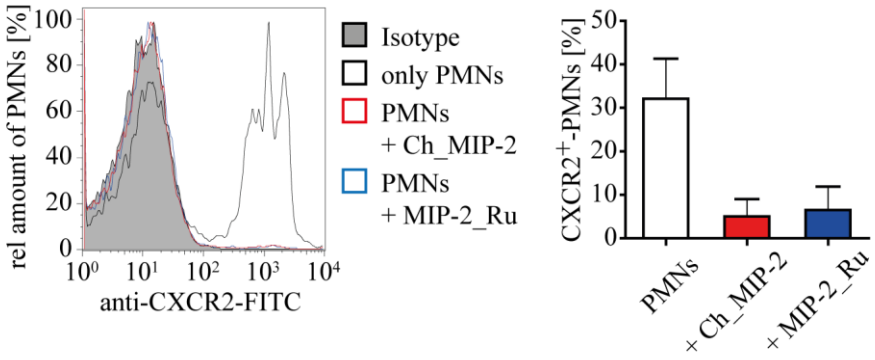

Fig 4.8: Internalization of CXCR2 after exposure to MIP-2 variants. Murine wt PMNs ($1*10^5$) from the bone marrow were incubated with 860 ng Ch-MIP-2 (red) or 860 ng MIP-2_Ru (blue) or PBS (black) at 37°C for 5 min, and then stained with anti-CXCR2 antibody (2 µg/ml). CXCR2 density was determined by flow cytometry. The left panel show an example of such an experiment. The right panel shows the summary of all experiments. Data shown are mean ± SEM from all experiments with n=2. Ch_MIP-2 and MIP-2_Ru reduced CXCR2 positive population from 32(±2)% to 5(±4)% and 6(±5)% respectively. There was no significant difference between CH-MIP-2's and MIP-2_Ru's ability to invoke CXCR2 internalization.

Since I expected Ch_MIP-2 to be inert, I repeated the experiments with PR3/NE deficient PMNs to exclude the activation of Ch_MIP-2 and MIP-2(1-73) to a more active form by mPR3 and mNE from wt PMNs (**Fig 4.9 A**).

The PR3/NE deficient mPMNs were incubated and stained as described above (**Fig 4.5** and **Fig 4.7**). It was more difficult to define clear populations of $CXCR2^+$ mPMNs (**Fig 4.9 B**). I set a gate, so 11.1±0.4% of wt mPMNs were CXCR2 positive. As expected, incubation with MIP-2_Ru decreased the amount of $CXCR2^+$-cells to 3.2±0.1%.

Interestingly, Ch_MIP-2 did not change the levels of CXCR2 on the surface. I also repeated the comparison between MIP-2(1-73) and MIP-2(5-73) (**Fig4.9 B**). There was

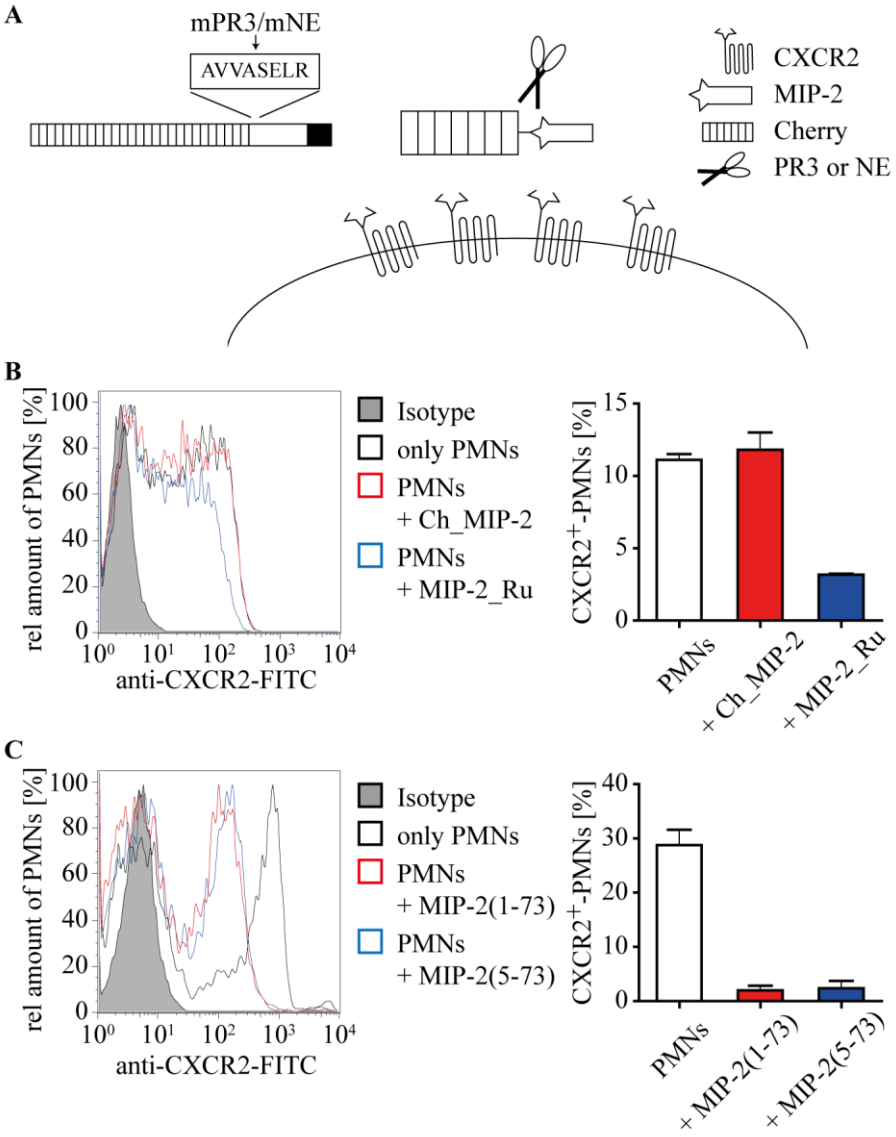

Fig 4.9: Different ability of Ch_MIP-2 and MIP-2_Ru to internalize CXCR2. (**A**) Wt mPMNs can use their own mPR3 and mNE to convert Ch-MIP-2 to its active form and wt mPMNs can therefore also convert MIP-2(1-73) to the more chemotactic form MIP-2(5-73). To avoid this, the experiment from **Fig 4.8** was repeated with PR3/NE deficient mPMNs. (**B**) Knockout PMNs ($1*10^5$) from the bone marrow were incubated at 37°C for 5 min with 860 ng Ch-MIP-2 (red) or MIP-2_Ru (blue). Cells treated only with PBS are depicted black. The PMNs were stained with 2 µg/ml anti-CXCR2 antibody (second antibody: FITC-coupled anti-rat antibody; 2.5 µg/ml). CXCR2 positive cells were counted and compared. Data shown is the mean ± SEM from all experiments with n=2. Only MIP-2_Ru but not Ch_MIP-2 was able to induce CXCR2 internalization in PR3/NE deficient mPMNs (**C)** PR3/NE deficient mPMNs were incubated with 200 ng MIP-2(1-73) (red) or MIP-2(5-73) (blue) before they were stained with anti-CXCR2 antibody as described above. Data shown is the mean ± SEM from all experiments with n=4. There was no significant difference between MIP-2(1-73) and MIP-2(5-73).

no significant difference between those two MIP-2 variants. Both decreased the population of $CXCR2^+$ cells from 31.3±0.5% to 4.2±2.8% (MIP-2(1-73)) or 3.4±2.0% (MIP-2(5-73).

4.1.4 Other chemokines as substrates

Based on the known N-terminal sequences of three other CXC ELR^+ chemokines, three fluorescence substrates were synthesized by EMC microcollections GmbH (**A**). After the cleavage of these substrates the fluorescence can be measured (excitation: 320 nm,

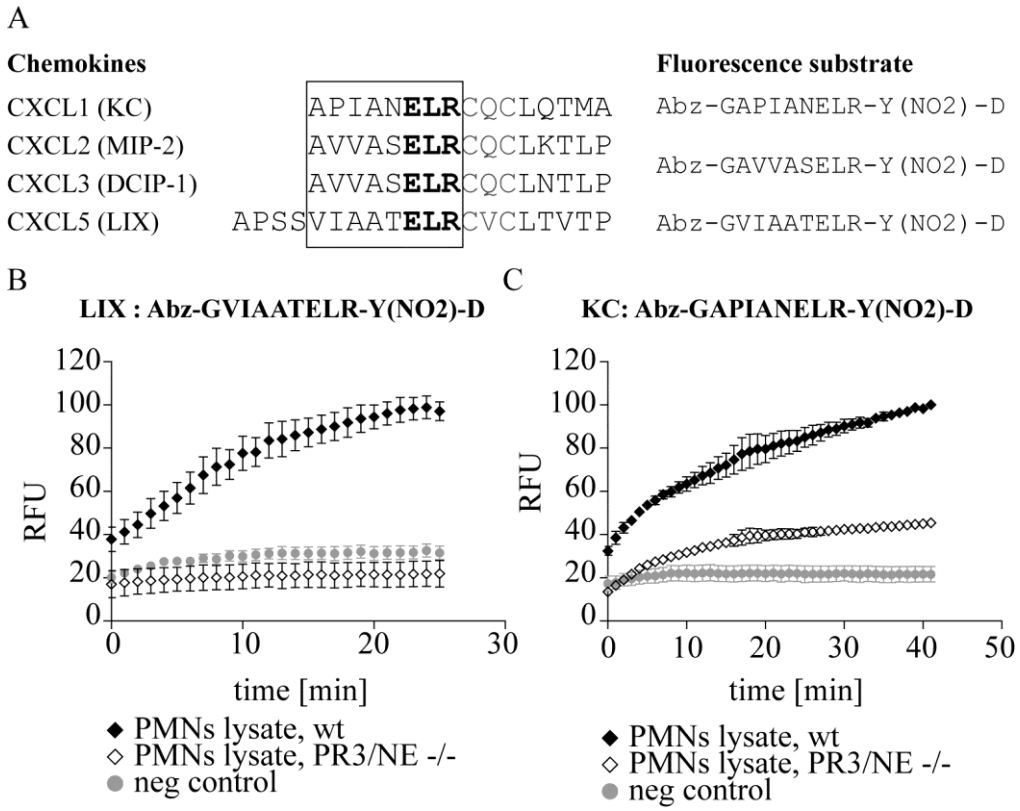

Fig 4.10: Processing of other chemokines by mNE or mPR3. (**A**) There are three other murine CXC ELR^+ chemokines that may also be processed by mPR3 and mNE. To answer this question, two additional FRET-substrates representing the N-terminus from the other chemokines were ordered. Cleavage of the substrates by mPR3 or mNE results in fluorescence that can be measured. (**B**) The LIX substrate Abz-GVIAATELR-Y(NO2)-D was incubated with lysates from $1.5*10^6$ wt (black squares) or PR3/NE deficient PMNs (white squares). The negative control was only substrate and buffer (grey dots). Data shown is the mean ± SEM of 3 independent experiments each conducted in triplicates. The LIX substrate is cleaved by the lysate of wt PMNs, but not by the lysate of PR3/NE-deficient PMNs. (**C**) The KC substrate Abz-GAPIANELR-Y(NO2)-D is incubated with lysates from $1.5*10^6$ wt (black squares) or PR3/NE deficient (white squeares) PMNs. The negative control was only substrate and buffer (grey dots). Data shown is the mean ± SEM of 3 independent experiments each conducted in triplicates. The KC-substrate is cleaved by lysate of wt and PR3/NE knockout lysate, although cleavage was more efficient with lysate of wt PMNs.

emission: 405 nm). The substrates were added to the lysates from 1.5*10^6 mPMNs at room temperature and the measurement was immediately started. The LIX substrate (Abz-GVIAATELR-Y(NO2)-D) showed a similar pattern as the MIP-2 substrate (Abz-GAVVASELR-Y(NO2)-D). It was cleaved by wt lysate, but not by the PR3/NE knockout lysate. By contrast, the KC substrate (Abz-GAPIANELR-Y(NO2)-D) could be cleaved by lysate of wt and PR3/NE-deficient PMNs, although the cleavage by double knockout lysate was diminished.

4.2 NE escapes inhibition by self-cleavage

4.2.1 Self-cleavage of NE

4.2.1.1 Identification of self-cleavage sites

After the removal of the propeptide of mNE with enterokinase, the molecular weight shift was routinely checked on a SDS-PAGE to ensure complete activation of mNE. In doing so it was discovered that in addition to the expected mature form of mNE two smaller bands appeared around 20 kDa. Edman sequencing revealed that both bands featured the N-terminal sequence of mNE. Thus, at some point during enterokinase treatment mNE must have been cleaved in the C-terminal region (**Fig 4.11 A**). After

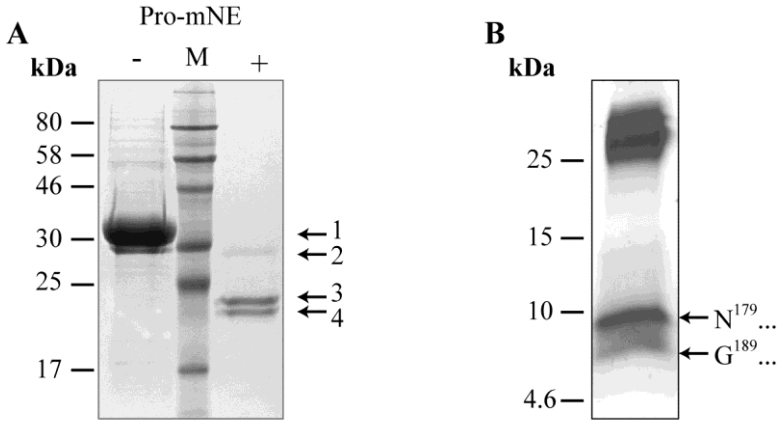

Fig 4.11: Two self-cleavage sites of mNE identified. (**A**) Purified mNE before (1) (left lane; 5 µg) and after the incubation with enterokinase (right lane; 3 µg) was analyzed by SDS-PAGE and Coomassie Blue staining. The middle lane contains the prestained protein marker (NEB, P7708). Two additional bands (3, 4), besides the mature mNE (2) were detected after EK incubation (right lane). Edman sequencing revealed that the bands 3 and 4 started with the mature N-terminus and were therefore identified as N-terminal fragments of mNE. (**B**) Using a small peptide 18% tris-tricine SDS gel, the small C-terminal fragments from mNE (5 µg loaded) not visible in panel **A** were separated and subjected to Edman sequencing. Edman sequencing revealed two cleavage sites at V^{178}/N^{179} and A^{188}/G^{189}. Edman sequencing was carried out by Reinhard Mentele (Core facility of MPI Biochemistry).

running an 18% tris-tricine gel with 5% crosslinking, I was able to separate the two small C-terminal fragments. These fragments were blotted on membranes for Edman sequencing. Cleavage of mNE occurred between V^{178}/N^{179} and A^{188}/G^{189}, indicating a self-cleavage of mNE, as these are elastase-like and not enterokinase cleavage sites (**Fig 4.11 B**). In the following intact mNE will be called single chain (sc) and the nicked form two chain (tc) mNE.

4.2.1.2 Self-cleavage of mNE changes its activity

Activation of mNE (1-2 mg/ml) was observed over a time course with the addition of enterokinase (25-50 µg/ml) as a starting point. At different time points aliquots were taken and frozen at -20°C, thus stopping the reaction (**Fig 4.12**). For SDS-PAGE 2 µg per time point of mNE was loaded and160 ng per time point was used for the activity assay. The amount of sc-mNE gradually decreased while concentration of tc-mNE increased. The tc-mNE represented the most predominant form after 24 hours (**Fig 4.12**, upper panel). This process did not stop, when I added the enterokinase specific D_4K-cmk inhibitor, verifying our suspicion of self-cleavage as the mechanism generating tc-mNE. In addition the activity of mNE at each time point was measured using

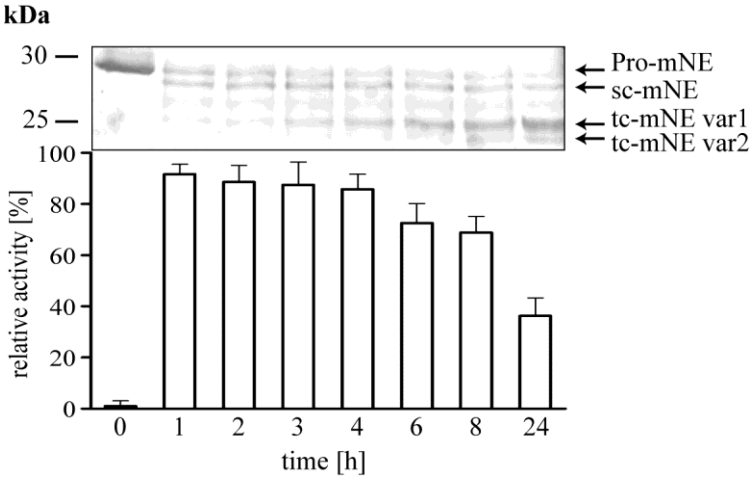

Fig 4.12: Self-cleavage of mNE changes its activity. At time point zero enterokinase (Roche; 25-50 µg/ml) was added to mNE (1-2 mg/ml). In two experiments enterokinase inhibitor D_4K-cmk was added after 1.5 hours. Each lane of a 15% SDS polyacrylamide gel stained with Coomassie was loaded with 2 µg mNE and 160 ng mNE were used for each activity assay. This gel is representative of 5 independent experiments. Activity measurements were always done in triplicates with Abz-GAVVASELR-Y(NO2)-D as the substrate. Data shown is mean ± SEM of all experiments (n=5). The y-axis shows the activity of mNE with the highest activity of each experiment set to 100%. Increasing amount of mNE was nicked over the time, even in the presence of enterokinase specific inhibitor. Thus nicking was indeed the result of a self-cleavage of mNE. The increase of tc-mNE and decrease of sc-mNE over time was paralleled by a slow, gradual decline in activity.

Abz-GAVVASELR-Y(NO2)-D as a substrate. The decrease of sc-NE and increase of tc-NE correlated with reduced activity over time.

4.2.2 Does NE inactivate itself via self-cleavage?

4.2.2.1 Western blot analysis of different mNE variants using a cmk inhibitor

To further investigate the decline of activity, I used a biotinylated AAPV-cmk inhibitor. Only active mNE can covalently react with the inhibitor, thus only active mNE is visualized in a western blot (**Fig 4.13 A**). Murine NE with a concentration of 80 µM was incubated with 0.5 mM AAPV-cmk at 37°C for 30 minutes. The six time's molar excess of the inhibitor ensured a complete inhibition of active mNE. I always added the AAPV-cmk inhibitor to the mix at the last possible moment, because AAPV-cmk is instable in aqueous solutions. A 15% SDS gel was run, where 1 µg was loaded for western blot analysis and 8 µg for Coomassie staining. Tc-mNE variant 1 gave a much stronger signal than tc-mNE variant 2 in the western blot, although the Coomassie stained gel indicated that equal amounts of both variants were present in the sample (**Fig 4.13 B**).

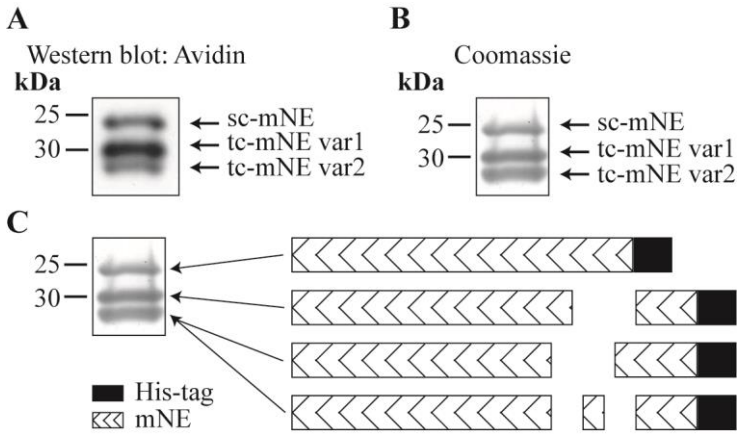

Fig 4.13: Western blot analysis of mNE with cmk inhibitor indicates inactivation of mNE variant. Biotinylated NE inhibitor AAPV-cmk (0.5 mM) was incubated with 80 µM mNE at 37°C for 30 min. The biotinylated AAPV-cmk forms a covalent complex with mNE. (**A**) The sample was split and 1 µg mNE was separated by SDS-PAGE (15%) and blotted. After the membrane was blocked with 5% (w/v) Non-Fat Dry Milk Blocker (Bio-Rad) the membrane was incubated with 0.5 µg/ml avidin-HRP (Invitrogen, 43-4423) at room temperature for one hour. (**B**) 8 µg of the sample was loaded on a 15% SDS-PAGE gel and stained with Coomassie. All three variants of mNE were able to react with AAPV-cmk. While Coomassie gel staining revealed an equal amount of variant 1 and 2, the signal of variant 1 in western blot analysis is much more prominent than that of variant 2. (**C**) The band labeled as variant 2 actually is derived from two different forms of mNE, which are cut at one or two positions. These two forms appeared to differ in their activities and most likely account for these discrepancies.

The gel showed only two large big N-terminal fragments that were separated from the small C-terminal fragments after reduction in the sample buffer. The band called tc-mNE variant 2 was derived from a mixture of mNE, which had been nicked once or twice (**Fig 4.13 C)**. On the other hand tc-mNE variant 1 exclusively consisted of single cut mNE. A different behavior of the single- and double- cut mNE with regards to AAPV-cmk inhibition might be a reason for the observed divergence between western blot analysis and Comassie staining.

4.2.2.2 Mass spectrometry analysis of different mNE variants using a cmk inhibitor

For further analysis via mass spectrometry, I needed homogenously glycosylated tc-mNE. After removal of the glycosylation sites mNE was no longer expressed in HEK293EBNA cells (data not shown). Therefore, in cooperation with U-protein

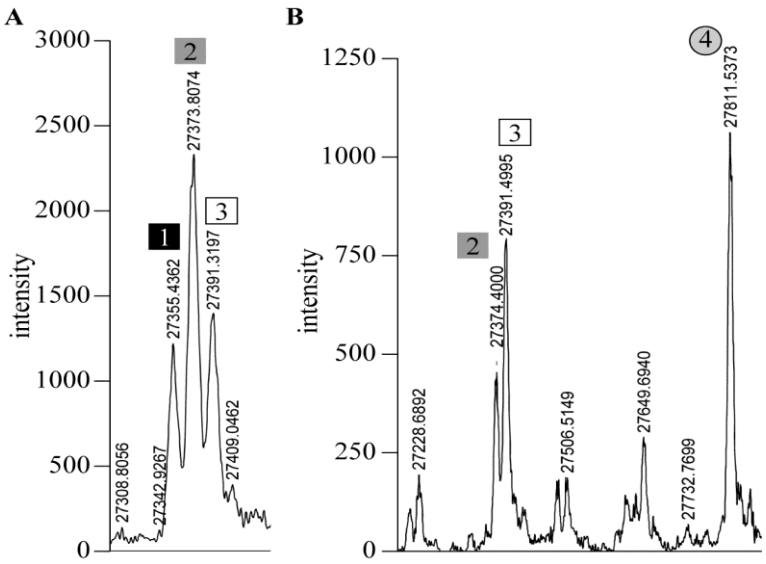

Fig 4.14: Mass spectrometry analysis of mNE exposed to a cmk inhibitor indicates inactivation of the double-nicked mNE variant. Pro-mNE was expressed in HEK293ED (U-Protein Express-BE, Utrecht) cells to achieve homogenous glycosylation. Purified pro-mNE (0.35 mg/ml) was incubated with enterokinase (NEB; 50 ng/ml) at 37°C over night. (**A**) The digest was then analysed by mass spectrometry performed by E. Weyher at the MPI of biochemistry. Peak 1 shows the homogenously glycosylated mNE (MW: 27.355 kDa). With each self-cleavage the molecular weight increased by the size of a water molecule resulting in peak 2 and 3. Clearly in this sample the most prominent peak was the single nicked mNE (2), while the peak for intact (1) and double (3) -nicked mNE had roughly the same height. (**B**) AAPA-cmk inhibitor (0.5 mg/ml) was added to the converted mNE from **A** and incubated at 37°C for 30 minutes. After adding AAPA-cmk inhibitor peak 1 completely disappeared and peak 2 was considerably diminished, leaving peak 3 as the most prominent one. As a result I got a new peak (4) with a MW of 27.811 kDa, which is the expected weight for the complex between single-nicked mNE and AAPA-cmk.

Express-BE (Utrecht), tc-mNE was expressed in HEK293ES cells, a N-glycosylation deficient cell line, which produces proteins with short homogenous carbohydrate chains and the supernatant was sent to us for purification. Purified pro_mNE (0.35 mg/ml) with special glycosylation was incubated with enterokinase (NEB; 50 ng/ml) at 37°C over night. For inhibition 0.5 mM unbiotinylated AAPA-cmk inhibitor was added to the converted mNE and incubated at 37°C for 30 minutes. Mass spectrometry analyses were performed by Elisabeth Weyher (core facility of the MPI Biochemistry). Sc-mNE without AAPA-cmk inhibitor had a molecular weight of 27.355 kDa as could be seen in peak 1 (**Fig 4.14 A**). Each time when mNE cleaved itself, a peptide bond was hydrolyzed and one water molecule (18 Da) was gained resulting in peak 2 and 3 with a molecular weight of 27.373 or 27.391 kDa respectively. The molecular weight of AAPA-cmk inhibitor is 475 Da. Because a hydrochloride is released during the AAPA-cmk reaction with mNE, the complex has a theoretical weight of 27.794 kDa. Although a complex of this size had not been found, peak 1 (sc-mNE) disappeared after the addition of the AAPA-cmk indicating that sc-mNE reacted completely with AAPA-cmk (**Fig 4.14 B**). Peak 2 (once cleaved mNE) was significantly reduced and a peak for the mNE-inhibitor complex (27.811 kDa), peak 4, appeared. There was still a considerably amount of double nicked mNE, while no signal for a protease-inhibitor complex was detected. Altogether, these results suggested that double-nicked mNE was inactive.

4.2.3 Resistant mNE

The first indication that the cleavage site A^{188}/G^{189} might have been more important was found in the order of cleavage. Murine pro-mNE (0.5 mg/ml) was incubated with EK (50 ng/ml) at room temperature for two hours (**Fig 4.15 A**). After that AAPA-cmk (0.5 mg/ml) was added to stop the self-cleavage of mNE. I loaded 2.5 µg of this converted mNE with (**Fig 4.15 A**, left lane) and without (**Fig 4.15 A**, right lane) AAPA-cmk on a 15% SDS gel. I detected tc-mNE variant 1 that resulted from the self-cleavage of mNE between A^{188} and G^{189} although I added AAPA-cmk after two hours. Furthermore, trypsin cleaved itself at the same topological site as mNE (K^{188}/D^{189} compared to A^{188}/G^{189}) (**Fig 4.15 B**). Interestingly, self-cleavage of trypsin at this site resulted in a specificity change. This cleavage site is conserved in NE across many species (**Fig 4.15.C)**.

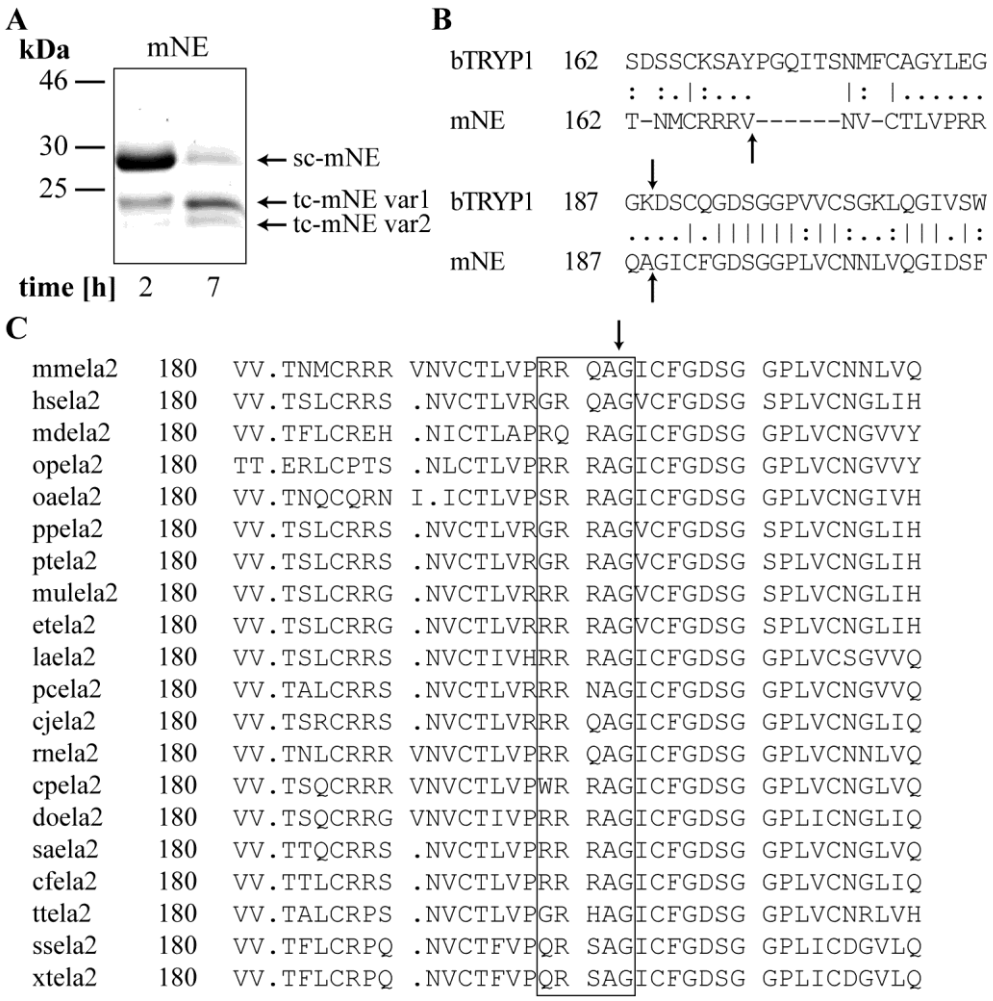

Fig 4.15: Cleavage between A^{188} and G^{189} might change activity of mNE. (**A**) To pro-mNE(wt) (0.5 mg/ml) 50 ng/ml enterokinase was added and incubated at room temperature for two hours. Then AAPA-cmk (0.5 mg/ml) or PBS was added to the digest and incubated at 37°C for 2 hours. The two digests (2.5 µg mNE per lane) with (left lane) and without (right lane) AAPA-cmk were loaded on a 15% Coomassie stained SDS gel. In contrast to tc-mNE var 2, tc-mNE was already detected two hours after the conversion of pro-mNE with enterokinase. Tc-mNE var 1 was a product of self-cleavage at A^{188}/G^{189}; therefore mNE cleaved itself first at A^{188}/G^{189}. (**B**) Trypsin also cleaves itself at the same topological site (K^{188}/D^{189}) similar to mNE at $A^{188}/G^{189}$and thereby changes its specificity. (**C**) This cleavage site A^{188}/G^{189} is conserved in many NE homologues from many species.

Taken together the cleavage site A^{188}/G^{189} appeared to show functional relevance. That is why I mutated $Q^{187}A^{188}$ to $K^{187}G^{188}$ to prevent the self-cleavage. To test whether this mutated mNE was stable I repeated the experiment of chapter 4.2.1.2. Mutated pro-mNE (1.1 mg/ml) was incubated with EK (NEB; 78 ng/ml) at 37°C. Enterokinase inhibitor D_4K-cmk inhibitor was added after two hours. At each time point an aliquot of 2 µg and 160 ng of mutated mNE was withdrawn for Coomassie blue gel and for an activity assay respectively (**Fig 4.16**). Sc-mNE was almost exclusively seen even after 24 hours. Only

little cleavage at the second self-cleavage site V^{178}/N^{179} was detected. In accordance to these findings the activity of the mutated mNE was stable. The activity was measured as described in chapter 4.2.1 using Abz-GAVVASELR-Y(NO2)-D as a substrate. Because the mutated form of mNE is a stable single-chain form, I suppose that this mutated form of mNE represents the natural sc-mNE and will refer to it as such. Data shown were mean ±SEM of three independent experiments.

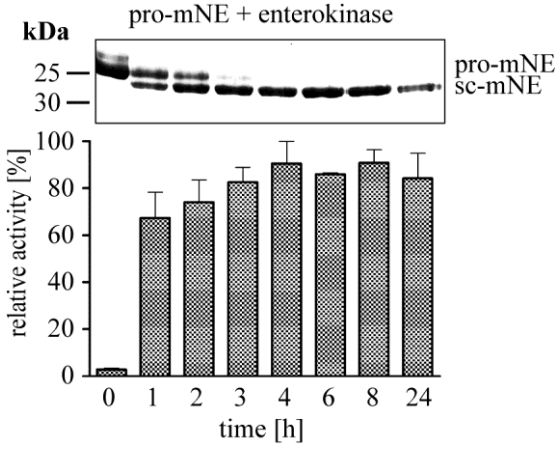

Fig 4.16: Mutation of $Q^{187}A^{188}$ to $K^{187}G^{188}$ prevented self-cleavage of mNE. To test whether the mutation was able to abolish self-cleavage, 1.1 mg/ml mutated pro-mNE was activated with EK (NEB; 78 ng/ml) at time point zero. After 1.5 hours the D_4K-cmk inhibitor was added to inactivate enterokinase. For each time point 2 µg mNE was loaded on a 15% SDS polyacrylamide gel for subsequent Coomassie staining. An activity assay with 160 ng mNE and Abz-GAVVASELR Y(NO2)-D as a substrate was also performed for each time point. This gel is representative of 3 independent experiments. Activity measurements were always done in triplicates. Data shown is the mean +/- SEM of all experiments. No self-cleavage at A^{188}/G^{189} was detected and only slight self-cleavage at V^{178}/N^{179} was found. The activity is stable even after 24 hours, thus elimination of self-cleavage site A^{188}/G^{189} was successful.

4.2.4 Titration of sc-and tc-mNE

4.2.4.1 Determination of α1PI concentration

Direct titration of mNE is not possible at present, because a suitable titration reagent is not available. Titrated α1PI was needed for the accurate determination of active mNE. Trypsin (Sigma Aldrich) was dissolved in 1 mM HCl and burst titrated as described in **chapter 3.3.1** (data not shown). A constant concentration of 200 nM trypsin was incubated with varying concentrations of α1PI at 37°C for one hour. Residual activity was measured with 200 µM Boc-Gln-Gly-Arg-AMC resulting in a typical enzymatic curve (**Fig 4.17 A**). The initial phase of the curve was always linear and the slope was the

maximum velocity (v_{max}) that can be achieved with this amount of active enzyme and substrate concentration. The slope was reciprocally proportional to the volume of α1PI used, so the total portion of active α1PI could be determined by extrapolation (**Fig 4.17 B**). The intersection with the x-axis indicates the amount of α1PI needed to completely inhibit trypsin. I always dissolved 1 mg α1PI (Athens research) in 500 µl water. The normal concentration was then approximately 4 µM active α1PI.

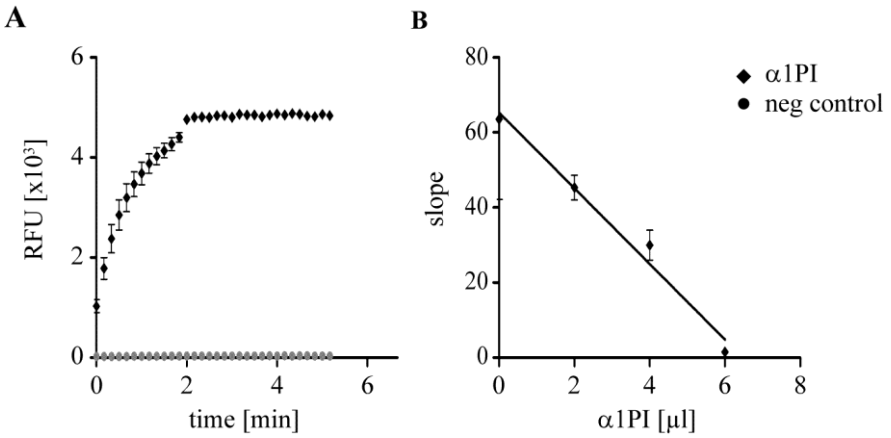

Fig 4.17: Determination of α1PI concentration. For an accurate determination of α1PI concentration, α1PI was titrated with burst titrated trypsin. Increasing α1PI concentrations were incubated with 200 nM trypsin at 37°C for one hour. (**A**) The remaining trypsin activity was measured using 200 µM Boc-Gln-Gly-Arg-AMC as a substrate (excitation: 350 nm, emission: 450 nm). The fluorescence is given in relative fluorescence units (RFU). The graph shown is an example for the described reaction. 200 nM trypsin was incubated with 64 nM α1PI at 37°C for one hour. (**B**) The slope of the linear part of the curve in **A** is the maximum velocity and is directly correlated with the concentration of active trypsin. The amount of α1PI was then plotted against the slope to extrapolate the volume of α1PI needed to inhibit trypsin completely. Graphs shown are typical examples for reactions described.

Sc- and tc-mNE were then titrated in a similar fashion. In order to work with the same sc/tc-mNE ratio every time, I determined the concentration of mNE using absorbance measurement or BCA assay and converted wt mNE at a concentration of 0.5 mg/ml. Tc-mNE was titrated with Boc-APnV-4-chloro-SBzl (**Fig 4.18 A**) and the active tc-mNE concentration was approximately 5-6 µM in this case (**Fig 4.18 C**). Because the mutation protected mNE from self-cleavage, the concentration during activation was not critical. Different initial concentrations of sc-mNE were titrated and thus there was not one common concentration for titrated sc-mNE.

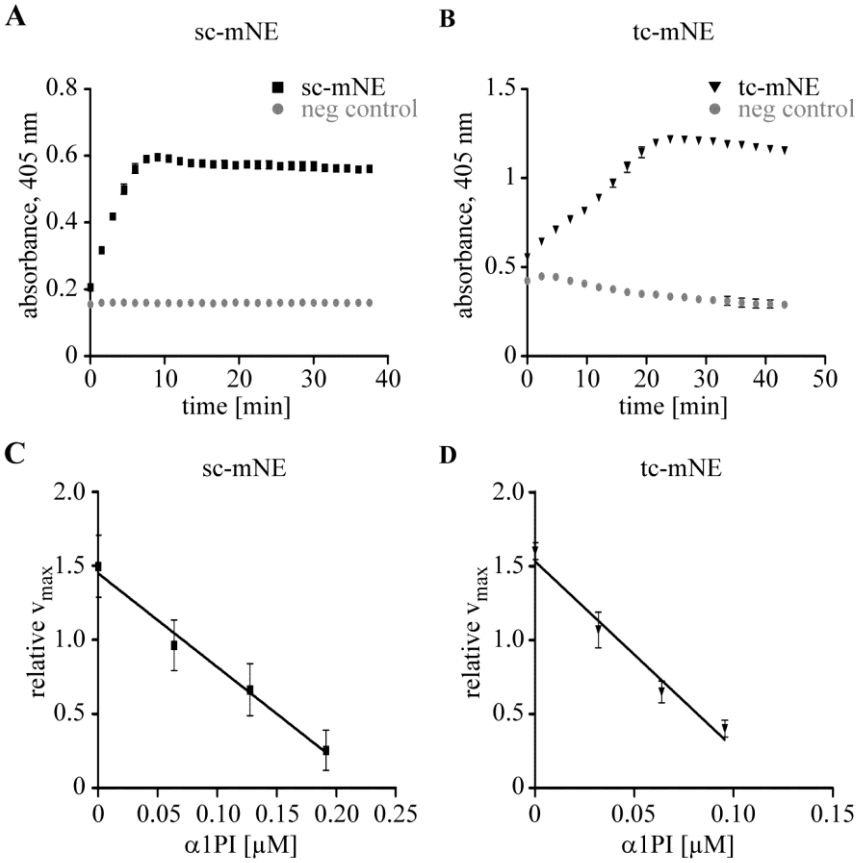

Fig 4.18: Titration of sc- and tc-mNE. Determination of the concentration of active sc- and tc-mNE was done similarly as for α1PI. In this case the concentration of sc- or tc-mNE respectively was held constant and the α1PI concentration was varied. (**A**) The remaining activity of sc-mNE was measured with 0.5 mM AAPV-pNA The negative control was only substrate and buffer (grey dots). (**B**) The remaining activity of tc-mNE was measured with 1 mM APnV-Sbzl and 0.5 mM DTNB. The negative control was only substrate and buffer (grey dots). As an example the graph of sc-mNE and tc-mNE without α1PI are shown in **A** and **B**. (**C, D**) Plotting the concentration of α1PI against relative v_{max} (slope of linear section in the curves) results in a linear regression line, which is extrapolated by using GraphPad Prism. The x-intercept showed the concentration needed to completely inactivate mNE. Because α1PI and mNE react in a 1:1 ratio, the x-intercept equals the concentration of active mNE used. From these values, the concentration of the stock solution of mNE can then be calculated. Graphs shown are examples for described reactions.

4.2.5 Testing of different substrates

Testing sc- and tc-mNE towards several substrates, I observed differences between these two forms. I chose the two most interesting substrates and analyzed them in detail. Both substrates represent the reactive center loop sequence of two serpins, which are natural serine protease inhibitors.

I used 231 nM tc-mNE and 23 nM sc-mNE and varied the substrate concentration between one to 80 µM. Since RFU was proportional to the substrate concentration, relative fluorescence units (RFU) were converted to substrate concentration. Fitting the subsequent Michaelis-Menten curve (**Eq. 3**) (**Fig 4.19 A, B**) with GraphPad Prism revealed that RCL of α1PI (Mca-GEAIPMSIPPEVK(Dnp)-rr) was a eight times better substrate for sc-mNE than tc-mNE with K_{cat}/K_M=14.9 (±0.7)*10^{+4} $M^{-1}s^{-1}$ for sc-mNE and

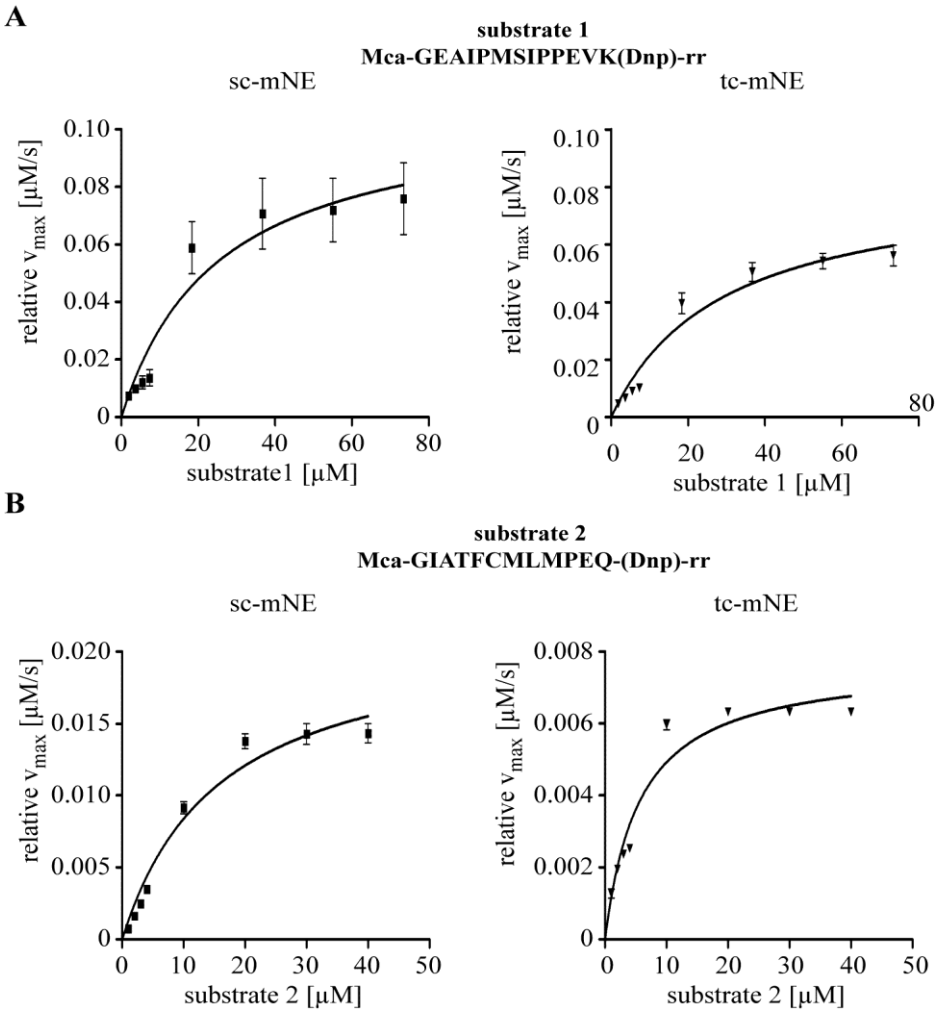

Fig 4.19: Activities of sc- and tc-mNE towards two different substrates. (**A**) Substrate concentration was varied (1-80 µM), while protease concentration was kept constant (sc-mNE=0.23 uM and tc-mNE=2.3 uM). Plotting substrate concentration against the relative maximum velocity v_{max} (slope of linear section in the graphs) renders a graph that was fitted to Michaelis-Menten kinetics (**Eq. 4**) using GraphPad Prism. K_{cat} and K_M for sc- and tc-mNE can be calculated using **Eq. 3, 4.** (**A**) The reactivity of sc- (left panel) and tc-mNE (right panel) towards the α1PI-substrate (Mca-GEAIPMSIPPEVK(Dnp)-rr) was determined as described above. (**B**) The reactivity of sc- (left panel) and tc-mNE (right panel) towards the MNEI-substrate (Mca-GIATFCMLPEQ(Dnp)-rr) was determined as described above. Each experiment was done in triplicate and data shown is mean +/- SEM (n=3). The conditions for the measurement of the fluorescence: excitation: 320 nm, emission: 405 nm. The results are listed in **Tab 4.1.**

1.8 (±0.7)*10^{+4} $M^{-1}s^{-1}$ for tc-mNE (**Tab**). Responsible for the difference is the turnover number k_{cat}, which is more than eleven times better for sc-mNE (k_{cat}=3.9 (±1.7) s^{-1}) than tc-mNE (k_{cat}=0.35 (±0.03) s^{-1}). In contrast, there was almost no difference between the Michaelis constant K_M of sc-mNE (K_M=27.8(±7)) and tc-mNE (K_M=20.9(±6)). Constants calculated here, are mean ±SEM from three independent experiments.

substrate		**K_M [µM]**	**k_{cat} [s^{-1}]**	**k_{cat}/K_M [$M^{-1}s^{-1}$]**
substrate 1	sc-mNE	27.8(±7)	3.92 (±1.73)	14. 9(±0.7)*10^4
Mca-GEAIPMSIPPEVK(Dnp)-rr	tc-mNE	20.9(±6)	0.35(±0.03)	1.8(±0.7)*10^4
substrate 2	sc-mNE	21(±1)	0.99(±0.71)	4 (±2)*10^4
Mca-GIATFCMLMPEQ-(Dnp)-rr	tc-mNE	2 (±2)	0.02(±0.01)	2 (±2)*10^4

By contrast, the substrate Mca-GIATFCMLMPEQ-(Dnp)-rr representing the RCL of MNEI was cleaved by sc- and tc-mNE almost equally well with k_{cat}/K_M of 4 (±2)*10^{+4} $M^{-1}s^{-1}$ and 2 (±2)*10^{+4} $M^{-1}s^{-1}$, respectively (**Fig 4.19 C, D**). Similar to the RCL of MNEI, k_{cat} for sc-mNE (0.99(±0.71)) was better than for tc-mNE (0.02 (±0.01), but the almost ten times lower K_M of tc-mNE (2(±2)) compared to sc-mNE (21(±1)) compensated this to a high degree. Constants calculated here, were mean ±SEM from three independent experiments.

4.2.6 Inhibitors

Until now, I only looked at the ability of mNE to cleave the RCL sequence of SERPINs. Cleavage of RCL is necessary, but not enough to inhibit mNE and to form mNE-inhibitor complexes. First, I ensured that sc- and tc-mNE could still form complexes with α1PI and were still irreversible inhibited. To demonstrate this, 6 µg sc-mNE and tc-mNE were incubated with 15.6 µg α1PI at 37°C and the reaction was interrupted at different time points by taking aliquots, containing 1 µg of mNE and 2.6 µg α1PI, and boiling them immediately with reducing sample buffer at 95°C (**Fig 4.20 A, B**). The ester-bond between mNE and α1PI was stable even after reduction, thus the mNE- α1PI complexes could be identified in a reducing SDS gel by the shift in the molecular weight. Sc-mNE has a molecular weight of 25 kDa and α1PI one of 52 kDa. After formation of the ester bond a small C-terminal portion of α1PI (4 kDa) was lost. Therefore the sc-mNE-α1PI complex was 73 kDa. Within seconds sc-mNE had completely reacted with α1PI, as

could be seen by the disappearance of sc-mNE and the emerging of th sc-mNE-α1PI complex at 73 kDa. Identification of the tc-mNE-α1PI complex was somewhat more difficult. The ester bond between mNE and α1PI was between the Ser195 from mNE and Met358 from α1PI. After reduction the tc-mNE fell apart and only its C-terminal part with 7 kDa remained bound to α1PI. The tc-mNE- α1PI complex had therefore a molecular weight of 55 kDa and run slightly above α1PI on a reducing SDS gel. After 30 seconds the first complexes were seen. But even after 20 min the reaction was not finished yet.

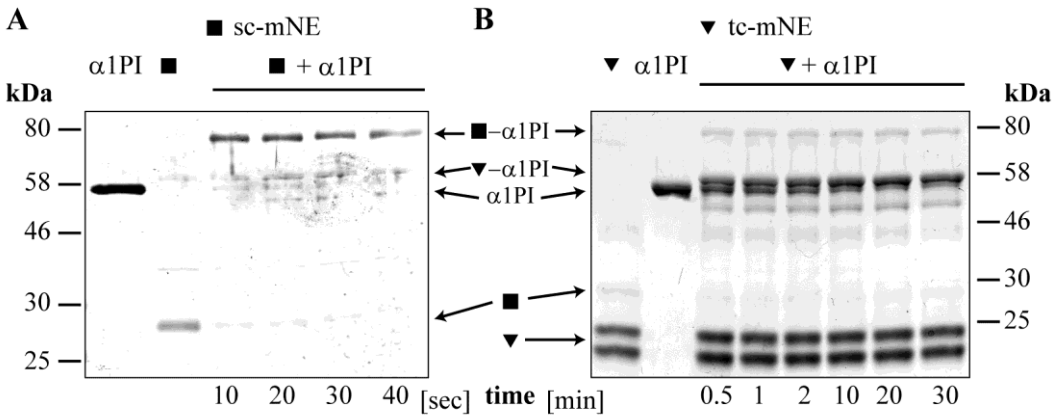

Fig 4.20: Complexation between the tc-mNE and α1P is impaired. (**A**) Sc-mNE (black square; 6 µg) was incubated with 15.6 µg α1PI at 37°C. Aliquots with 1 µg sc-mNE and 2.6 µg α1PI were taken at different time points and immediately boiled in reducing sample buffer at 95°C. Sc-mNE disappeared within seconds. At the same time, a band at approximately 73 kDa appeared. This position corresponds to the MW of the sc-mNE- α1PI complex, thus sc-mNE forms a complex with α1PI during the first 30 seconds. (**B**) The experiment of **A** was repeated with tc-mNE (black triangle). In contrast to sc-mNE, tc-mNE-α1PI complex formed much slower. Since only the C-terminus of tc-mNE remains attached to the complex after reduction, the tc-mNE-α1PI complex is much smaller and runs only slightly above natural α1PI. Even after 20 minutes I saw a reduction of the α1PI band and an increase of the tc-mNE-α1PI band, indicating that the reaction was still not finished at that time point. Gels shown are representative of three independent experiments.

Although complex formation between tc-mNE and α1PI was considerably slower, α1PI could still inhibit tc-mNE irreversibly. As described in **chapter 3.3.3** k_{obs} was determined by adding mNE to mixes of different α1PI amounts (0-0.73 µM) and a constant substrate amount (Mca-GEAIPTSIPPEVK(Dnp)-rr; 152.12 µM). The resulting competition between substrate and α1PI gave characteristic curves (**Fig 4.21 A, B**) that were fitted to **Eq. 8** using GrapPad Prism. All experiments were done in duplicates and repeated thrice. The

calculated k_{obs} values were then plotted against the corresponding α1PI concentration (**Fig 4.21 C, D**) and fitted to fit **Eq. 8** in GraphPad Prism**.** K_{ass} was the constant that describes the association rate between mNE and α1PI to form an initial encounter complex and was in this case the speed limiting factor. While sc-mNE had a K_{ass} of 4.6 (±0.5)*10^{+6} $M^{-1}s^{-1}$, tc-mNE had a K_{ass} of 3.1(±1.4)*10^{+5} $M^{-1}s^{-1}$ with α1PI, meaning sc-mNE was 15 times faster inhibited by α1PI than tc-mNE. Constants calculated here, were mean ±SEM from three independent experiments.

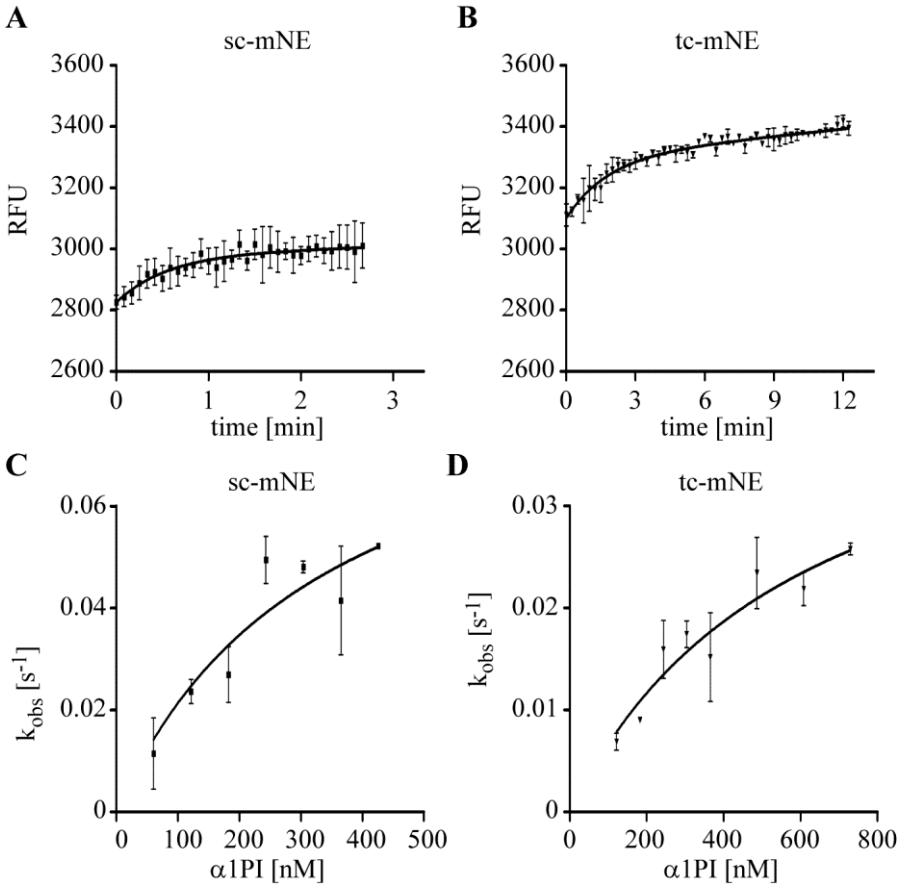

Fig 4.21: Tc-mNE inhibition with α1PI impaired. (**A**) Sc-mNE (10 nM) is given to a mix of 152.12 µM substrate and varying α1PI concentrations (0-0.73 µM). The y-axis shows the fluorescence in relative fluorescence units (RFU) (excitation: 320 nm, emission: 405 nm). The subsequent curves were fitted with GraphPad Prism to **Eq. 8**. Data shown are examples with ± SEM and n=2. The graph is an example and 0.18 µM α1PI was used in this experiment. (**B**) The experiments in **A** were repeated in **B** with the same conditions by substituting sc-mNE with tc-mNE. As an example a graph with 0.12 µM α1PI is shown. (**C**,**D**) The resulting k_{obs} values were than plotted against α1PI concentration to determine K_{ass}. The resulting graph is fitted to **Eq. 9** using GraphPad Prism. Data shown is mean ± SEM of all experiments (n=3). Nicking of mNE resulted in an 15 times slower inhibition of α1PI (K_{ass}(sc-mNE)= 4.6(±0.5)*10^{+6} $M^{-1}s^{-}1$ and K_{ass}(tc-mNE)= 3.1(±1.4)*10^{+5} $M^{-1}s^{-1}$).

4.2.6.1 Z-α1PI

Z- α1PI was expressed in HEK293 cells and purified via Ni-column (data not shown). The sequence is listed in the appendix (**8.2.5**). As Z-α1PI is prone to polymerization, Z-α1PI was only stable at 4°C for one day. Experiments had to be performed on the same day and titration of active Z- α1PI was not possible. To estimate the concentration, different amounts of Z- α1PI were incubated with 100 nM sc-mNE at room temperature for 30 minutes. Thereafter 20 µM substrate (MCA-GEAIPTSIPPEVK(Dnp)-rr) was added to measure residual sc-mNE activity. The minimal amount of Z-α1PI needed to inhibit sc-mNE completely, was then incubated with 100 nM sc- or tc-mNE at room temperature for 5 minutes. By adding 20 µM substrate (MCA-GEAIPTSIPPEVK(Dnp)-rr) the remaining active tc-mNE was measured. In contrast to sc-mNE, tc-mNE was still active. Therefore tc-mNE was poorly inhibited by Z- α1PI compared to the sc-mNE. This experiment was repeated three times with different batches of Z- α1PI.

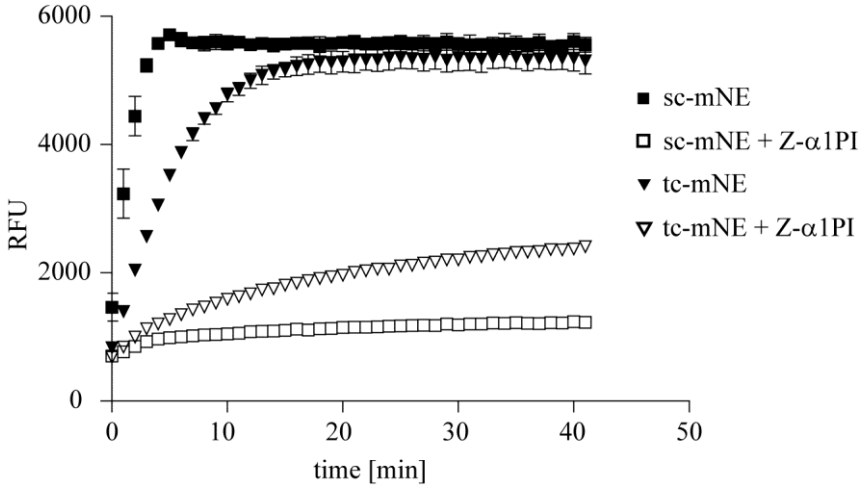

Fig 4.22: Inhibition of sc- and tc-mNE by Z-α1PI. To estimate the concentration of active Z-α1PI sc-mNE was incubated with varying amounts of Z-α1PI at room temperature for 30 minutes. The residual activity was measured by adding 20 µM substrate (MCA-GEAIPTSIPPEVK(Dnp)-rr). The amount of Z-α1PI was plotted against the slope. The x-axis intercept is the minimal amount necessary to inhibit 100 nM sc-mNE completely. This calculated amount of Z-α1PI was incubated with 100 nM sc- (white squares) and tc-mNE (white triangles) at room temperature for 5 minutes before adding substrate to the reaction. While sc-mNE was completely inhibited after 5 minutes, tc-mNE still showed some activity. For positive control sc- (black squares) or tc-mNE (black triangles) were incubated with 20 µM substrate. Data ±SEM are representative of three experiments.

4.2.6.2 Small molecule inhibitor

Besides the natural inhibitor α1PI I also tested whether inhibition by AZ111177, a small molecule inhibitor designed for therapeutic use, was also affected. The inhibitor was kindly provided by Astra Zeneca along with the information that the mechanism of inhibition is reversible. For reversible inhibition the dissociation constant K_D was the negative reciprocal value of K_{ass}, and was used to compare inhibition strength. To this purpose, Michaelis-Menten curves with different AZ111177 concentration were determined (**Fig 4.23**). GraphPad Prism was used to calculate K_i from these by fitting these graphs to **Eq. 6**. All experiments were done in duplicates and repeated thrice. The K_i of sc-mNE is 1.7 (±2) µM. Compared to this, K_i of tc-mNE is 17 times worse (K_i of tc-mNE= 27.9 (±27) µM). Constants calculated here, were mean ±SEM from three

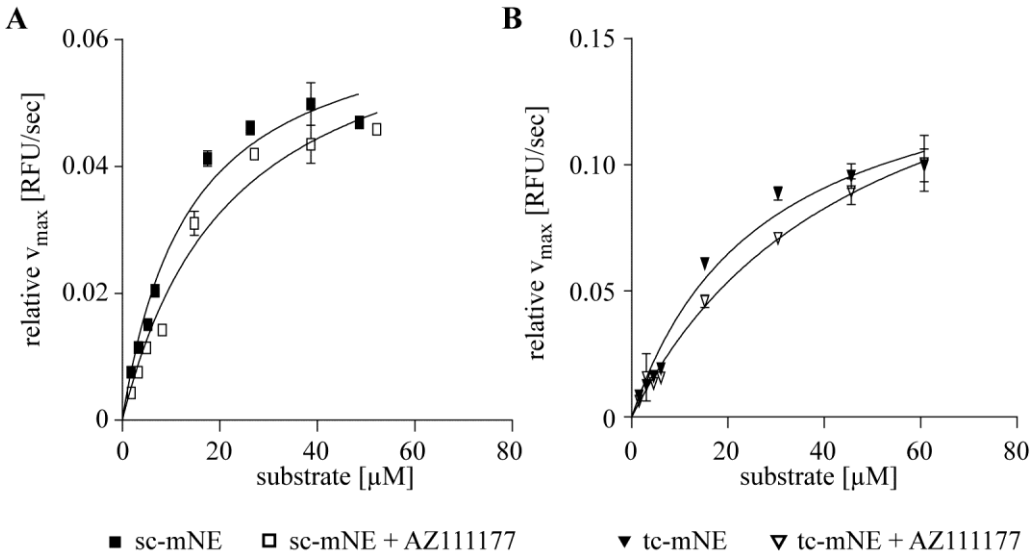

Fig 4.23: Inhibition of tc-mNE by AZ111177 was worse than that of sc-mNE. (**A**) Relative maximum v_{max} (slope of linear section in the curves) of sc-mNE (23.81 nM) with varying substrate concentration (MCA-GEAIPTSIPPEVK(Dnp)-rr; 1-80 µM) was plotted against substrate concentrations. The graph is fitted to the Michaelis-Menten equation **Eq. 4**. This procedure is repeated with sc-mNE that was incubated with different AZ111177 concentrations (20-800 nM) at 37°C for one hour beforehand. For the graph shown here 20 nM AZ111177 was used. (**B**) The experiment described in **A** was repeated with tc-mNE. As an example a graph with 2 µM AZ111177 is shown. Data shown are representative for three independent experiments. Filled symbols represent graphs of uninhibited sc- (black squares) or tc-mNE (black triangle). Hollow symbols show a graph in the presence of the inhibitor. All experiments were done in duplicates and repeated thrice. The graphs were fitted to **Eq. 6** with GraphPad Prism. With K_i (sc-mNE)= 1.712(±2) µM and K_i (tc-mNE)= 27.922 (±27) µM, inhibition of tc-mNE is 17 times worse than that of sc-mNE by AZ111177.

independent experiments.

4.2.7 Natural occurrence of tc-mNE

To adress the question, whether the tc-mNE form also occurs *in-vivo*, I analyzed the PMNs as NE was stored there in a large quantity there. I investigated murine as well as human PMNs. Murine PMNs were isolated from bone marrow cells using a percoll gradient. Whole PMNs lysate from $1*10^6$ mPMNs was separated on 15% reducing SDS gel and blotted (**Fig. 4.15 A**). The mebrane was incubated with 1µg/ml anti-hNE antibody

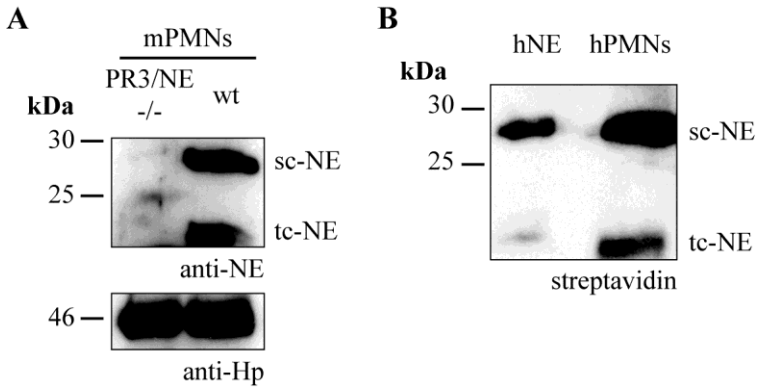

Fig 4.24: Tc-NE was found in PMNs. Both human and murine PMNs were investigated for the existence of tc-NE. (**A**) Lysate of $1*10^6$ mPMNs was separated by SDS-PAGE and after blotting the membrane was incubated with 1 µg/ml anti-hNE antibody (Abcam; ab68672), which cross reacts with mNE, at 4°C over night.. The second antibody HRP-coupled anti-rabbit antibody was 1:5000 diluted and incubated at room temperature for 1 hour. To demonstrate the specificity of the anti-hNE antibody for mNE, lysate of PR3/NE deficient PMNs was loaded on the same gel. In wt hPMNs two bands corresponding to sc- and tc-mNE respectively could be found, while no bands were visible in the knockout lysate. The membrane was incubated in stripping buffer (200 mM glycine, 0.1% SDS, pH 2.2) to remove the antibodies at room temperature for 30 minutes. The membrane was incubated with anti-human haptoglobin antibody (Dako; 1:1000 diluted) at 4°C over night. Detection of haptoglobin ensured that I had compared equal amounts of wt (right lane) and PR3/NE deficient (left lane) PMN lysate. All experiments were repeated thrice. (**B**) Lysate of $3*10^6$ hPMNs was first inhibited with 20 nmol biotinylated AAPV-cmk inhibitor, which reacts covalently with hNE. To isolated hNE, I first immunoprecipitated it with 4.4 µg anti-hNE (QED; 13203) and subsequently purified the hNE-antibody complexes with the help of 30 µl Protein G-dynabeads (Invitrogen). After boiling the beads with loading buffer and performing a SDS-PAGE the samples were blotted on a membrane. HRP-coupled streptavidin (Millipore; OR03L) was added in a 1:1000 dilution and incubated at room temperature for 1 hour. The co-migration of the two bands with a MW of about 20 kDa from control hNE (Elastin products; 500 ng) and the PMNs lysate strongly suggests that the band observed in neutrophil lysates is identical with that obtained by self-cleavage. All experiments were repeated thrice.

(Abcam; ab68672) that was crossreacting with mNE. I was able to identify sc- and tc-mNE. As a control lysate from $1*10^6$ PR3/NE deficient PMNs were loaded on the same gel. No bands were detected at the appropiate height. To ensure that an equal amount of wt and PR3/NE knockout lysate was compared, the membrane was stripped with stripping buffer (200 nM glycine, 0.1% SDS, pH 2.2) at room temperature for 1 hour. Then the mebrane was incubated with an anti-haptoglobin antibody Dako; 1:1000 dilution).

For human PMNs I had to change my protocol as there was no antibody available, which was sensitive enough to detect tc-mNE by western blot. Therefore, lysate of $3*10^6$ hPMNs was first covalently inhibited with 20 nmol biotinylated AAPV-cmk inhibitor, before an immunoprecipitation with 4.4 µg anti-hNE antibody (QED; 13203) was performed. The Protein G dynabeads (Invitrogen; 30 µl), which were used to capture the hNE-antibody complexes, were boiled at 95°C with sample buffer and analyzed on a 15% SDS gel. After blotting the samples on a membrane, the mebrane was incubated with 1:1000 diluted HRP-coupled streptavidin (Millipore; OR03L). As only active mNE could react with AAPA-cmk inhibitor, only active hNE was detected with this method. Commercially availabe hNE (Elastin products) was loaded as a control on the gel (500 ng per lane). The bands of the immunoprecipitated hPMNs corresponded to the bands that were also seen in the control hNE. Both sc- and tc-hNE were found in hPMNs. All experiments were repeated three times.

5 Discussion

In recent years, emerging evidence revealed a regulatory role of NSPs in immune defense reactions and not only a merely destructive role. Besides the degradation of pathogens and ECM, extracellular NSPs were specifically involved in controlling and directing the inflammatory process (Pham, 2008). In this study, the role of extracellular PR3 and NE during inflammation was investigated in more detail. I focused especially on the impact of these NSPs on chemokine regulation. To this end several methods and tools were developed with the final goal to investigate the processing of chemokines via NSPs *in vivo*. In the course of this research, I also found a modified form of NE, which was further analyzed. By nicking itself, NE could change specificity and could escape from efficient inhibition by α1PI.

5.1 NSP regulate inflammation by processing chemokines

PR3/NE deficient mice showed an attenuated response towards IC-mediated inflammation. Not only were less neutrophils recruited to the inflammation site, but also oxidative burst reaction was diminished (Kessenbrock et al., 2008). The degradation of progranulin, an anti-inflammatory protein, has been identified as one target of PR3 and NE. The prolonged bioactivity of intact progranulin in the absence of PR3 and NE, was in part responsible for the impaired IC-mediated inflammatory reaction (Kessenbrock et al., 2008). Of course, progranulin was hardly the only protein these proteases were encountering. Chemokines are key players for leukocyte recruitment and also control inflammation. Worthy of note here was that chemokines have been found in different isoforms *in vivo*. For IL-8 at least ten different isoforms could be identified (Proost et al., 2008). Trimming of the N-terminus in various ways was detected, which was likely caused by proteolytic cleavage. At present it is unknown, which protease is responsible for the processing of IL-8. Based on *in vitro* studies several candidates, e.g. hPR3, had been proposed (Mortier et al., 2008; Padrines et al., 1994; Wolf et al., 2008).

As proteolytic processing is most likely implicated in the generation of isoforms of chemokines, chemokines are plausible substrate candidates for PR3 and NE (Mortier et al., 2008; Wolf et al., 2008). Moreover neutrophils have been reported to be a source of chemokines (Kasama et al., 2005; Scapini et al., 2000). Interestingly, both IL-8 and MIP-2, members of the family of CXC ELR^+ chemokines, belonged to this group of

neutrophil-derived chemokines (Scapini et al., 2000). Cathepsin G was able to influence the MIP-2 levels in a non-proteolytically function (Raptis et al., 2005). I addressed the question of whether NSPs also influence MIP-2 in a proteolytic way. I could indeed show that mPR3 as well as mNE was able to cleave MIP-2 after Ala^4 *in vitro*. In an under-agarose assay this shortened MIP-2 was able to attract more neutrophils than intact MIP-2. This finding is in accordance to the oberservation that IL-8 was also cleaved by hPR3 *in vitro* and this isoform was also more chemotactic than the unprocessed precursor (Nourshargh et al., 1992; Padrines et al., 1994).

My new observation supported the view that both mPR3 and mNE play a pro-inflammatory role in antibacterial defense responses (Kessenbrock et al., 2011). A substrate featuring the N-terminal sequence of MIP-2 was incubated with lysate of wt or PR3/NE deficient PMNs. As this substrate was only cleaved by the lysate of wt but not by that of PR3/NE deficient PMNs, mPR3 and mNE are the only proteases among many other endoproteases present in PMNs that are able to process MIP-2. In contrast to our substrate, the MIP-2 N-terminus was not protected. Hence, exopeptidases could trim the N-terminus and could still be involved in MIP-2 processing. For a better understanding, MIP-2 was incubated with TNF-α primed mPMNs. In this experiment, all proteases including exopeptidases of mPMNs were competing with each other for MIP-2. After immunoprecipitation, I blotted MIP-2 on a membrane for Edman sequencing. Incubation with wt, but not with PR3/NE knockout mPMNs yielded N-terminally processed MIP-2(5-73). Full length MIP-2 was not completely converted and was identified in both samples. This experiment confirmed our previous finding with the MIP-2 substrate. PR3 and NE seemed to be the only proteases in mPMNs that could process MIP-2.

I tried to understand the impact of N-terminal trimming on its chemotactic activity. For this purpose I produced not only intact and processed MIP-2, but also N-terminally and C-terminally elongated versions. Ch_MIP-2 was chemotactically inert, but could be activated by mPR3 or mNE cleavage. This switch from inactive to active could be demonstrated more easily than the conversion of MIP-2(1-73) to MIP-2(5-73), which resulted only in an enhancement of the chemotactic activity. As the N-terminal extension of MIP-2(1-73) was rather large, I first had to test whether mPR3 and mNE still maintained the ability to cleave Ch_MIP-2. This was indeed the case and I therefore proceeded with the next experiment.

Binding of chemotactically active MIP-2 triggered receptor internalization. Wild type mPMNs isolated from the bone marrow were incubated with all four variants of MIP-2. Then remaining CXCR2 receptors on the surface were measured and compared with the amount of CXCR2 receptors on untreated mPMNs. Since binding to the receptor was a prerequisite to induce its internalization and responses in PMNs, it was a measure for the strength of MIP-2 binding. I expected that the more chemotactic forms of MIP-2 would bind better to CXCR2 resulting in a stronger reduction of CXCR2 on the surface. Surprisingly, all isoforms induced a similar reduction of CXCR2. Even Ch_MIP2 was able to bind to CXCR2, although this isoform was supposed to be chemotactically neutral. This unexpected result has been probably obtained, because wt PMNs were used in this experiment. Wt mPMNs carry mPR3 and mNE. Due to the purification on a percoll gradient these mPMNs most likely were partially activated. Some active mPR3 and mNE were active on the surface of mPMNs and might have converted Ch_MIP-2 to MIP-2(5-73). MIP-2(5-73) in turn could bind to CXCR2 and thereby triggered receptor internalization. To verify my hypothesis, I used PR3/NE deficient mPMNs. As these knockout mPMNs did not express mPR3 and mNE anymore, they should be unable to convert Ch_MIP2 and hence CXCR2 should remain on the surface. In line with my prediction CXCR2 on PR3/NE deficient mPMNs did not get internalized after incubation with Ch_MIP-2, while the other three isoforms still induced receptor internalization. With this experiment, I was able to demonstrate that active mPR3 and mNE is on the surface of activated wt mPMNs. This finding is remarkable, because mPR3 and mNE were normally stored in the primary granules, which were the type of granules to be discharged last (Borregaard et al., 2007).

I did not detect a difference between MIP-2(1-73), MIP-2(5-73) and MIP-2_Ru. The chemotactic strength was either not correlated to the binding affinity to the receptor or I used too much MIP-2, and so saturated the receptor with all variants. I tried to lower the amount of MIP-2, but still could not see a difference. I think the concentration of MIP-2 was not measured accurately enough to notice small differences in bioactivity.

MIP-2 is not the only CXC ELR^+ chemokine; there is also KC (CXCL1), DCIP-1 (CXCL3) and LIX (CXCL5). As the N-terminal sequence showed suitable cleavage sites for mPR3 and mNE, I tested whether one of the other chemokines could also be processed. DCIP-1 had actually the same N-terminal sequence as MIP-2 and thus could definitely be processed by mPR3 and mNE. As done in the case of MIP-2, substrates

featuring the N-terminal sequence of these chemokines were ordered. Lysates of wt mPMNs could cleave all three sequences, implying that all chemokines could be processed by neutrophil proteases. After incubating the LIX- substrate with lysates of PR3/NE knockout mPMNs, I did not observe any cleavage. The only endoproteases of mPMNs capable of cleaving LIX were found to be mPR3 and mNE. But the substrate did not feature the whole N-terminus of LIX as LIX had a longer N-terminus than the other chemokines. So other proteases could still cleave the remaining N-terminus not covered by the substrate. In fact, it has been reported that MMP-8 could process LIX after Ser^4 and that this cleavage enhanced its chemotactic activity (Tester et al., 2007). LIX could be further shortened by mPR3 and was thus an interesting target for mNE. Besides that the longer N-terminus protected LIX from exopeptidase trimming. The KC-derived substrate, however, was still cleaved by the lysate of PR3/NE deficient mPMNs. Evidently, some other endoproteases could also cleave KC.

In conclusion, mPR3 and mNE could process the N-terminus of some CXC ELR^+ chemokines. In the case of MIP-2 this led to an enhancement of the chemotactic properties. Lysate, supernatant and mPMNs were able to cleave MIP-2 and to induce CXCR2 receptor internalization. Of course *in vivo* evidence for these processing events are needed. Detecting MIP-2 was very hard as the concentration range is normally between 100-1000 pM. To this end I have set up a cooperation with David Meierhoff (MPI Berlin). Targeted mass spectrometry was very sensitive and the detection limit of MIP-2 was down to 1 fM. Up to now, we have established a working protocol. At the moment, we are analyzing biological samples from different inflammatory mouse models to see how chemokines are modified at the N-terminus *in vivo*.

5.2 NE escapes inhibition by self-cleavage

During the studies of NE, the appearance of two unexplained bands after enterokinase conversion attracted my interest. Further analysis revealed these as fragments of NE. Since only enterokinase and mNE were present in the sample, one of these two proteases came into question. The cleavage sites V^{178}/N^{179} and A^{188}/G^{189} pointed to mNE, as mNE was said to prefer small aliphatic residues (Hedstrom, 2002), whereas enterokinase cleaved after D_4K. NE was still cleaved, despite the addition of an enterokinase specific inhibitor (D_4K-cmk). This was the final proof for the self-cleavage of mNE. There were several possible functions for the self-cleavage. As already mentioned, self-cleavage of

trypsin was an important mechanism for the termination of its activity and could lead to either inactivation or even a change in specificity (Kay and Kassell, 1971; Whitcomb et al., 1996). Failure of this self-limiting mechanism actually resulted in a disease, called pancreatitis (Simon et al., 2002; Whitcomb et al., 1996). The question was therefore, whether these possibilities also applied to mNE. Especially the cleavage of the A^{188}/G^{189} peptide bond held great promise of uncovering new elastase properties. Not only was this site conserved throughout many species homologues, but also matched a self-cleavage site in trypsin at a topologically equivalent position (K^{188}/D^{189}). This cleavage site was located on a loop, which shaped the S1 pocket (Specificity et al., 1989). It has been shown that residue 189 is very important for substrate specificity. For example the Asp^{189} in trypsin was responsible for its preference to cleave after Arg or Lys (Hedstrom, 2002). Cleavage at this position was therefore of significant relevance for the activity of mNE. Moreover, this site A^{188}/G^{189} seemed to be the highly favored cleavage site in mNE, as it was always cleaved first. Once cleaved, a small portion of mNE was further processed at a second self-cleavage site. This suggests that the prime cleavage at A^{188}/G^{189} made the other minor cleavage site $V^{178}N^{179}$ more accessible to mNE.

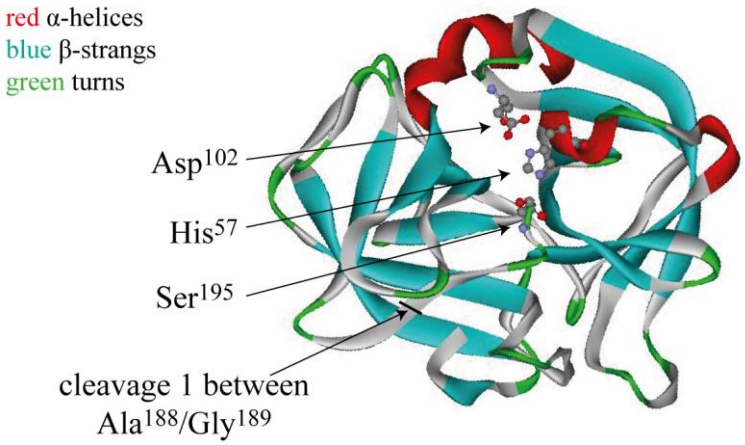

Fig 5.1: Autocleavage of human NE. Human NE is shown in the standard orientation according to Wolfram Bode. α-helices in red, β-sheets in blue and turns are painted in green. The catalytic triad residues, His^{57}, Asp^{102} and Ser^{195}, are depicted with their respective side chains. Human NE cleaved itself between Ala^{188} and Gly^{189}. As this loops is located on a loop that is essential for the shaping of the S1 pocket, a cleavage at this site is expected to have an impact on the substrate specificity of hNE. The raw data for the structure of hNE was obtained from the RCSB protein data bank (file number: 3Q76) and modified using the program Viewer Lite 5.0 (Accelrys Inc, San Diego).

Initial experiments on the activity of nicked mNE showed that it was moderately diminished but not completely destroyed. Thus, the primary purpose of this self-cleavage site was not the inactivation of mNE, although we found some hints that the double-cleaved mNE might be inactive. The first clue for this conclusion was found in an experiment, where a mixture of sc- and tc-mNE was incubated with biotinylated AAPV-inhibitor to visualize active mNE (**Fig4.12**). If all of the mNE retained its activity, the signals of the western blot and Coomassie staining should be the same. As the lower band was clearly weaker in the western blot compared to the amount of protein in this band, I suggested that the tc-mNE did not react with the inhibitor. As the lower band contained both a single-nicked mNE (cleaved between V^{178} and N^{179}) and a double-nicked mNE, a plausible interpretation was the loss of activity after the double-cut. But at this point in time, I had not shown the existence of double-nicked mNE. Every time when a peptide bond was hydrolyzed in mNE, a water molecule of 18 Da was added to the mNE molecule. As mass spectrometry was sensitive enough to actually detect the gained water molecule, NE was analyzed by mass spectrometry. Indeed, intact, single- and double-nicked mNE could be clearly differentiated. As expected, the peak for sc-mNE disappeared after the addition of the AAPV-cmk inhibitor. To my surprise, a small peak of single-cut mNE remained. But the highest unreactive peak was without a doubt the double-nicked mNE, which did not react with the inhibitor. I expected two new peaks for mNE-cmk complexes, but only found one. This peak was identified as the single-nicked mNE-cmk complex, so the intact mNE-cmk complex was missing. Altogether, I could show that double nicked mNE exist. And all the evidence indicated that double-nicked mNE was inactive.

Double-cutting of mNE occurred only to a small degree. Up to eight hours of incubation the lion's share of mNE modification was the single-nicked form, cleaved at A^{188}/G^{189}. Cleavage of trypsin at K^{188}/D^{189}, the topological precedent of the A^{188}/G^{189} cleavage in mNE, resulted in a change of specificity (Keil-Dlouhá et al., 1971; Smith and Shaw, 1969). Trypsin gained a chymotrypsin-like specificity (Keil-Dlouhá et al., 1971). Although, profiling of protease specificity with tandem mass spectrometry by Oliver Schilling did not reveal a drastic change of specificity in tc-mNE, I was nevertheless able to detect a change in substrate preferences. After testing several substrates, I recognized that tc-mNE had a narrower range of substrate specificity. While the tc-mNE activity was almost the same for certain substrates, it worsened considerably for others. A substrate

featuring the RCL of MNEI (Mca-GIATFCMLMPEQ-(Dnp)-rr) was a good example to illustrate this finding. The K_M/k_{cat} was in the same order for sc- and tc-mNE. By contrast the substrate with the RCL of α1PI (Mca-GEAIPMSIPPEVK(Dnp)-rr) was truly interesting. This sequence was a much worse substrate for tc-mNE than for sc-mNE. Because cleavage of the RCL was an absolute prerequisite for irreversible inhibition of mNE by α1PI, tc-NE appeared to be poorly inhibited by α1PI. As α1PI was demonstrated to be the most important inhibitor for mNE in our body, it was an exciting finding (Travis and Salvesen, 1983). NE was a protease with a very broad cleavage range. Why would this enzyme only cleave itself to reduce its substrate spectrum? One hypothesis for the function of this self-limiting substrate specificity is the following. Through self-inflicted restriction, NE could escape its inhibition by α1PI and could act longer on certain substrates. This would enable NE to focus its activity on a narrow circle of substrates. An ideal substrate for a long lasting activity should have an amplifying and regulatory function, as this would leverage the prolonged NE activity further. At present our knowledge about the most relevant regulatory substrates of NE is very limited, because most previous studies focused on the destructive nature of NE. Hence, I was unable to evaluate a suitable substrate in support of my hypothesis. Although I was unable to substantiate my idea along these lines, there was still the interesting observation of an impaired inhibition of tc-mNE by α1PI. The tc-mNE could not only enhance inflammation by regulating biological mediators, but could also have a longer action time to generate damage. In the introduction I already mentioned that patients with the Z-allel had reduced α1PI plasma levels. Low plasma levels and the impaired NE inhibition were blamed for the development of lung emphysema (Garver et al., 1986; Lomas et al., 1993). Because the Z-variant of α1PI tended to aggregate, it was speculated that these inclusion bodies themselves were responsible for emphysema development (Carrell et al., 1994; Gooptu et al., 2009). But it has also been reported, that patients that completely lacked α1PI in their plasma and are therefore unable to produce aggregates, still developed emphysema (Garver et al., 1986; Satoh et al., 1988). Hence impaired inhibition of tc-mNE by α1PI and prolonged activity appeared to be a pathogenic factor for emphysema.

First, I had to determine, whether tc-mNE was indeed less well inhibited by α1PI than sc-mNE. Although α1PI still formed complexes with tc-mNE, these complexes were formed more slowly. While sc-mNE reacted with α1PI within seconds, the reaction of

tc-mNE with α1PI took around 30 minutes. Not only complex formation was compromised, but also formation of the encounter complex was worse. The reaction of α1PI with mNE was described in two steps: First an encounter complex had to be assembled. Up to this time point the reaction was still reversible (Gettins, 2002; Travis and Salvesen, 1983). In the second step the enzyme attacked the RCL of α1PI and mNE and α1PI formed a covalent acyl-enzyme complex (Gettins, 2002; Travis and Salvesen, 1983). In a substrate reaction the substrate would be freed from the enzyme after hydrolysis of the acyl bond. But with α1PI a conformational change of α1PI distorted the active center of mNE, so the catalytical function of mNE was lost and mNE was irrevocably bound to α1PI (Gettins, 2002; Huntington, 2011; Travis and Salvesen, 1983). Here, the formation of the encounter complex was the limiting step. The parameter K_{ass} described the association rate between α1PI and mNE and was therefore a good indicator for inhibition efficiency. K_{ass} was 15 times worse for α1PI and tc-mNE, than α1PI and sc-mNE. Of course tc-mNE was not as efficient in cleaving certain substrates. It was e.g. five times worse for the substrate Mca-GIATFCMLMPEQ-(Dnp)-rr. But this 15-fold functional impairment toward tc-mNE was comparable with the reduction of α1PI levels in homozygous Z allel carrier (10-15%). Individuals that carried the Z α1PI as well as the normal M α1PI had only a 25-40% decrease in the plasma levels of α1PI ((Zorzetto et al., 2008). Under normal conditions these individuals were not at risk to develop emphysema. Only if an additional environmental factor added to it, these persons showed some decline in lung functions (Thun et al., 2012). If for example these persons developed a severe lung inflammatory disease, the high neutrophil infiltration of the lung would lead to increased levels of tc-mNE. I could clearly show that tc-mNE was less well inhibited by Z- α1PI as I could still detect tc-mNE activity, when sc-mNE was already inhibited. Since these high levels of tc-mNE were not properly inhibited, the risk for emphysema development would be tremendously increased. A high amount of tc-mNE alone might not lead to emphysema, but in combination with a trigger from the environment, e.g. smoking, infections, lung inflammation etc., it might worsen the prognosis.

I was able to show that α1PI inhibition was impaired after NE has nicked itself. But as we already knew that the substrate specificity was diminished, the question as to whether tc-mNE could still trigger emphysema remained to be answered. These studies have not been included in this thesis, but are currently performed in cooperation with Önder Yildirim. A first series of installation experiments showed that tc-mNE was still

pathogenic (data not shown). Tc-mNE was instilled into the respiratory tract of wt mice and after two months, emphysema development was observed. The data are still preliminary and have to be confirmed.

Today, patients suffering from severe α1PI deficiency were already treated with α1PI infusions in some European countries. But individuals that were only heterozygous for the Z-allel were not regarded as severely α1PI deficient and were thus not treated by α1PI substitution therapy. Conversely, NE has already been recognized as a drug target for the prevention or treatment of lung disease. Consequently, many inhibitors have been developed to target NE in the past decade. None of these inhibitors were successful in clinical trial or approved by the authorities. It is still not known why these inhibitors failed. One possible reason might be the overlooked tc-mNE. In cooperation with Astra Zeneca I obtained one of these failed inhibitors and compared its efficiency against sc- and tc-mNE. The difference in their ability to inhibit sc- and tc-mNE was indeed greater than that of α1PI. Tc-mNE was insufficiently blocked by AZ111177 and therefore escaped these inhibitors. This may be the reason why this substance could not prevent further damage.

Last but not least, as all experiments so far were done *in vitro*, the existence of tc-mNE *in vivo* had to be verified. In their native forms, the difference between sc- and tc-mNE was only one water molecule. Hence, western blot analysis under reducing conditions was the easiest way to detect tc-mNE. Since PMNs were the main source of NE, they were my first target. With the help of recombinant mNE, I was able to find an anti-hNE antibody that crossreacted with mNE and was suited for western blot analysis. The lysate of PR3/NE deficient PMNs was loaded as a negative control. I found two bands in wt PMN lysate that were clearly missing in PR3/NE deficient lysate. On these grounds I concluded that these bands were mNE. The upper band had the expected weight for sc-mNE, while the lower band is most likely tc-mNE. With this antibody tc-mNE had been successfully detected in a biological sample. The purification of mPMNs made use of a percoll gradient. PMNs were slightly activated by this procedure and so tc-mNE could be an artifact of the purification. That is why I repeated the experiments with whole bone marrow cells. The result was the same as with mPMNs (data not shown). In the case of hPMNs, I did not merely prove the existence of the tc-mNE form, but also demonstrated that it is active. By incubating the lysate with biotinylated AAPV-cmk inhibitor first, I have tagged all active hNE molecules. Subsequent immunoprecipitation with an anti-hNE

antibody had guaranteed the identification of hNE. I was able to detect active sc- and tc-hNE in hPMNs. Further evidence for the natural occurrence of tc-NE could be found in the literature. Starkey et al. purified elastase from spleen using CM-cellulose and verified its identity with different substrates (Starkey and Barrett, 1976). SDS-PAGE of elastase revealed three distinct bands under reducing conditions at around 27, 15-20 and 10-13 kDa. The sizes of these bands were estimated from the gel and fitted our data very well. In another study NE was purified from leukocytes. Additional to the purification with CM-cellulose a column with aprotinin, a serine protease inhibitor, was used (Baugh and Travis, 1976). Although the authors did not comment on this, a second band was visible after the purification with aprotinin. Since a marker was missing on the SDS gel, I was not able to judge whether the size fits tc-mNE. During i*n vitro* studies with hNE, tc-hNE appeared after 168 hours (Padrines et al., 1989). Relatively low concentrations of only 100 nM were used. This was probably the reason that the reaction took so long. In an attempt to elucidate the biosynthetic profile of hNE during PMN maturation, Garwicz et al. differentiated bone marrow progenitor cells and analyzed them at different days (Garwicz et al., 2005). After immunoprecipitation with an anti-hNE antibody, the samples were run on a SDS-PAGE. Two bands were visible on the SDS-PAGE. Clearly the nicking of NE has already been seen since 1976, but obviously ignored as unimportant or an artifact from purification. These findings as well pointed to the existence of tc-NE *in vivo.*

Taken together our studies showed that tc-NE was able to escape inhibition. Bearing the pathophysiological role of NE in mind, this was especially important, as tc-NE was longer active and could cause damage for a longer period of time. Up to now tc-mNE was never considered as a separate target during the development of therapeutical inhibitors and therefore these inhibitors were not designed to inactivate the tc-NE sufficiently. In an attempt to find a suitable inhibitor, I mutated the RCL of α1PI. I replaced Met^{358} with Met, Thr and Cys, because the difference between sc-and tc-mNE was smaller when using substrates featuring these mutations (data not shown). All three α1PI variants were able to inhibit sc- and tc-mNE irreversible, but I did not determine yet whether these α1PI variants inhibit tc-mNE better.

5.3 Conclusion

In conclusion, these studies demonstrated the beneficial and destructive effects of PR3 and NE as pro-inflammatory actors. I could show that PR3 and NE process chemokines, thereby enhancing the chemotactic properties of the chemokines. The PMNs were attracted to the inflammatory site by a chemokine gradient. Once they arrived at the inflammatory site they released PR3 and NE. Because of the high inhibitor concentrations, PR3 and NE were probably only active in a small area surrounding the neutrophil (Campbell et al., 1999). In this small activity zone, PR3 and NE could convert the chemokines to their more active form. This in turn would steepen the gradient and accelerate the recruitment of other neutrophils.

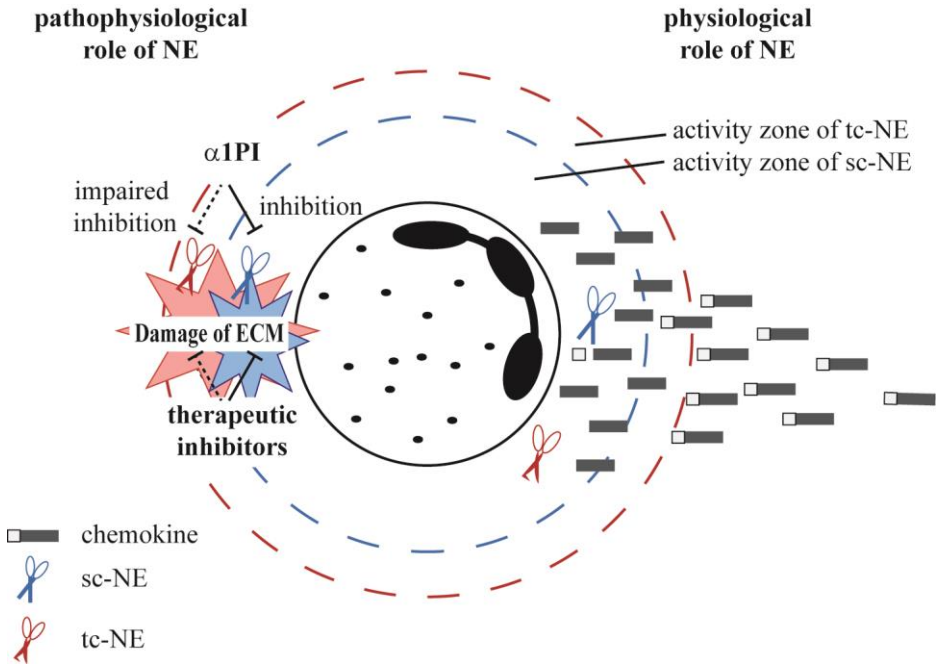

Fig 5.2: Impact of extracellular NE. PR3 and NE are only active in a small area around the neutrophil before they are inactivated by the high inhibitor concentrations in their surroundings. Chemokines that are in the action radius are converted to their more active form by PR3 and NE. This steepens the chemokine gradient and accelerates the neutrophil recruitment. The action radius of the tc-mNE (red) is larger than that of the sc-mNE (blue), because it is more slowly inhibited by α1PI. This protracted activity of tc-mNE also extends the time during which tc-mNE can generate damage. Small molecule inhibitors developed against NE, inhibited tc-NE only insufficiently.

On the one hand the pro-inflammatory quality of extracellular functions warranted a fast response towards intruders; on the other hand uncontrolled activity of NE would be harmful and could cause emphysema. In this work, I was able to show a mechanism, in which NE could escape inhibition by α1PI. NE cleaved itself at high concentration as found in phagolysosomes. The resulting tc-NE had a narrower substrate specificity, which in turn impaired inhibition by the natural inhibitor α1PI. The action radius of tc-NE was therefore larger than that of sc-NE. Small molecule inhibitors developed for therapeutic applications inhibited tc-NE insufficiently.

Understanding the pro-inflammatory role of NE and PR3 is necessary for better intervention during disease. In chronic inflammation inhibition of NE might prove beneficial. The existence of tc-NE should be taken into account for the development of suitable inhibitors for both forms of NE.

6 Bibliography

Appelberg, R. (2007). Neutrophils and intracellular pathogens: beyond phagocytosis and killing. Trends Microbiol. *15*, 87–92.

Baggiolini, M. (2001). Chemokines in pathology and medicine. J. Intern. Med. *250*, 91–104.

Barnes, P.J., Shapiro, S.D., and Pauwels, R.A. (2003). Chronic obstructive pulmonary disease: molecular and cellular mechanisms. Eur. Respir. J. *22*, 672–688.

Barroso, B., Abello, N., and Bischoff, R. (2006). Study of human lung elastin degradation by different elastases using high-performance liquid chromatography/mass spectrometry. Anal. Biochem. *358*, 216–224.

Baugh, R.J., and Travis, J. (1976). Human leukocyte granule elastase: rapid isolation and characterization. Biochemistry *15*, 836–841.

Beatty, K., Matheson, N., and Travis, J. (1984). Kinetic and chemical evidence for the inability of oxidized alpha 1-proteinase inhibitor to protect lung elastin from elastolytic degradation. Hoppe. Seylers. Z. Physiol. Chem. *365*, 731–736.

Belaaouaj, A., McCarthy, R., Baumann, M., Gao, Z., Ley, T.J., Abraham, S.N., and Shapiro, S.D. (1998). Mice lacking neutrophil elastase reveal impaired host defense against gram negative bacterial sepsis. Nat. Med. *4*, 615–618.

Belaaouaj, A., Kim, K.S., and Shapiro, S.D. (2000). Degradation of outer membrane protein A in Escherichia coli killing by neutrophil elastase. Science *289*, 1185–1188.

Benarafa, C., Cooley, J., Zeng, W., Bird, P.I., and Remold-O'Donnell, E. (2002). Characterization of four murine homologs of the human ov-serpin monocyte neutrophil elastase inhibitor MNEI (SERPINB1). J. Biol. Chem. *277*, 42028–42033.

Berg, J.M., Tymoczko, J.L., and Stryer, L. (2003). Biochemie (New York: Spektrum Akademischer Verlag).

Bode, W. (1979). The transition of bovine trypsinogen to a trypsin-like state upon strong ligand binding. II. The binding of the pancreatic trypsin inhibitor and of isoleucine-valine and of sequentially related peptides to trypsinogen and to p-guanidinobenzoate-trypsinoge. J. Mol. Biol. *127*, 357–374.

Bode, W., Schwager, P., and Huber, R. (1978). The transition of bovine trypsinogen to a trypsin-like state upon strong ligand binding. The refined crystal structures of the bovine trypsinogen-pancreatic trypsin inhibitor complex and of its ternary complex with Ile-Val at 1.9 A resolution. J. Mol. Biol. *118*, 99–112.

Borregaard, N. (2010). Neutrophils, from marrow to microbes. Immunity *33*, 657–670.

Borregaard, N., Sørensen, O.E., and Theilgaard-Mönch, K. (2007). Neutrophil granules: a library of innate immunity proteins. Trends Immunol. *28*, 340–345.

Brinkmann, V., Reichard, U., Goosmann, C., Fauler, B., Uhlemann, Y., Weiss, D.S., Weinrauch, Y., and Zychlinsky, A. (2004). Neutrophil extracellular traps kill bacteria. Science *303*, 1532–1535.

Brodrick, J.W., Largman, C., Johnson, J.H., and Geokas, M.C. (1978). Human cationic trypsinogen. Purification, characterization, and characteristics of autoactivation. J. Biol. Chem. *253*, 2732–2736.

Campbell, E.J., Campbell, M.A., Boukedes, S.S., and Owen, C.A. (1999). Quantum proteolysis by neutrophils: implications for pulmonary emphysema in α1-antitrypsin deficiency. J. Clin. Invest. *104*, 337–344.

Campbell, E.J., Campbell, M.A., and Owen, C.A. (2000). Bioactive proteinase 3 on the cell surface of human neutrophils: quantification, catalytic activity, and susceptibility to inhibition. J. Immunol. *165*, 3366–3374.

Carrell, R.W., Whisstock, J., and Lomas, D.A. (1994). Conformational changes in serpins and the mechanism of α1-antitrypsin deficiency. Am. J. Respir. Crit. Care Med. *150*, S171–175.

Chen, J.M., Montier, T., and Férec, C. (2001). Molecular pathology and evolutionary and physiological implications of pancreatitis-associated cationic trypsinogen mutations. Hum. Genet. *109*, 245–252.

Chua, F., and Laurent, G.J. (2006). Neutrophil elastase: mediator of extracellular matrix destruction and accumulation. Proc. Am. Thorac. Soc. *3*, 424–427.

Clark-Lewis, I., Schumacher, C., Baggiolini, M., and Moser, B. (1991). Structure-activity relationships of interleukin-8 determined using chemically synthesized analogs. Critical role of NH2-terminal residues and evidence for uncoupling of neutrophil chemotaxis, exocytosis, and receptor binding activities. J. Biol. Chem. *266*, 23128–23134.

Cooley, J., Takayama, T.K., Shapiro, S.D., Schechter, N.M., and Remold-O'Donnell, E. (2001). The serpin MNEI inhibits elastase-like and chymotrypsin-like serine proteases through efficient reactions at two active sites. Biochemistry *40*, 15762–15770.

Dale, D.C., Bolyard, A.A., and Aprikyan, A. (2002). Cyclic neutropenia. Semin. Hematol. *39*, 89–94.

Dale, D.C., Boxer, L., and Liles, W.C. (2008). The phagocytes: neutrophils and monocytes. Blood *112*, 935–945.

Dalgıc, B., Bukulmez, A., and Sarı, S. (2011). Eponym: Papillon-Lefevre syndrome. Eur. J. Pediatr. *170*, 689–691.

Dean, R.A., Cox, J.H., Bellac, C.L., Doucet, A., Starr, A.E., and Overall, C.M. (2008). Macrophage-specific metalloelastase (MMP-12) truncates and inactivates ELR+ CXC

chemokines and generates CCL2, -7, -8, and -13 antagonists: potential role of the macrophage in terminating polymorphonuclear leukocyte influx. Blood *112*, 3455–3464.

Döring, G., Frank, F., Boudier, C., Herbert, S., Fleischer, B., and Bellon, G. (1995). Cleavage of lymphocyte surface antigens CD2, CD4, and CD8 by polymorphonuclear leukocyte elastase and cathepsin G in patients with cystic fibrosis. J. Immunol. *154*, 4842–4850.

Duranton, J., and Bieth, J.G. (2003). Inhibition of proteinase 3 by α1-antitrypsin in vitro predicts very fast inhibition in vivo. Am. J. Respir. Cell Mol. Biol. *29*, 57–61.

Fujita, J., Nelson, N.L., Daughton, D.M., Dobry, C. a, Spurzem, J.R., Irino, S., and Rennard, S.I. (1990). Evaluation of elastase and antielastase balance in patients with chronic bronchitis and pulmonary emphysema. Am. Rev. Respir. Dis. *142*, 57–62.

Garver, R.I., Mornex, J.F., Nukiwa, T., Brantly, M., Courtney, M., LeCocq, J.P., and Crystal, R.G. (1986). Alpha 1-antitrypsin deficiency and emphysema caused by homozygous inheritance of non-expressing alpha 1-antitrypsin genes. N. Engl. J. Med. *314*, 762–766.

Garwicz, D., Lennartsson, A., Jacobsen, S.E.W., Gullberg, U., and Lindmark, A. (2005). Biosynthetic profiles of neutrophil serine proteases in a human bone marrow-derived cellular myeloid differentiation model. Haematologica *90*, 38–44.

Gettins, P.G.W. (2002). Serpin structure, mechanism, and function. Chem. Rev. *102*, 4751–4804.

Gooptu, B., and Lomas, D. a (2009). Conformational pathology of the serpins: themes, variations, and therapeutic strategies. Annu. Rev. Biochem. *78*, 147–176.

Gooptu, B., Ekeowa, U.I., and Lomas, D.A. (2009). Mechanisms of emphysema in alpha1-antitrypsin deficiency: molecular and cellular insights. Eur. Respir. J. *34*, 475–488.

De Haar, S.F., Jansen, D.C., Schoenmaker, T., De Vree, H., Everts, V., and Beertsen, W. (2004). Loss-of-function mutations in cathepsin C in two families with Papillon-Lefèvre syndrome are associated with deficiency of serine proteinases in PMNs. Hum. Mutat. *23*, 524.

De Haar, S.F., Hiemstra, P.S., van Steenbergen, M.T.J.M., Everts, V., and Beertsen, W. (2006). Role of polymorphonuclear leukocyte-derived serine proteinases in defense against Actinobacillus actinomycetemcomitans. Infect. Immun. *74*, 5284–5291.

Hedstrom, L. (2002). Serine protease mechanism and specificity. Chem. Rev. *102*, 4501–4524.

Heinz, A., Jung, M.C., Jahreis, G., Rusciani, A., Duca, L., Debelle, L., Weiss, A.S., Neubert, R.H.H., and Schmelzer, C.E.H. (2012). The action of neutrophil serine proteases on elastin and its precursor. Biochimie *94*, 192–202.

Henriksen, P.A., and Sallenave, J. (2008). Human neutrophil elastase: mediator and therapeutic target in atherosclerosis. Int. J. Biochem. Cell Biol. *40*, 1095–1100.

Hopkins, P.C., Carrell, R.W., and Stone, S.R. (1993). Effects of mutations in the hinge region of serpins. Biochemistry *32*, 7650–7657.

Hortin, G.L., Sviridov, D., and Anderson, N.L. (2008). High-abundance polypeptides of the human plasma proteome comprising the top 4 logs of polypeptide abundance. Clin. Chem. *54*, 1608–1616.

Horwitz, M.S., Duan, Z., Korkmaz, B., Lee, H.-H., Mealiffe, M.E., and Salipante, S.J. (2007). Neutrophil elastase in cyclic and severe congenital neutropenia. Blood *109*, 1817–1824.

Huntington, J. a (2011). Serpin structure, function and dysfunction. J. Thromb. Haemost. *9 Suppl 1*, 26–34.

Janeway, C.A.J., Travers, P., Walport, M., and Slomchik, M. (2005). Immunobiology: The immune system in health and disease (Garland Science Publishing).

Kallenberg, C.G.M., Heeringa, P., and Stegeman, C. a (2006). Mechanisms of Disease: pathogenesis and treatment of ANCA-associated vasculitides. Nat. Clin. Pract. Rheumatol. *2*, 661–670.

Kasama, T., Miwa, Y., Isozaki, T., Odai, T., Adachi, M., and Kunkel, S.L. (2005). Neutrophil-derived cytokines: potential therapeutic targets in inflammation. Curr. Drug Targets. Inflamm. Allergy *4*, 273–279.

Kay, J., and Kassell, B. (1971). The autoactivation of trypsinogen. J. Biol. Chem. *246*, 6661–6665.

Keil-Dlouhá, V., Zylber, N., Imhoff, J.-M., Tong, N.-T., and Keil, B. (1971). Proteolytic activity of pseudotrypsin. FEBS Lett. *16*, 291–295.

Kelly, E., Greene, C.M., and McElvaney, N.G. (2008). Targeting neutrophil elastase in cystic fibrosis. Expert Opin. Ther. Targets *12*, 145–157.

Kessenbrock, K., Fröhlich, L., Sixt, M., Lämmermann, T., Pfister, H., Bateman, A., Belaaouaj, A., Ring, J., Ollert, M., Fässler, R., et al. (2008). Proteinase 3 and neutrophil elastase enhance inflammation in mice by inactivating antiinflammatory progranulin. J. Clin. Invest. *118*, 2438–2447.

Kessenbrock, K., Krumbholz, M., Schönermarck, U., Back, W., Gross, W.L., Werb, Z., Gröne, H.-J., Brinkmann, V., and Jenne, D.E. (2009). Netting neutrophils in autoimmune small-vessel vasculitis. Nat. Med. *15*, 623–625.

Kessenbrock, K., Dau, T., and Jenne, D.E. (2011). Tailor-made inflammation: how neutrophil serine proteases modulate the inflammatory response. J. Mol. Med. (Berl). *89*, 23–28.

Klein, C. (2009). Congenital neutropenia. Hematology Am. Soc. Hematol. Educ. Program 344–350.

Korkmaz, B., Horwitz, M.S., Jenne, D.E., and Gauthier, F. (2010). Neutrophil elastase, proteinase 3, and cathepsin G as therapeutic targets in human diseases. Pharmacol. Rev. *62*, 726–759.

Lawrence, T., Willoughby, D.A., and Gilroy, D.W. (2002). Anti-inflammatory lipid mediators and insights into the resolution of inflammation. Nat. Rev. Immunol. *2*, 787–795.

Liou, T.G., and Campbell, E.J. (1995). Nonisotropic enzyme-inhibitor interactions: a novel nonoxidative mechanism for quantum proteolysis by human neutrophils. Biochemistry *34*, 16171–16177.

Liu, Z., Zhou, X., Shapiro, S.D., Shipley, J.M., Twining, S.S., Diaz, L.A., Senior, R.M., and Werb, Z. (2000). The serpin α1-proteinase inhibitor is a critical substrate for gelatinase B/MMP-9 in vivo. Cell *102*, 647–655.

Lomas, D.A., Evans, D.L., Stone, S.R., Chang, W.S., and Carrell, R.W. (1993). Effect of the Z mutation on the physical and inhibitory properties of α1-antitrypsin. Biochemistry *32*, 500–508.

Makowski, G.S., and Ramsby, M.L. (2005). Autoactivation profiles of calcium-dependent matrix metalloproteinase-2 and -9 in inflammatory synovial fluid: effect of pyrophosphate and bisphosphonates. Clin. Chim. Acta. *358*, 182–191.

McDonald, M.R., and Kunitz, M. (1941). The effect of calcium and other ions on the autocatalytic formation of trypsin from trypsinogen. J. Gen. Physiol. *25*, 53–73.

Metcalf, D. (1991). Control of granulocytes and macrophages: molecular, cellular, and clinical aspects. Science *254*, 529–533.

Mortier, A., Van Damme, J., and Proost, P. (2008). Regulation of chemokine activity by posttranslational modification. Pharmacol. Ther. *120*, 197–217.

Nathan, C. (2006). Neutrophils and immunity: challenges and opportunities. Nat. Rev. Immunol. *6*, 173–182.

Nourshargh, S., Perkins, J.A., Showell, H.J., Matsushima, K., Williams, T.J., and Collins, P.D. (1992). A comparative study of the neutrophil stimulatory activity in vitro and pro-inflammatory properties in vivo of 72 amino acid and 77 amino acid IL-8. J. Immunol. *148*, 106–111.

Owen, C.A., and Campbell, E.J. (1999). The cell biology of leukocyte-mediated proteolysis. J. Leukoc. Biol. *65*, 137–150.

Owen, C.A., Campbell, M.A., Sannes, P.L., Boukedes, S.S., and Campbell, E.J. (1995). Cell surface-bound elastase and cathepsin G on human neutrophils: a novel, non-

oxidative mechanism by which neutrophils focus and preserve catalytic activity of serine proteinases. J. Cell Biol. *131*, 775–789.

Padrines, M., Schneider-Pozzer, M., and Bieth, J.G. (1989). Inhibition of neutrophil elastase by alpha-1-proteinase inhibitor oxidized by activated neutrophils. Am. Rev. Respir. Dis. *139*, 783–790.

Padrines, M., Wolf, M., Walz, a, and Baggiolini, M. (1994). Interleukin-8 processing by neutrophil elastase, cathepsin G and proteinase-3. FEBS Lett. *352*, 231–235.

Perera, N.C., Schilling, O., Kittel, H., Back, W., Kremmer, E., and Jenne, D.E. (2012). NSP4, an elastase-related protease in human neutrophils with arginine specificity. Proc. Natl. Acad. Sci. U. S. A. *109*, 6229–6234.

Pham, C.T.N. (2006). Neutrophil serine proteases: specific regulators of inflammation. Nat. Rev. Immunol. *6*, 541–550.

Pham, C.T.N. (2008). Neutrophil serine proteases fine-tune the inflammatory response. Int. J. Biochem. Cell Biol. *40*, 1317–1333.

Proost, P., Loos, T., Mortier, A., Schutyser, E., Gouwy, M., Noppen, S., Dillen, C., Ronsse, I., Conings, R., Struyf, S., et al. (2008). Citrullination of CXCL8 by peptidylarginine deiminase alters receptor usage, prevents proteolysis, and dampens tissue inflammation. J. Exp. Med. *205*, 2085–2097.

Raptis, S.Z., Shapiro, S.D., Simmons, P.M., Cheng, A.M., and Pham, C.T.N. (2005). Serine protease cathepsin G regulates adhesion-dependent neutrophil effector functions by modulating integrin clustering. Immunity *22*, 679–691.

Reeves, E.P., Lu, H., Jacobs, H.L., Messina, C.G.M., Bolsover, S., Gabella, G., Potma, E.O., Warley, A., Roes, J., and Segal, A.W. (2002). Killing activity of neutrophils is mediated through activation of proteases by K+ flux. Nature *416*, 291–297.

Rinderknecht, H. (1986). Activation of pancreatic zymogens. Normal activation, premature intrapancreatic activation, protective mechanisms against inappropriate activation. Dig. Dis. Sci. *31*, 314–321.

Roghanian, A., and Sallenave, J. (2008a). Neutrophil elastase (NE) and NE inhibitors: canonical and noncanonical functions in lung chronic inflammatory diseases (cystic fibrosis and chronic obstructive pulmonary disease). J. Aerosol Med. Pulm. Drug Deliv. *21*, 125–144.

Roghanian, A., and Sallenave, J.-M. (2008b). Neutrophil elastase (NE) and NE inhibitors: canonical and noncanonical functions in lung chronic inflammatory diseases (cystic fibrosis and chronic obstructive pulmonary disease). J. Aerosol Med. Pulm. Drug Deliv. *21*, 125–144.

Satoh, K., Nukiwa, T., Brantly, M., Garver, R.I., Hofker, M., Courtney, M., and Crystal, R.G. (1988). Emphysema associated with complete absence of alpha 1- antitrypsin in

serum and the homozygous inheritance [corrected] of a stop codon in an alpha 1-antitrypsin-coding exon. Am. J. Hum. Genet. *42*, 77–83.

Scapini, P., Lapinet-Vera, J.A., Gasperini, S., Calzetti, F., Bazzoni, F., and Cassatella, M.A. (2000). The neutrophil as a cellular source of chemokines. Immunol. Rev. *177*, 195–203.

Senior, R.M., Tegner, H., Kuhn, C., Ohlsson, K., Starcher, B.C., and Pierce, J.A. (1977). The induction of pulmonary emphysema with human leukocyte elastase. Am. Rev. Respir. Dis. *116*, 469–475.

Simon, P., Weiss, F.U., Sahin-Toth, M., Parry, M., Nayler, O., Lenfers, B., Schnekenburger, J., Mayerle, J., Domschke, W., and Lerch, M.M. (2002). Hereditary pancreatitis caused by a novel PRSS1 mutation (Arg-122 → Cys) that alters autoactivation and autodegradation of cationic trypsinogen. J. Biol. Chem. *277*, 5404–5410.

Smith, R.L., and Shaw, E. (1969). Pseudotrypsin. A modified bovine trypsin produced by limited autodigestion. J. Biol. Chem. *244*, 4704–4712.

Specificity, S., Inhibitorst, M., Bode, W., Meyer, E., and Powers, J.C. (1989). Perspectives in Biochemistry Human Leukocyte and Porcine Pancreatic Elastase : X-ray Crystal Structures ,. *28*.

Starkey, P.M., and Barrett, A.J. (1976). Neutral proteinases of human spleen. Purification and criteria for homogeneity of elastase and cathepsin G. Biochem. J. *155*, 255–263.

Stoller, J.K., and Aboussouan, L.S. (2012). A review of α1-antitrypsin deficiency. Am. J. Respir. Crit. Care Med. *185*, 246–259.

Tester, A.M., Cox, J.H., Connor, A.R., Starr, A.E., Dean, R.A., Puente, X.S., López-Otín, C., and Overall, C.M. (2007). LPS responsiveness and neutrophil chemotaxis in vivo require PMN MMP-8 activity. PLoS One *2*, e312.

Thun, G.-A., Ferrarotti, I., Imboden, M., Rochat, T., Gerbase, M., Kronenberg, F., Bridevaux, P.-O., Zemp, E., Zorzetto, M., Ottaviani, S., et al. (2012). SERPINA1 PiZ and PiS heterozygotes and lung function decline in the SAPALDIA cohort. PLoS One *7*, e42728.

Travis, J., and Salvesen, G.S. (1983). Human plasma proteinase inhibitors. Annu. Rev. Biochem. *52*, 655–709.

Travis, J., Shieh, B.H., and Potempa, J. (1988). The functional role of acute phase plasma proteinase inhibitors. Tokai J. Exp. Clin. Med. *13*, 313–320.

Voynow, J.A., Fischer, B.M., and Zheng, S. (2008). Proteases and cystic fibrosis. Int. J. Biochem. Cell Biol. *40*, 1238–1245.

Whitcomb, D.C., Gorry, M.C., Preston, R.A., Furey, W., Sossenheimer, M.J., Ulrich, C.D., Martin, S.P., Gates, L.K., Amann, S.T., Toskes, P.P., et al. (1996). Hereditary

pancreatitis is caused by a mutation in the cationic trypsinogen gene. Nat. Genet. *14*, 141–145.

Wolf, M., Albrecht, S., and Märki, C. (2008). Proteolytic processing of chemokines: implications in physiological and pathological conditions. Int. J. Biochem. Cell Biol. *40*, 1185–1198.

Zhou, A., Carrell, R.W., and Huntington, J.A. (2001). The serpin inhibitory mechanism is critically dependent on the length of the reactive center loop. J. Biol. Chem. *276*, 27541–27547.

Zhu, J., Nathan, C., Jin, W., Sim, D., Ashcroft, G.S., Wahl, S.M., Lacomis, L., Erdjument-Bromage, H., Tempst, P., Wright, C.D., et al. (2002). Conversion of proepithelin to epithelins: roles of SLPI and elastase in host defense and wound repair. Cell *111*, 867–878.

Zorzetto, M., Russi, E., Senn, O., Imboden, M., Ferrarotti, I., Tinelli, C., Campo, I., Ottaviani, S., Scabini, R., von Eckardstein, A., et al. (2008). SERPINA1 gene variants in individuals from the general population with reduced α1-antitrypsin concentrations. Clin. Chem. *54*, 1331–1338.

7 Abbreviations

α1PI	a1-protease inhibitor
ABTS	2,2'-azino-bis(3-ethylbenzothiazoline-6-sulphonic acid)
Abz	2-aminobenzoyl
AMC	7-amino-4-methylcoumarin
ANCA	antineutrophil cytoplasmic autoantibodies
ATP	adenosine-5'-triphosphate
BCA	bicinchoninic acid
CG	cathepsin G
Ch	cherry
cmk	chloromethyl ketone
COPD	chronic obstructive pulmonary disease
CXCR2	C-X-C chemokine receptor type 2
DNA	deoxyribonucleic acid
DPPI	dipeptidyl peptidase I
EBNA	Epstein-Barr nuclear antigen
ECM	extracellular matrix
EDDnp	N-(2,4-dinitrophenyl)ethylenediamine
EDTA	ethylenediaminetetraacetic acid
ELISA	enzyme-linked immunosorbent assay
FCS	fetal calf serum
Fret	fluorescence resonance energy transfer
GPA	granulomatosis with polyangiitis
HBSS	Hank's balanced salt solution
HEK	human embryonic kidney cells
HRP	horseraddish peroxidase
IC	immune complex
IL-8	interleukin-8
K_{ass}	association constant
k_{cat}	catalytical constant
K_i	inhibitor constant
$K_{i(app)}$	apparent inhibitor constant
K_M	Michaelis-Menten concentration

ko	knockout
k_{obs}	observed constant
LIX	LPS-induced CXC ckemokine
MIP-2	macrophage inflammatory protein 2
MMP	matrix metalloproteinase
MNEI	monocyte neutrophil elastase inhibitor
NE	neutrophil elastase
NPGB	p-nitrophenyl p-guanidinobenzoate hydrochloride
NSP	neutrophil serine protease
PBMC	peripheral blood mononuclear cell
PBS	phosphate buffered saline
PCR	polymerase chain reaction
PEI	polyethylenimine
PLS	Papillon-Lefèvre sndrome
PMA	phorbol myristate acetate
PMN	polymorphonuclear neutrophilic granulocytes
pNA	p-nitroanilide
PR3	proteinase 3
PVDF	polyvinylidene fluoride
RCL	reactive center loop
ROS	reactive oxgen species
ROS	reactive oxygen species
RPMI	Roswell Park Memorial Institute medium
Ru	ruby
SBzl	thiobenzyl ester
sc	single chain
SDS	sodium dodecyl sulfate
TAE	tris-acetate-EDTA
tc	two chain
TNFα	tumor necrosis factor α
TPCK	L-1-tosylamide-2-phenylethyl chloromethyl ketone
v_{max}	maximum velocity
wt	wildtype
Z a1PI	Z variant of a1PI

8 Appendix

8.1 Vector map of pTT5

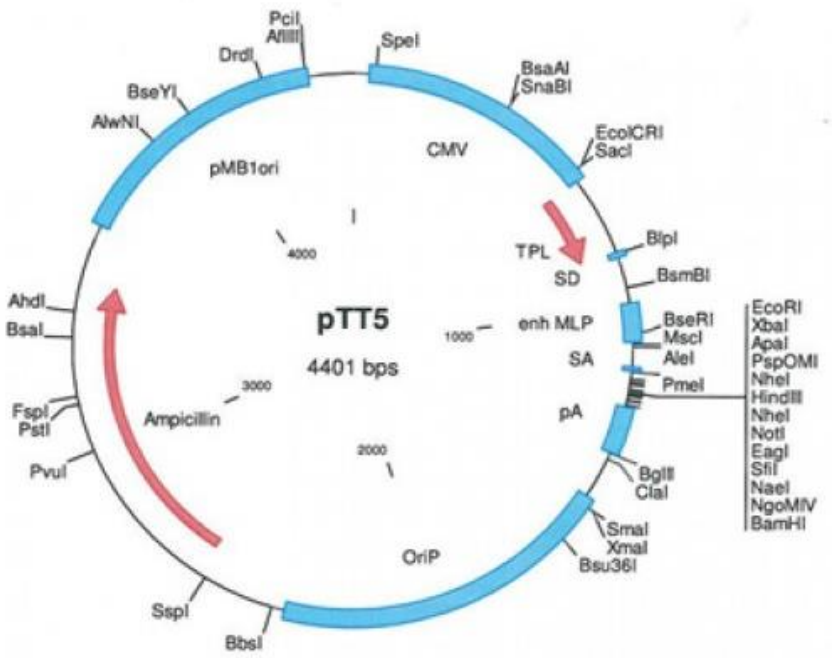

OriP: EBV origin of replication

pMB1 ori: bacterial origin of replication

CMV: Cytomegalovirus promoter

TPL: adenovirus tripartite leader

SD: splice donor

enh. MLP: enhanced major late promoter

SA: splice acceptor

pA: rabbit beta-globin polyadenylation site

8.2 Sequence of expressed proteins

Grey: Signalpeptide

Fat: His-tag

Underlined: propeptide with enterokinase cleavage site

8.2.1 pTT5_NGS_mNE(wt)_st.H6

```
M  E  T  D  T  L  L  L  W  V  L  L  L  W  V  P  G
ATGGAGACAGACACACTCCTGCTATGGGTACTGCTGCTCTGGGTACCAGG
         ^10       ^20       ^30       ^40       ^50
 S  T  G  S  R  M  H  R  N  G  S  H  V  D  D  D  D
TTCCACTGGTAGCCGCATGCACCGCAACGGCAGCCACGTGGATGACGACG
         ^60       ^70       ^80       ^90       ^100
  K  I  V  G  G  R  P  A  R  P  H  A  W  P  F  M
ACAAGATTGTTGGTGGCCGGCCGGCCCGGCCCCATGCTTGGCCCTTCATG
         ^110      ^120      ^130      ^140      ^150
A  S  L  Q  R  R  G  G  H  F  C  G  A  T  L  I  A
GCATCCCTGCAGAGGCGTGGAGGTCATTTCTGTGGTGCCACCCTCATTGC
         ^160      ^170      ^180      ^190      ^200
 R  N  F  V  M  S  A  A  H  C  V  N  G  L  N  F  R
CAGGAACTTCGTCATGTCAGCAGCCCACTGTGTGAACGGCCTAAATTTCC
         ^210      ^220      ^230      ^240      ^250
  S  V  Q  V  V  L  G  A  H  D  L  R  R  Q  E  R
GGTCAGTGCAGGTAGTGCTGGGAGCCCATGACCTGCGGCGACAGGAGCGC
         ^260      ^270      ^280      ^290      ^300
T  R  Q  T  F  S  V  Q  R  I  F  E  N  G  F  D  P
ACTCGACAGACCTTCTCTGTGCAGCGGATCTTCGAGAATGGCTTTGACCC
         ^310      ^320      ^330      ^340      ^350
 S  Q  L  L  N  D  I  V  I  I  Q  L  N  G  S  A  T
ATCACAACTGCTGAACGACATTGTGATTATCCAGCTCAATGGCTCCGCTA
         ^360      ^370      ^380      ^390      ^400
  I  N  A  N  V  Q  V  A  Q  L  P  A  Q  G  Q  G
CCATTAACGCCAACGTGCAGGTGGCCCAGCTGCCTGCCCAGGGCCAGGGC
         ^410      ^420      ^430      ^440      ^450
V  G  D  R  T  P  C  L  A  M  G  W  G  R  L  G  T
GTGGGTGACAGAACTCCATGTCTGGCCATGGGCTGGGGCAGGTTGGGCAC
         ^460      ^470      ^480      ^490      ^500
 N  R  P  S  P  S  V  L  Q  E  L  N  V  T  V  V  T
AAACAGACCATCACCCAGTGTGCTACAAGAGCTCAATGTGACAGTGGTGA
         ^510      ^520      ^530      ^540      ^550
  N  M  C  R  R  R  V  N  V  C  T  L  V  P  R  R
CTAACATGTGCCGCCGTCGTGTGAACGTATGCACTCTGGTGCCACGTCGG
         ^560      ^570      ^580      ^590      ^600

Q  A  G  I  C  F  G  D  S  G  G  P  L  V  C  N  N
CAGGCAGGCATCTGCTTCGGGGACTCTGGCGGACCCTTGGTCTGTAACAA
         ^610      ^620      ^630      ^650      ^650
```

```
 L  V  Q  G  I  D  S  F  I  R  G  G  C  G  S  G  L
CCTTGTCCAAGGCATTGACTCCTTCATCCGAGGAGGCTGTGGATCTGGAT
         ^660      ^670      ^680      ^690      ^700
  Y  P  D  A  F  A  P  V  A  E  F  A  D  W  I  N
TGTACCCAGATGCCTTCGCCCCTGTGGCTGAGTTTGCAGATTGGATCAAT
         ^710      ^720      ^730      ^740      ^750
S  I  I  R  K  P  R  H  H  H  H  H  H
TCCATTATTCGAAAGCCTAGGCATCATCACCATCACCAT
         ^760      ^770      ^780
```

8.2.2 pTT5_NGS_mNE-KG187/8_st.H6

```
M  E  T  D  T  L  L  L  W  V  L  L  L  W  V  P  G
ATGGAGACAGACACACTCCTGCTATGGGTACTGCTGCTCTGGGTACCAGG
         ^10       ^20       ^30       ^40       ^50
 S  T  G  S  R  M  H  R  N  G  S  H  V  D  D  D  D
TTCCACTGGTAGCCGCATGCACCGCAACGGCAGCCACGTGGATGACGACG
         ^60       ^70       ^80       ^90       ^100
  K  I  V  G  G  R  P  A  R  P  H  A  W  P  F  M
ACAAGATTGTTGGTGGCCGGCCGGCCCGGCCCCATGCTTGGCCCTTCATG
         ^110      ^120      ^130      ^140      ^150
A  S  L  Q  R  R  G  G  H  F  C  G  A  T  L  I  A
GCATCCCTGCAGAGGCGTGGAGGTCATTTCTGTGGTGCCACCCTCATTGC
         ^160      ^170      ^180      ^190      ^200
 R  N  F  V  M  S  A  A  H  C  V  N  G  L  N  F  R
CAGGAACTTCGTCATGTCAGCAGCCCACTGTGTGAACGGCCTAAATTTCC
         ^210      ^220      ^230      ^240      ^250
  S  V  Q  V  V  L  G  A  H  D  L  R  R  Q  E  R
GGTCAGTGCAGGTAGTGCTGGGAGCCCATGACCTGCGGCGACAGGAGCGC
         ^260      ^270      ^280      ^290      ^300
T  R  Q  T  F  S  V  Q  R  I  F  E  N  G  F  D  P
ACTCGACAGACCTTCTCTGTGCAGCGGATCTTCGAGAATGGCTTTGACCC
         ^310      ^320      ^330      ^340      ^350
 S  Q  L  L  N  D  I  V  I  I  Q  L  N  G  S  A  T
ATCACAACTGCTGAACGACATTGTGATTATCCAGCTCAATGGCTCCGCTA
         ^360      ^370      ^380      ^390      ^400
  I  N  A  N  V  Q  V  A  Q  L  P  A  Q  G  Q  G
CCATTAACGCCAACGTGCAGGTGGCCCAGCTGCCTGCCCAGGGCCAGGGC
         ^410      ^420      ^430      ^440      ^450
V  G  D  R  T  P  C  L  A  M  G  W  G  R  L  G  T
GTGGGTGACAGAACTCCATGTCTGGCCATGGGCTGGGGCAGGTTGGGCAC
         ^460      ^470      ^480      ^490      ^500
 N  R  P  S  P  S  V  L  Q  E  L  N  V  T  V  V  T
AAACAGACCATCACCCAGTGTGCTACAAGAGCTCAATGTGACAGTGGTGA
         ^510      ^520      ^530      ^540      ^550
  N  M  C  R  R  R  V  N  V  C  T  L  V  P  R  R
CTAACATGTGCCGCCGTCGTGTGAACGTATGCACTCTGGTGCCACGTCGA
         ^560      ^570      ^580      ^590      ^600
K  G  G  I  C  F  G  D  S  G  G  P  L  V  C  N  N
AAGGGTGGCATCTGCTTCGGGGACTCTGGCGGACCCTTGGTCTGTAACAA
         ^610      ^620      ^630      ^650      ^650
```

```
 L  V  Q  G  I  D  S  F  I  R  G  G  C  G  S  G  L
CCTTGTCCAAGGCATTGACTCCTTCATCCGAGGAGGCTGTGGATCTGGAT
         ^660      ^670      ^680      ^690      ^700
  Y  P  D  A  F  A  P  V  A  E  F  A  D  W  I  N
TGTACCCAGATGCCTTCGCCCCTGTGGCTGAGTTTGCAGATTGGATCAAT
         ^710      ^720      ^730      ^740      ^750
S  I  I  R  K  P  R  H  H  H  H  H  H
TCCATTATTCGAAAGCCTAGGCATCATCACCATCACCAT
         ^760      ^770      ^780
```

8.2.3 pTT5_ MIP-(5-73)_H6

```
M  E  T  D  T  L  L  L  W  V  L  L  L  W  V  P  G
ATGGAGACAGACACACTCCTGCTATGGGTACTGCTGCTCTGGGTACCAGG
         ^10       ^20       ^30       ^40       ^50
 S  T  G  S  E  L  R  C  Q  C  L  K  T  L  P  R  V
TTCCACTGGTAGTGAACTGCGCTGTCAATGCCTGAAGACCCTGCCAAGGG
         ^60       ^70       ^80       ^90       ^100
  D  F  K  N  I  Q  S  L  S  V  T  P  P  G  P  H
TTGACTTCAAGAACATCCAGAGCTTGAGTGTGACGCCCCCAGGACCCCAC
         ^110      ^120      ^130      ^140      ^150
C  A  Q  T  E  V  I  A  T  L  K  G  G  Q  K  V  C
TGCGCCCAGACAGAAGTCATAGCCACTCTCAAGGGCGGTCAAAAAGTTTG
         ^160      ^170      ^180      ^190      ^200
 L  D  P  E  A  P  L  V  Q  K  I  I  Q  K  I  L  N
CCTTGACCCTGAAGCCCCCCTGGTTCAGAAAATCATCCAAAAGATACTGA
         ^210      ^220      ^230      ^240      ^250
  K  G  K  A  N  T  G  H  H  H  H  H  H
ACAAAGGCAAGGCTAACACCGGTCATCATCACCATCACCAT
         ^260      ^270      ^280      ^290
```

8.2.4 pTT5_EK_MIP-2(1-73)_H6

```
M  E  T  D  T  L  L  L  W  V  L  L  L  W  V  P  G
ATGGAGACAGACACACTCCTGCTATGGGTACTGCTGCTCTGGGTACCAGG
         ^10       ^20       ^30       ^40       ^50
S  T  G  D  G  S  L  Q  G  D  D  D  D  K  A  V  V
TTCCACTGGTGACGGGTCCCTGCAGGGCGACGACGACGACAAGGCTGTTG
         ^60       ^70       ^80       ^90       ^100
  A  S  E  L  R  C  Q  C  L  K  T  L  P  R  V  D
TGGCCAGTGAACTGCGCTGTCAATGCCTGAAGACCCTGCCAAGGGTTGAC
         ^110      ^120      ^130      ^140      ^150
F  K  N  I  Q  S  L  S  V  T  P  P  G  P  H  C  A
TTCAAGAACATCCAGAGCTTGAGTGTGACGCCCCCAGGACCCCACTGCGC
         ^160      ^170      ^180      ^190      ^200
 Q  T  E  V  I  A  T  L  K  G  G  Q  K  V  C  L  D
CCAGACAGAAGTCATAGCCACTCTCAAGGGCGGTCAAAAAGTTTGCCTTG
         ^210      ^220      ^230      ^240      ^250
  P  E  A  P  L  V  Q  K  I  I  Q  K  I  L  N  K
ACCCTGAAGCCCCCCTGGTTCAGAAAATCATCCAAAAGATACTGAACAAA
         ^260      ^270      ^280      ^290      ^300
```

```
G  K  A  N  T  G  H  H  H  H  H  H
GGCAAGGCTAACACCGGTCATCATCACCATCACCAT
         ^310      ^320      ^330
```

8.2.5 pTT5_MIP-2(5-73)_Ruby_H6

```
M  E  T  D  T  L  L  L  W  V  L  L  L  W  V  P  G
ATGGAGACAGACACACTCCTGCTATGGGTACTGCTGCTCTGGGTACCAGG
         ^10       ^20       ^30       ^40       ^50
 S  T  G  S  E  L  R  C  Q  C  L  K  T  L  P  R  V
TTCCACTGGTAGTGAACTGCGCTGTCAATGCCTGAAGACCCTGCCAAGGG
         ^60       ^70       ^80       ^90       ^100
  D  F  K  N  I  Q  S  L  S  V  T  P  P  G  P  H
TTGACTTCAAGAACATCCAGAGCTTGAGTGTGACGCCCCCAGGACCCCAC
         ^110      ^120      ^130      ^140      ^150
C  A  Q  T  E  V  I  A  T  L  K  G  G  Q  K  V  C
TGCGCCCAGACAGAAGTCATAGCCACTCTCAAGGGCGGTCAAAAAGTTTG
         ^160      ^170      ^180      ^190      ^200
 L  D  P  E  A  P  L  V  Q  K  I  I  Q  K  I  L  N
CCTTGACCCTGAAGCCCCCCTGGTTCAGAAAATCATCCAAAAGATACTGA
         ^210      ^220      ^230      ^240      ^250
  K  G  K  A  N  T  G  S  G  G  G  E  D  N  S  L
ACAAAGGCAAGGCTAACACCGGTTCTGGTGGCGGTGAGGATAACAGCCTG
         ^260      ^270      ^280      ^290      ^300
I  K  E  N  M  R  M  K  V  V  L  E  G  S  V  N  G
ATCAAAGAAAACATGCGGATGAAGGTGGTGCTGGAAGGCAGCGTGAACGG
         ^310      ^320      ^330      ^340      ^350
 H  Q  F  K  C  T  G  E  G  E  G  N  P  Y  M  G  T
CCACCAGTTCAAGTGCACCGGCGAGGGCGAGGGCAACCCCTACATGGGCA
         ^360      ^370      ^380      ^390      ^400
  Q  T  M  R  I  K  V  I  E  G  G  P  L  P  F  A
CCCAGACCATGCGGATCAAAGTGATCGAGGGCGGACCTCTGCCCTTCGCC
         ^410      ^420      ^430      ^440      ^450
F  D  I  L  A  T  S  F  M  Y G  S  R  T  F  I  K
TTCGACATCCTGGCCACATCCTTCATGTACGGCAGCCGGACCTTCATCAA
         ^460      ^470      ^480     ^490      ^500
 Y  P  K  G  I  P  D  F  F  K  Q  S  F  P  E  G  F
GTACCCCAAGGGCATCCCCGATTTCTTCAAGCAGAGCTTCCCCGAGGGCT
         ^510      ^520      ^530      ^540      ^550
  T  W  E  R  V  T  R  Y  E  D  G  G  V  I  T  V
TCACCTGGGAGAGAGTGACCAGATACGAGGACGGCGGCGTGATCACCGTG
         ^560      ^570      ^580      ^590      ^600
M  Q  D  T  S  L  E  D  G  C  L  V  Y  H  A  Q  V
ATGCAGGACACCAGCCTGGAAGATGGCTGCCTGGTGTACCATGCCCAGGT
         ^610      ^620      ^630      ^640      ^650
 R  G  V  N  F  P  S  N  G  A  V  M  Q  K  K  T  K
CAGGGGCGTGAATTTTCCCAGCAACGGCGCCGTGATGCAGAAGAAAACCA
         ^660      ^670      ^680      ^690      ^700
  G  W  E  P  N  T  E  M  M  Y  P  A  D  G  G  L
AGGGCTGGGAGCCCAACACCGAGATGATGTACCCCGCTGACGGCGGACTG
         ^710      ^720      ^730      ^740      ^750
```

```
R  G  Y  T  H  M  A  L  K  V  D  G  G  G  H  L  S
AGAGGCTACACCCACATGGCCCTGAAGGTGGACGGCGGAGGGCACCTGAG
         ^760       ^770       ^780       ^790       ^800
 C  S  F  V  T  T  Y  R  S  K  K  T  V  G  N  I  K
CTGCAGCTTCGTGACCACCTACCGATCCAAGAAAACCGTGGGCAACATCA
         ^810       ^820       ^830       ^840       ^850
  M  P  G  I  H  A  V  D  H  R  L  E  R  L  E  E
AGATGCCCGGCATCCACGCCGTGGACCACCGGCTGGAAAGGCTGGAAGAG
         ^860       ^870       ^880       ^890       ^900
S  D  N  E  M  F  V  V  Q  R  E  H  A  V  A  K  F
TCCGACAACGAGATGTTCGTGGTGCAGCGGGAGCACGCCGTGGCCAAGTT
         ^910       ^920       ^930       ^940       ^950
A  G  L  P  G  G  H  H  H  H  H  H
CGCCGGCCTGCCTGGAGGGCACCATCACCATCACCAT
         ^960       ^970       ^980
```

8.2.6 pTT5_ Cherry_MIP-2(1-73)_H6

```
M  E  T  D  T  L  L  L  W  V  L  L  L  W  V  P  G
ATGGAGACAGACACACTCCTGCTATGGGTACTGCTGCTCTGGGTACCAGG
         ^10        ^20        ^30        ^40        ^50
 S  T  G  D  V  S  K  G  E  E  D  N  M  A  I  I  K
TTCCACTGGTGACGTGAGCAAGGGCGAGGAGGATAACATGGCCATCATCA
         ^60        ^70        ^80        ^90        ^100
  E  F  M  R  F  K  V  H  M  E  G  S  V  N  G  H
AGGAGTTCATGCGCTTCAAGGTGCACATGGAGGGCTCCGTGAACGGCCAC
         ^110       ^120       ^130       ^140       ^150
E  F  E  I  E  G  E  G  E  G  R  P  Y  E  G  T  Q
GAGTTCGAGATCGAGGGCGAGGGCGAGGGCCGCCCCTACGAGGGCACCCA
         ^160       ^170       ^180       ^190       ^200
 T  A  K  L  K  V  T  K  G  G  P  L  P  F  A  W  D
GACCGCCAAGCTGAAGGTGACCAAGGGTGGCCCCCTGCCCTTCGCCTGGG
         ^210       ^220       ^230       ^240       ^250
  I  L  S  P  Q  F  M  Y  G  S  K  A  Y  V  K  H
ACATCCTGTCCCCTCAGTTCATGTACGGCTCCAAGGCCTACGTGAAGCAC
         ^260       ^270       ^280       ^290       ^300
P  A  D  I  P  D  Y  L  K  L  S  F  P  E  G  F  K
CCCGCCGACATCCCCGACTACTTGAAGCTGTCCTTCCCCGAGGGCTTCAA
         ^310       ^320       ^330       ^340       ^350
 W  E  R  V  M  N  F  E  D  G  G  V  V  T  V  T  Q
GTGGGAGCGCGTGATGAACTTCGAGGACGGCGGCGTGGTGACCGTGACCC
         ^360       ^370       ^380       ^390       ^400
  D  S  S  L  Q  D  G  E  F  I  Y  K  V  K  L  R
AGGACTCCTCCCTGCAGGACGGCGAGTTCATCTACAAGGTGAAGCTGCGC
         ^410       ^420       ^430       ^440       ^450
G  T  N  F  P  S  D  G  P  V  M  Q  K  K  T  M  G
GGCACCAACTTCCCCTCCGACGGCCCCGTAATGCAGAAGAAGACCATGGG
         ^460       ^470       ^480       ^490       ^500
 W  E  A  S  S  E  R  M  Y  P  E  D  G  A  L  K  G
CTGGGAGGCCTCCTCCGAGCGGATGTACCCCGAGGACGGCGCCCTGAAGG
         ^510       ^520       ^530       ^540       ^550
```

```
  E  I  K  Q  R  L  K  L  K  D  G  G  H  Y  D  A
GCGAGATCAAGCAGAGGCTGAAGCTGAAGGACGGCGGCCACTACGACGCT
         ^560      ^570      ^580      ^590      ^600
E  V  K  T  T  Y  K  A  K  K  P  V  Q  L  P  G  A
GAGGTCAAGACCACCTACAAGGCCAAGAAGCCCGTGCAGCTGCCCGGCGC
         ^610      ^620      ^630      ^640      ^650
 Y  N  V  N  I  K  L  D  I  T  S  H  N  E  D  Y  T
CTACAACGTCAACATCAAGTTGGACATCACCTCCCACAACGAGGACTACA
         ^660      ^670      ^680      ^690      ^700
  I  V  E  Q  Y  E  R  A  E  G  R  H  S  T  G  G
CCATCGTGGAACAGTACGAACGCGCCGAGGGCCGCCACTCCACCGGCGGC
         ^710      ^720      ^730      ^740      ^750
M  D  E  L  Y  K  S  G  G  G  G  V  P  G  S  T  G
ATGGACGAGCTGTACAAGTCTGGTGGCGGTGGGGTACCAGGTTCCACTGG
         ^760      ^770      ^780      ^790      ^800
 A  V  V  A  S  E  L  R  C  Q  C  L  K  T  L  P  R
TGCTGTTGTGGCCAGTGAACTGCGCTGTCAATGCCTGAAGACCCTGCCAA
         ^810      ^820      ^830      ^840      ^850
  V  D  F  K  N  I  Q  S  L  S  V  T  P  P  G  P
GGGTTGACTTCAAGAACATCCAGAGCTTGAGTGTGACGCCCCCAGGACCC
         ^860      ^870      ^880      ^890      ^900
H  C  A  Q  T  E  V  I  A  T  L  K  G  G  Q  K  V
CACTGCGCCCAGACAGAAGTCATAGCCACTCTCAAGGGCGGTCAAAAAGT
         ^910      ^920      ^930      ^940      ^950
 C  L  D  P  E  A  P  L  V  Q  K  I  I  Q  K  I  L
TTGCCTTGACCCTGAAGCCCCCCTGGTTCAGAAAATCATCCAAAAGATAC
         ^960      ^970      ^980      ^990      ^1000
  N  K  G  K  A  N  T  G  H  H  H  H  H  H
TGAACAAAGGCAAGGCTAACACCGGTCATCATCACCATCACCAT
         ^1010     ^1020     ^1030
```

8.2.7 pTT5_α1PI_342K

```
M  E  T  D  T  L  L  L  W  V  L  L  L  W  V  P  G
ATGGAGACAGACACACTCCTGCTATGGGTACTGCTGCTCTGGGTACCAGG
         ^10       ^20       ^30       ^40       ^50
 S  T  G  E  D  P  Q  G  D  A  A  Q  K  T  D  T  S
TTCCACTGGTGAGGATCCCCAGGGAGATGCTGCCCAGAAGACAGATACAT
         ^60       ^70       ^80       ^90       ^100
  H  H  D  Q  D  H  P  T  F  N  K  I  T  P  N  L
CCCACCATGATCAGGATCACCCAACCTTCAACAAGATCACCCCCAACCTG
         ^110      ^120      ^130      ^140      ^150
A  E  F  A  F  S  L  Y  R  Q  L  A  H  Q  S  N  S
GCTGAGTTCGCCTTCAGCCTATACCGCCAGCTGGCACACCAGTCCAACAG
         ^160      ^170      ^180      ^190      ^200
 T  N  I  F  F  S  P  V  S  I  A  T  A  F  A  M  L
CACCAATATCTTCTTCTCCCCAGTGAGCATCGCTACAGCCTTTGCAATGC
         ^210      ^220      ^230      ^240      ^250
  S  L  G  T  K  A  D  T  H  D  E  I  L  E  G  L
TCTCCCTGGGGACCAAGGCTGACACTCACGATGAAATCCTGGAGGGCCTG
         ^260      ^270      ^280      ^290      ^300
```

```
N  F  N  L  T  E  I  P  E  A  Q  I  H  E  G  F  Q
AATTTCAACCTCACGGAGATTCCGGAGGCTCAGATCCATGAAGGCTTCCA
         ^310      ^320      ^330      ^340      ^350
 E  L  L  R  T  L  N  Q  P  D  S  Q  L  Q  L  T  T
GGAACTCCTCCGTACCCTCAACCAGCCAGACAGCCAGCTCCAGCTGACCA
         ^360      ^370      ^380      ^390      ^400
  G  N  G  L  F  L  S  E  G  L  K  L  V  D  K  F
CCGGCAATGGCCTGTTCCTCAGCGAGGGCCTGAAGCTAGTGGATAAGTTT
         ^410      ^420      ^430      ^440      ^450
L  E  D  V  K  K  L  Y  H  S  E  A  F  T  V  N  F
TTGGAGGATGTTAAAAAGTTGTACCACTCAGAAGCCTTCACTGTCAACTT
         ^460      ^470      ^480      ^490      ^500
 G  D  T  E  E  A  K  K  Q  I  N  D  Y  V  E  K  G
CGGGGACACCGAAGAGGCCAAGAAACAGATCAACGATTACGTGGAGAAGG
         ^510      ^520      ^530      ^540      ^550
  T  Q  G  K  I  V  D  L  V  K  E  L  D  R  D  T
GTACTCAAGGGAAAATTGTGGATTTGGTCAAGGAGCTTGACAGAGACACA
         ^560      ^570      ^580      ^590      ^600
V  F  A  L  V  N  Y  I  F  F  K  G  K  W  E  R  P
GTTTTTGCTCTGGTGAATTACATCTTCTTTAAAGGCAAATGGGAGAGACC
         ^610      ^620      ^630      ^640      ^650
 F  E  V  K  D  T  E  E  E  D  F  H  V  D  Q  V  T
CTTTGAAGTCAAGGACACCGAGGAAGAGGACTTCCACGTGGACCAGGTGA
         ^660      ^670      ^680      ^690      ^700
  T  V  K  V  P  M  M  K  R  L  G  M  F  N  I  Q
CCACCGTGAAGGTGCCTATGATGAAGCGTTTAGGCATGTTTAACATCCAG
         ^710      ^720      ^730      ^740      ^750
H  S  K  K  L  S  S  W  V  L  L  M  K  Y  L  G  N
CACAGTAAGAAGCTGTCCAGCTGGGTGCTGCTGATGAAATACCTGGGCAA
         ^760      ^770      ^780      ^790      ^800
 A  T  A  I  F  F  L  P  D  E  G  K  L  Q  H  L  E
TGCCACCGCCATCTTCTTCCTGCCTGATGAGGGGAAACTACAGCACCTGG
         ^810      ^820      ^830      ^840      ^850
  N  E  L  T  H  D  I  I  T  K  F  L  E  N  E  D
AAAATGAACTCACCCACGATATCATCACCAAGTTCCTGGAAAATGAAGAC
         ^860      ^870      ^880      ^890      ^900
R  R  S  A  S  L  H  L  P  K  L  S  I  T  G  T  Y
AGAAGGTCTGCCAGCTTACATTTACCCAAACTGTCCATTACTGGAACCTA
         ^910      ^920      ^930      ^940      ^950
 D  L  K  S  V  L  G  Q  L  G  I  T  K  V  F  S  N
TGATCTGAAGAGCGTCCTGGGTCAACTGGGCATCACTAAGGTCTTCAGCA
         ^960      ^970      ^980      ^990      ^1000
  G  A  D  L  S  G  V  T  E  E  A  P  L  K  L  S
ATGGGGCTGACCTCTCCGGGGTCACAGAGGAGGCACCCCTGAAGCTCTCC
         ^1010     ^1020     ^1030     ^1040     ^1050
K  A  V  H  K  A  V  L  T  I  D  K  K  G  T  E  A
AAGGCCGTGCATAAGGCTGTGCTGACCATCGACAAGAAAGGGACTGAAGC
         ^1060     ^1070     ^1080     ^1090     ^1100
 A  G  A  M  F  L  E  A  I  P  M  S  I  P  P  E  V
TGCTGGGGCCATGTTCCTCGAGGCCATACCCATGAGTATACCCCCCGAGG
         ^1110     ^1120     ^1130     ^1140     ^1150
```

```
  K   F   N   K   P   F   V   F   L   M   I   E   Q   N   T   K
TCAAGTTCAACAAACCCTTTGTCTTCTTAATGATTGAACAAAATACCAAG
         ^1160     ^1170     ^1180     ^1190
S   P   L   F   M   G   K   V   V   N   P   T   Q   K   T   G  H
TCTCCCCTCTTCATGGGAAAAGTGGTGAATCCCACCCAAAAAACCGGTCA
         ^1210     ^1220     ^1230     ^1240     ^1250
 H   H   H   H   H
TCATCACCATCACCAT
         ^1260
```

8.3 List of constructs

name of construct	vector	insert	method	oligonucleotide	restriction enzymes
pTT5_S_mNE(wt)_H_6	pTT5	pcDNA5/FRT_S_mNE_H_6	Subklonierung	-	NheI + NaeI/PmeI
pTT5_NGS_mNE(wt)_H_6	pTT5_S_mNE(wt)_H_6		Oligoduplex	DJ3385/DJ3386	PmlI + KpnI
pTT5_NGS_mNE-KG188/9_H_6	pTT5_NGS_mNE(wt)_H_6		Oligoduplex	DJ3395/3396	AlfI
pTT5_NGS_mNE(wt)_st.H_6	pTT5_S_mNE(wt)_H_6		Oligoduplex	DJ3397/DJ3398	BstBI + BamHI
pTT5_NGS_mNE-KG187/8_st.H_6	pTT5_NGS_mNE-KG188/9_H_6		Oligoduplex	DJ3397/DJ3398	BstBI + BamHI
pCDNA5/FRT_S_mNE-KG187/8_w/o-glyc_H_6	pcDNA5/FRT_S_mNE_H_6	pTT5_S_mNE(wt)_H_6	PCR	DJ3469/DJ3470	AleI +BstXI/EagI
pTT5_NGS_mNE(wt)_w/o-glyc_st.H_6	pTT5	pCDNA5/FRT_S_mNE(wt)_w/o-glyc_H_6	Subklonierung		EagI + BmgBI
pTT5_NGS_mNE(A195)_st.H_6	pTT5_NGS_mNE(wt)_st.H_6		Oligoduplexe	DJ3532/DJ3533	AlfI
pTT5_ MIP-(5-73)_H_6	pTT5	cDNA	PCR	DJ3310/DJ3311	AgeI + KpnI
pTT5_MIP-2(1-73)_H_6	pTT5	cDNA	PCR	DJ3309/DJ3310	AgeI + KpnI
pTT5_EK_MIP-2(1-73)	pTT5	cDNA	PCR	DJ3354/DJ3340	Age + SfbI
pTT5_EK_MIP-2(1-73)_H_6	pTT5	pTT5_EK_MIP-2(73)	PCR	DJ3310/DJ3376	AgeI + KpnI
pTT5_MIP-2(5-73)_Ruby_H_6	pTT5	cDNA	PCR	DJ3374/DJ3375	AgeI + BamHI
pTT5_ Cherry_MIP-2(1-73)_H_6	pTT5_MIP-2(73)	cDNA	PCR	DJ3341/DJ3342	KpnI
pTT5_α1PI_wt	pTT5	pUC57_hsa1pi	Subklonierung		KpnI + AgeI
pTT5_α1PI_M358T	pTT5_α1PI_wt		Oligoduplex	DJ3553/ DJ3554	AbsI + AccI
pTT5_α1PI_E342K	pTT5_α1PI_wt	pUC57_hsa1pi	PCR	DJ3557/ DJ3558	EcoRV + AbsI
pTT5_MNEI	pTT5				

Presentations at international conferences

02/2013 Oral presentation on "Decreased inhibitory capacity of natural α1-antitrypsin towards an autoprocessed two-chain form of neutrophil elastase". *26th International Winter School on Proteinases and Their Inhibitors.* Italy.

06/2012 Poster presentation of "Autoprocessing of neutrophil elastase near its active site counteracts alpha-1-antitrypsin inhibition" *Gordon Research Conference: Proteolytic Enzymes and Their Inhibitors.* Italy, 2010.

02/2011 Oral presentation on "Instability and self-digestion of neutrophil elastase". *26th International Winter School on Proteinases and Their Inhibitors.* Italy.

02/2010 Oral presentation on "Chemokines as targets of neutrophil serine proteases". *26th International Winter School on Proteinases and Their Inhibitors.* Italy.

9 Publications

- Anastasov, N., Bonzheim, I., Rudelius, M., Klier, M., **Dau, T**., Angermeier, D., Duyster, J., Pittaluga, S., Fend, F., Raffeld, M., et al. (2010). C/EBPβ expression in ALK-positive anaplastic large cell lymphomas is required for cell proliferation and is induced by the STAT3 signaling pathway. Haematologica 95, 760–767.

- Kessenbrock, K., **Dau, T**., and Jenne, D.E. (2011). Tailor-made inflammation: how neutrophil serine proteases modulate the inflammatory response. J. Mol. Med. (Berl). *89*, 23–28.*

- Mankan, A.K., **Dau, T**., Jenne, D., and Hornung, V. (2012). The NLRP3/ASC/Caspase-1 axis regulates IL-1β processing in neutrophils. Eur. J. Immunol. 42, 710–715.*

*these publications resulted from this Ph. D. thesis